



**CHALMERS**  
UNIVERSITY OF TECHNOLOGY

---



# Study of system earthing for 36 kV- collector grids for wind farms

Master's thesis in Electric Power Engineering

DAVID JANSSON  
PATRIK WADSTRÖM



## Abstract

For wind farms, it has become more common to use system voltage of 36 kV for the collector grids. However, in Sweden there are guidelines and standards for voltages up to 24 kV but low voltages result in higher losses. For power systems with voltage levels above 24 kV, clear instructions for how to perform system earthing are lacking; this means that many opportunities are allowed for 36 kV collector grids.

The purpose of this study is to identify different alternatives of how to system earth a wind farm with system voltage of 36 kV. This thesis consists of two major parts; a mapping of present solutions and a simulation part. By contacting different developers and owners of wind farms, their method for system earthing may be identified. Wind farms that are selected for the mapping consists of at least 10 wind turbines and with a construction voltage of 36 kV. The simulations will be performed on a model for different system earthing alternatives to investigate the behavior of fault current and transient overvoltages during line-faults. Also, the simulations will investigate the impact of a lightning impulse. The simulation model is based on a specific wind farm and the software that will be used for the power system analysis is PSCAD/EMTDC.

The result of the mapping indicates that the most common earthing method in Sweden is resonance earthing and for Europe, low-resistance earthing. In the simulations, it can be seen that the main difference between these two earthing methods is the fault current. The fault current is much greater for low-resistance earthing compared with resonance earthing. The simulation also indicates that the resonance earthed system causes the highest transient overvoltages compared with low-resistance earthing. The results of the lightning impulse simulations for resonance earthing shows that it is important to have a low value of the resistance of the earth electrode for a surge arrester to keep a lower voltage level.



## **Acknowledgements**

First of all, we would like to thank Sweco Energuide, department Kraftsystemanalys for all their help and support with this thesis. An extra big thanks to our supervisors at Sweco, Simon Lindroth and Gustav Holmquist and also the colleagues in the department, Fredrik Loodin and Christian Adolfsson. We would like to say thanks to our supervisor at Chalmers University of Technology, Tarik Abdulahovic for all the help with PSCAD and valuable comments on this thesis.

Big thanks to all the companies that took their time and answered our questions for the survey in this thesis.

David Jansson och Patrik Wadström, Gothenburg



# Contents

|          |   |           |
|----------|---|-----------|
| <b>1</b> | <b>Introduction</b>                         | <b>1</b>  |
| 1.1      | Background . . . . .                        | 1         |
| 1.2      | Aim . . . . .                               | 1         |
| 1.3      | Problem . . . . .                           | 2         |
| 1.4      | Scope . . . . .                             | 2         |
| 1.5      | Method . . . . .                            | 3         |
| <b>2</b> | <b>Theory</b>                               | <b>4</b>  |
| 2.1      | Unbalanced Faults . . . . .                 | 4         |
| 2.1.1    | Sequence Network . . . . .                  | 4         |
| 2.1.2    | Single Line-to-ground Fault . . . . .       | 6         |
| 2.1.3    | Line-to-Line Fault . . . . .                | 8         |
| 2.1.4    | Double Line-to-ground Fault . . . . .       | 10        |
| 2.2      | Earthing Methods . . . . .                  | 12        |
| 2.2.1    | Isolated Neutral System . . . . .           | 12        |
| 2.2.2    | Solidly Neutral Earthed System . . . . .    | 13        |
| 2.2.3    | Resistance Earthed System . . . . .         | 14        |
| 2.2.4    | Resonance Earthed System . . . . .          | 16        |
| 2.2.5    | Earthing Transformer . . . . .              | 19        |
| 2.3      | Earth Electrode . . . . .                   | 20        |
| 2.4      | Impulse Overvoltage . . . . .               | 22        |
| <b>3</b> | <b>Electrical Regulations and Standards</b> | <b>24</b> |
| <b>4</b> | <b>Mapping of Wind Farms</b>                | <b>26</b> |
| 4.1      | Survey Methodology . . . . .                | 26        |
| 4.2      | Selection of Wind Farms . . . . .           | 26        |
| <b>5</b> | <b>Description of the wind farm</b>         | <b>28</b> |
| 5.1      | Technical spec. . . . .                     | 28        |

---

|           |   |           |
|-----------|---|-----------|
| 5.2       | System earthing . . . . .               | 31        |
| 5.3       | Protection . . . . .                    | 31        |
| 5.4       | Earth resistance . . . . .              | 32        |
| <b>6</b>  | <b>Modeling</b>                         | <b>33</b> |
| 6.1       | Introduction to PSCAD/EMTDC . . . . .   | 33        |
| 6.2       | Cables . . . . .                        | 33        |
| 6.3       | Overhead lines . . . . .                | 35        |
| 6.4       | Wind turbine and transformers . . . . . | 36        |
| 6.5       | 77/33 kV-transformer . . . . .          | 36        |
| 6.6       | Utility grid . . . . .                  | 37        |
| 6.7       | Impulse overvoltages . . . . .          | 38        |
| <b>7</b>  | <b>Simulation</b>                       | <b>39</b> |
| 7.1       | Low-resistance earthing . . . . .       | 40        |
| 7.2       | Resonance earthing . . . . .            | 52        |
| 7.3       | Lightning impulses . . . . .            | 63        |
| 7.3.1     | Lightning impulse of 600 kV . . . . .   | 63        |
| 7.3.2     | Lightning impulse of 1 MV . . . . .     | 69        |
| <b>8</b>  | <b>Result</b>                           | <b>74</b> |
| 8.1       | Survey . . . . .                        | 74        |
| 8.2       | Simulation . . . . .                    | 75        |
| <b>9</b>  | <b>Discussion</b>                       | <b>79</b> |
| <b>10</b> | <b>Conclusion</b>                       | <b>81</b> |
|           | <b>References</b>                       | <b>83</b> |
|           | <b>Appendix</b>                         | <b>86</b> |

# 1

## Introduction

### 1.1 Background

In wind farms, it has become more common to use a system voltage of 36 kV for collector grids and the design of an electrical system is dependent on the voltage level.

In Sweden there are guidelines and standards for voltages up to 24 kV but low voltages result in higher losses. For power systems with voltage levels above 24 kV, clear instructions for how to perform system earthing are lacking; this means that many opportunities are allowed for 36 kV collector grids. With higher voltages, there needs to be more focus on operational and personal safety. Due to that there are lacking guidelines and standards for how to solve system earthing for higher voltages, questions occur regarding how to solve this and still keep high safety, follow regulations and detect fault currents. This becomes a challenge due to the poor grounding conditions, as it often is where wind farms are installed. In Sweden it is most common to use resonant earthed systems, but in other countries it is common to use low-resistance earthed systems. That is why it is suggested to do a survey of present solutions which can be used as a basis.

As a starting point, an earlier wind power research report will be used, written by Daniel Wall and Christer Liljegren, "Problems in the system related to wind power, an inventory". This report mentions the need for this kind of research and study. By conducting this study, it may be possible to increase the understanding of selection of system grounding on collector grids for wind farms at 36 kV.

### 1.2 Aim

The aim of this study is to identify different alternatives of how to system earth a wind farm with system voltage of 36 kV in Sweden and Europe and to identify pros and cons for the most common earthing methods. Furthermore, with simulations, investigate how the

collector grid for a specific wind farm behaves differently during line-faults, dependent on which earthing method that is used. Also, the simulations should investigate the impact of a lightning impulse for a resonance earthed system.

### 1.3 Problem

There are lacking guidelines and standards in Sweden when it comes to system earthing a wind farm with a system voltage of 36 kV. The problem that needs to be investigated is how to design an earthing system for these kinds of wind farms. The two major tasks that need to be solved are to perform a mapping of present solutions and perform simulations. Mapping of present solutions gives an overview of which methods for system earthing in wind farms are common for companies across Europe.

Mapping of present solutions and simulations should include and answer following questions:

- What is the most common method for system earthing in Europe?
- What are the pros and cons with the different methods for system earthing?
- How do line-faults affect the fault current, the voltage levels and transient over-voltages for a wind farm with the two most common methods for system earthing?
- How does lightning impulses affect the wind farm?
- How is the ohmic value of the earth electrode affecting a surge arresters ability to withstand a lightning impulse?
- What conclusions can be made?

### 1.4 Scope

The mapping will not include a full investigation of all wind farms in Sweden and Europe. The wind farms that will be selected will consist of at least 10 wind turbines and with a construction voltage of 36 kV. All possible faults that may occur will not be studied, only the most common faults will be analyzed. This study will not examine whether there is any correlation between manufacturer of components for wind farms and system earthing method. Costs of system earthing can have a big role in the choice of system earthing. However, how much costs affect the choice of system earthing will not be investigated.

Simulations will only be performed on the system earthing that appears to be the most common methods in Sweden and Europe. The model is based on an existing wind farm with some modifications. Faults that will be simulated are single line-to-ground faults, line-to-line faults and double line-to-ground faults. Furthermore, impulse overvoltages will only be simulated for the specific wind farm that the simulations are based on.

## 1.5 Method

The investigation will consist of two major parts; a mapping of present solutions and a simulation part. The mapping will include studies of scientific articles and reports for different methods for system earthing. By contacting different developers and owners of wind farms in Sweden and parts of Europe, their system earthing method may be identified.

The simulations will be performed on the model for different system earthing alternatives to investigate which parameters, and values of the parameters, that are important to achieve satisfactory operating conditions. The simulation software that will be used for power system analysis is PSCAD/EMTDC.

# 2

## Theory

### 2.1 Unbalanced Faults

#### 2.1.1 Sequence Network

A three-phase generator supplying a three-phase balanced load is illustrated in Figure 2.1, where the generator has an impedance  $Z_n$  between neutral and ground.

The phase voltage can be expressed as positive-sequence set of phasors, where  $a$  describes the phase rotation of  $120^\circ$ , where  $a = e^{j120^\circ}$  and  $a^2 = e^{j240^\circ}$  [1].

$$\mathbf{E}^{abc} = \begin{bmatrix} 1 \\ a^2 \\ a \end{bmatrix} E_a \quad (2.1)$$

It can be seen that by applying Kirchoff's voltage law to Figure 2.1, the phase voltages can be expressed as

$$V_a = E_a - Z_s I_a - Z_n I_n \quad (2.2)$$

$$V_b = E_b - Z_s I_b - Z_n I_n \quad (2.3)$$

$$V_c = E_c - Z_s I_c - Z_n I_n. \quad (2.4)$$

In Figure 2.1, all incoming currents is equal to all outgoing currents according to Kirchoff's current law in the neutral point,  $N$ , Therefore, can the phase currents be represented as

$$I_a + I_b + I_c = I_n. \quad (2.5)$$

By substituting  $I_n$  in (2.5) into (2.2), (2.3) and (2.4), the phase voltages can be expressed as

$$\mathbf{V}^{abc} = \mathbf{E}^{abc} - \mathbf{Z}^{abc} \mathbf{I}^{abc} \quad (2.6)$$

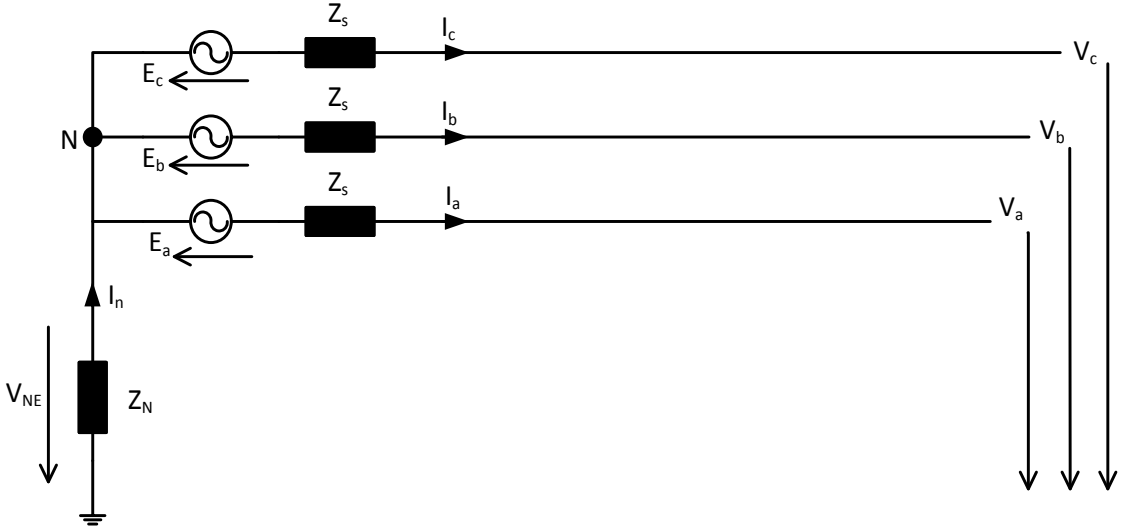


Figure 2.1: Three-phase generator with neutral impedance

or represented in matrix form as

$$\begin{bmatrix} V_a \\ V_b \\ V_c \end{bmatrix} = \begin{bmatrix} E_a \\ E_b \\ E_c \end{bmatrix} - \begin{bmatrix} Z_s + Z_n & Z_n & Z_n \\ Z_n & Z_s + Z_n & Z_n \\ Z_n & Z_n & Z_s + Z_n \end{bmatrix} \begin{bmatrix} I_a \\ I_b \\ I_c \end{bmatrix} \quad (2.7)$$

Transforming into symmetrical components from phase voltages and phase currents can be performed by multiplying with the *symmetrical components transformation matrix*,  $\mathbf{A}$  [1].

$$\mathbf{A} \mathbf{V}_a^{012} = \mathbf{A} \mathbf{E}_a^{012} - \mathbf{Z}^{abc} \mathbf{A} \mathbf{I}_a^{012} \quad (2.8)$$

where  $\mathbf{A}$  is

$$\mathbf{A} = \begin{bmatrix} 1 & 1 & 1 \\ 1 & a^2 & a \\ 1 & a & a^2 \end{bmatrix} \quad (2.9)$$

Solving the transformation into symmetrical components results in

$$\mathbf{V}_a^{012} = \mathbf{E}_a^{012} - \mathbf{A}^{-1} \mathbf{Z}^{abc} \mathbf{A} \mathbf{I}_a^{012} = \mathbf{E}_a^{012} - \mathbf{Z}^{012} \mathbf{I}_a^{012} \quad (2.10)$$

where

$$\mathbf{Z}^{012} = \mathbf{A}^{-1} \mathbf{Z}^{abc} \mathbf{A}. \quad (2.11)$$

Solving  $\mathbf{Z}^{012}$  results in

$$\mathbf{Z}^{012} = \begin{bmatrix} Z_s + 3Z_n & 0 & 0 \\ 0 & Z_s & 0 \\ 0 & 0 & Z_s \end{bmatrix} = \begin{bmatrix} Z_0 & 0 & 0 \\ 0 & Z_1 & 0 \\ 0 & 0 & Z_2 \end{bmatrix} \quad (2.12)$$

Since the generated emf in the circuit is balanced, only positive-sequence voltage occurs. Therefore,

$$\mathbf{E}_a^{012} = \begin{bmatrix} 0 \\ E_a \\ 0 \end{bmatrix}. \quad (2.13)$$

Now (2.10) can be rewritten to

$$\begin{bmatrix} V_a^0 \\ V_a^1 \\ V_a^2 \end{bmatrix} = \begin{bmatrix} 0 \\ E_a \\ 0 \end{bmatrix} - \begin{bmatrix} Z_0 & 0 & 0 \\ 0 & Z_1 & 0 \\ 0 & 0 & Z_2 \end{bmatrix} \begin{bmatrix} I_a^0 \\ I_a^1 \\ I_a^2 \end{bmatrix} \quad (2.14)$$

or

$$V_a^0 = -Z^0 I_a^0 \quad (2.15)$$

$$V_a^1 = E_a - Z^1 I_a^1 \quad (2.16)$$

$$V_a^2 = -Z^2 I_a^2. \quad (2.17)$$

The equations (2.15), (2.16), (2.17) above can be illustrated by the equivalent sequence network in Figure 2.2. From the sequence network it can be seen that the earthing

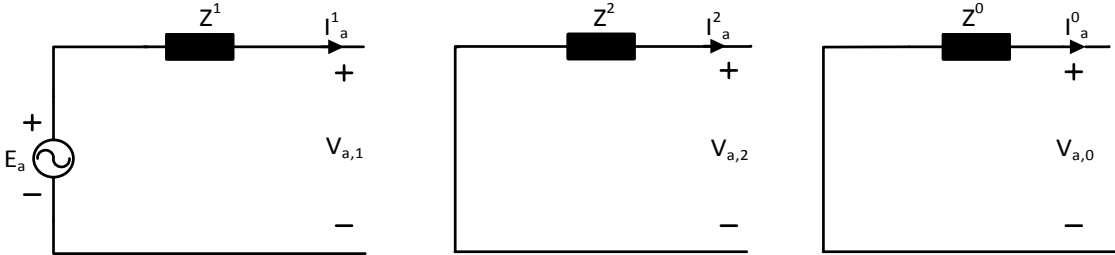


Figure 2.2: Positive, negative and zero sequence

impedance is affecting the zero sequence impedance because of  $Z^0 = Z_s + 3Z_n$  [1].

### 2.1.2 Single Line-to-ground Fault

Single line-to-ground (SLG) fault can occur in electrical distribution systems. This type of fault can be exemplified according to Figure 2.3. The generator in the figure has

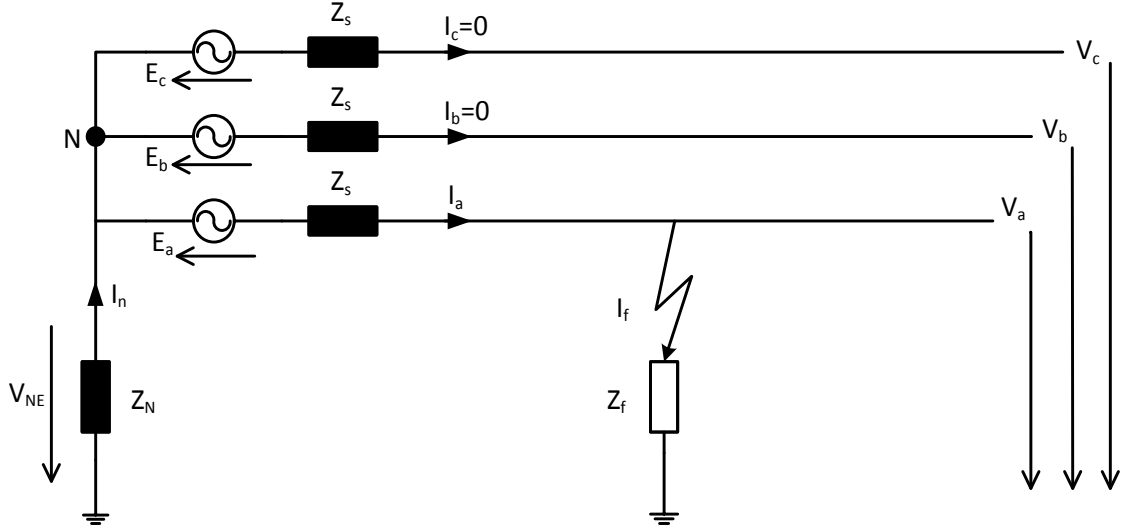


Figure 2.3: Single line-to-ground fault circuit

no-load condition and the neutral is connected through the impedance  $Z_N$  to ground. Phase  $a$  is exposed to a SLG fault through the impedance  $Z_f$  [1].

Performing power system calculations on SLG fault gives the boundary conditions at the fault location under the assumption of no-load condition to:

$$V_a = I_a Z_f \quad (2.18)$$

$$I_b = I_c = 0. \quad (2.19)$$

The symmetrical components of the currents can be written as

$$I_a^0 = \frac{1}{3}(I_a + I_b + I_c) \quad (2.20)$$

$$I_a^1 = \frac{1}{3}(I_a + aI_b + a^2I_c) \quad (2.21)$$

$$I_a^2 = \frac{1}{3}(I_a + a^2I_b + aI_c) \quad (2.22)$$

with the boundary condition,  $I_b = I_c = 0$ , the three equations above result in

$$I_a^0 = I_a^1 = I_a^2 = \frac{1}{3}I_a. \quad (2.23)$$

Describing the phase voltages in symmetrical components results in

$$V_a = V_a^0 + V_a^1 + V_a^2, \quad (2.24)$$

$$V_b = V_a^0 + a^2V_a^1 + aV_a^2, \quad (2.25)$$

$$V_c = V_a^0 + aV_a^1 + a^2V_a^2. \quad (2.26)$$

By substituting (2.18) and (2.23) into (2.24), the following can be obtained

$$V_a^0 + V_a^1 + V_a^2 = Z_f 3I_a^0. \quad (2.27)$$

The symmetrical components of phase voltage  $a$  can be described as

$$V_a^0 = -Z^0 I_a^0 \quad (2.28)$$

$$V_a^1 = E_a - Z^1 I_a^1 \quad (2.29)$$

$$V_a^2 = -Z^2 I_a^2. \quad (2.30)$$

Substituting  $I_a^1$  and  $I_a^2$  from (2.23) into (2.28), (2.29) and (2.30), the symmetrical components of phase voltage  $a$  can be rewritten as

$$V_a^0 = -Z^0 I_a^0 \quad (2.31)$$

$$V_a^1 = E_a - Z^1 I_a^0 \quad (2.32)$$

$$V_a^2 = -Z^2 I_a^0. \quad (2.33)$$

Now Equation (2.27) can be formulated by using (2.31), (2.32) and (2.33) as

$$-Z^0 I_a^0 + E_a - Z^1 I_a^0 - Z^2 I_a^0 = Z_f 3I_a^0. \quad (2.34)$$

Solving for  $I_a^0$

$$I_a^0 = \frac{E_a}{Z_1 + Z_2 + Z_0 + 3Z_f}. \quad (2.35)$$

Combining (2.23) and (2.35), the fault current can be expressed as

$$I_a = 3I_a^0 = \frac{3E_a}{Z_1 + Z_2 + Z_0 + 3Z_f}. \quad (2.36)$$

From (2.35) the symmetrical component of the phase current  $a$ ,  $I_a^0$  can be represented in Figure 2.4 by connecting the sequence networks in series [1].

### 2.1.3 Line-to-Line Fault

When a line-to-line (LL) fault occurs, it can be represented as in Figure 2.5. For simplification, the fault occurs for phase b and c. Assumption that it is initially in no-load condition is made. To present a LL fault in an equivalent sequence network, first thing to do is to determine the boundary conditions. This can be done from Figure 2.5.

$$V_b - V_c = Z_f I_b \quad (2.37)$$

$$I_b + I_c = 0 \quad (2.38)$$

$$I_a = 0. \quad (2.39)$$

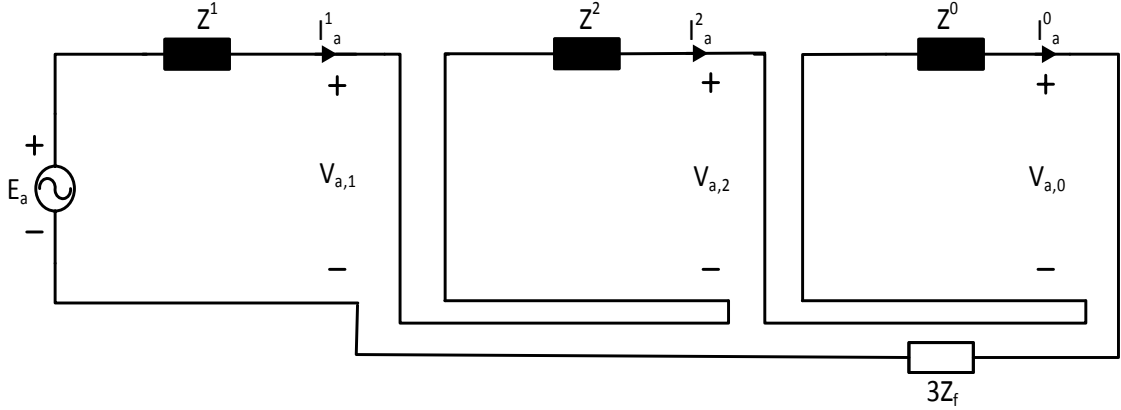


Figure 2.4: Single line-to-ground fault equivalent sequence network circuit

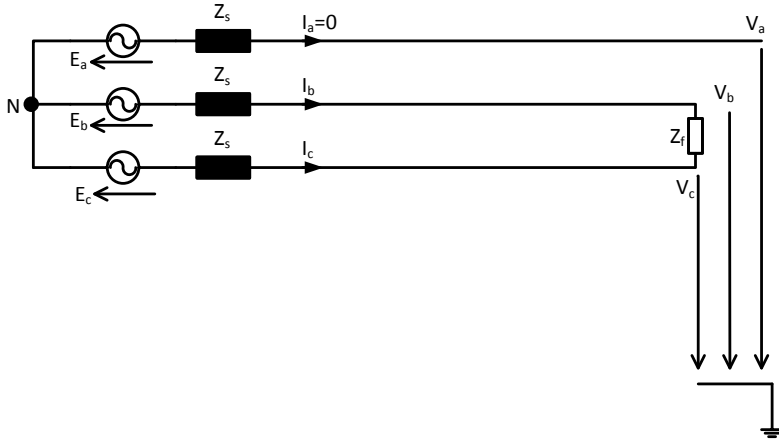


Figure 2.5: Line-to-Line fault

By substituting the boundary conditions in (2.37)-(2.39) into (2.20)-(2.22), the symmetrical components can be expressed as

$$I_a^0 = 0 \tag{2.40}$$

$$I_a^1 = \frac{1}{3}(a - a^2)I_b \tag{2.41}$$

$$I_a^2 = \frac{1}{3}(a^2 - a)I_b. \tag{2.42}$$

From (2.41) and (2.42) it can be noted that

$$I_a^1 = -I_a^2 \tag{2.43}$$

From (2.24)-(2.26) it is given that

$$V_b - V_c = (a^2 - a)(V_a^1 - V_a^2) = Z_f I_b. \tag{2.44}$$

Substituting  $V_a^1$  and  $V_a^2$  from (2.16) and (2.17) and using that  $I_a^2 = -I_a^1$ , following equation is given

$$(a^2 - a)[E_a - (Z_1 + Z_2)I_a^1] = Z_f I_b. \quad (2.45)$$

Then substitute  $I_b$  from (2.41), which gives

$$E_a - (Z_1 + Z_2)I_a^1 = Z_f \frac{3I_a^1}{(a - a^2)(a^2 - a)}. \quad (2.46)$$

Due to that  $(a - a^2)(a^2 - a) = 3$ , and by solving for  $I_a^1$ , (2.46) can be expressed as

$$I_a^1 = \frac{E_a}{Z_1 + Z_2 + Z_f} \quad (2.47)$$

which gives the phase currents as

$$\begin{bmatrix} I_a \\ I_b \\ I_c \end{bmatrix} = \begin{bmatrix} 1 & 1 & 1 \\ 1 & a^2 & a \\ 1 & a & a^2 \end{bmatrix} \begin{bmatrix} 0 \\ I_a^1 \\ -I_a^1 \end{bmatrix} \quad (2.48)$$

The fault current is

$$I_b = -I_c = (a^2 - a)I_a^1. \quad (2.49)$$

From (2.43) and (2.47) it is given that the positive- and negative sequence network is connected in opposition. The result of the sequence network is shown in Figure 2.6 [1].

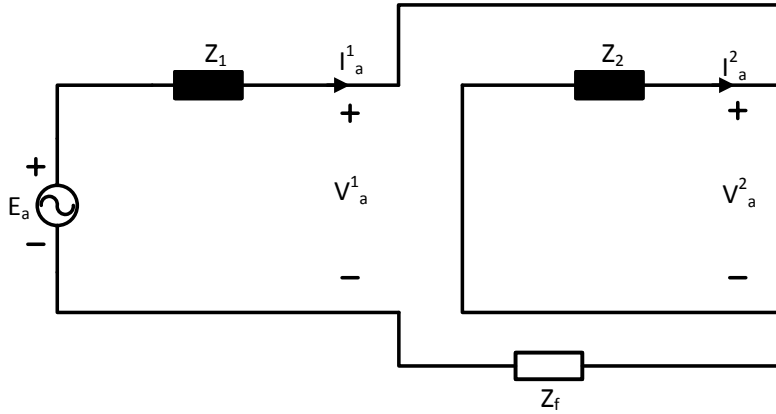


**Figure 2.6:** Line-to-Line fault sequence network

#### 2.1.4 Double Line-to-ground Fault

For a double line-to-ground fault (LLG), seen in Figure 2.7, the boundary conditions (when assuming initially no-load) is

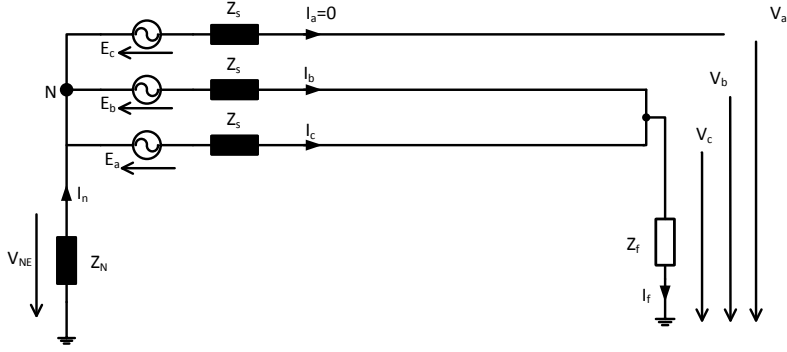


Figure 2.7: Double line-to-ground fault

$$V_b = V_c = Z_f(I_b + I_c) \quad (2.50)$$

$$I_a = I_a^0 + I_a^1 + I_a^2 = 0. \quad (2.51)$$

From the boundary conditions we have that  $V_b = V_c$  and then from (2.25) and (2.26) it can be noted that

$$V_a^1 = V_a^2. \quad (2.52)$$

If  $I_b$  and  $I_c$  are substituted for the symmetrical components, the following relation is obtained

$$\begin{aligned} V_b &= Z_f(I_a^0 + a^2 I_a^1 + a I_a^2 + I_a^0 + a I_a^1 + a^2 I_a^2) \\ &= Z_f(2I_a^0 - I_a^1 - I_a^2) \\ &= 3Z_f I_a^0. \end{aligned} \quad (2.53)$$

Then substitute (2.53) and (2.52) into (2.25)

$$\begin{aligned} 3Z_f I_a^0 &= V_a^0 + (a^2 + a)V_a^1 \\ &= V_a^0 - V_a^1. \end{aligned} \quad (2.54)$$

Substitute  $V_a^0$  and  $V_a^1$  from (2.54) with the symmetrical components in (2.15)-(2.17) and then solve for  $I_a^0$

$$I_a^0 = -\frac{E_a - Z_1 I_a^1}{Z_0 + 3Z_f}. \quad (2.55)$$

Then solve for  $I_a^2$  by substituting the symmetrical components of voltage into (2.52)

$$I_a^2 = -\frac{E_a - Z_1 I_a^1}{Z_2} \quad (2.56)$$

and to get  $I_a^1$ , substitute  $I_a^0$  and  $I_a^2$  into (2.51)

$$I_a^1 = \frac{E_a}{Z_1 + \frac{Z_2(Z_0 + 3Z_f)}{Z_2 + Z_0 + 3Z_f}}. \quad (2.57)$$

From (2.55),(2.56) and (2.57) the equivalent circuit for the sequence network can be drawn. It can be noted that the positive sequence should be connected in series with the negative sequence in parallel with the zero-sequence, shown in Figure 2.8 [1]. The fault current of a double line-to-ground fault can be presented as

$$I_f = I_b + I_c = 3I_a^0. \quad (2.58)$$

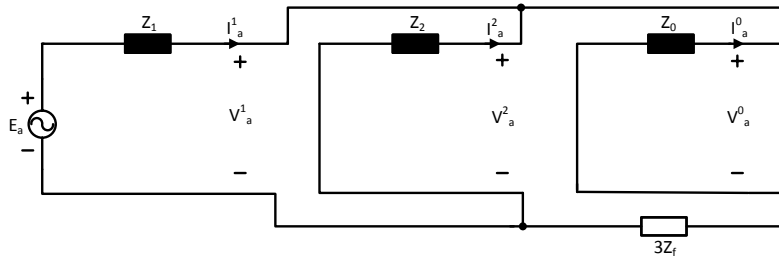


**Figure 2.8:** Double line-to-ground fault sequence network

## 2.2 Earthing Methods

### 2.2.1 Isolated Neutral System

When the system is isolated, it means that there is not any intentional connection between the system neutral and earth. But there are however capacitance between one phase and another, and between phase and earth  $X_0$ , see Figure 2.9. The capacitive coupling between two phases has a very low effect on the system earthing and can therefore be neglected.

Isolated systems are no longer recommended to use in power systems due to transient overvoltages. For an isolated system it is possible for transient overvoltages to occur all over the the system in account to recurring earth faults. It is possible for transient overvoltages to cause failure of insulation. To prevent overvoltages the system should be earthed with either a solid earth system or impedance earthing [2]. Another disadvantage, besides the high transients, is that, when a fault occurs, the voltage in the two healthy lines rises and affects the rating of the surge protective devices [3].

An advantage with an isolated system though, is that when a fault occurs, the capacitance between the lines and earth limits the fault current to be small. The current is limited to only a fraction of an ampere for small power systems and for bigger systems it can be up to tens of ampere [3].

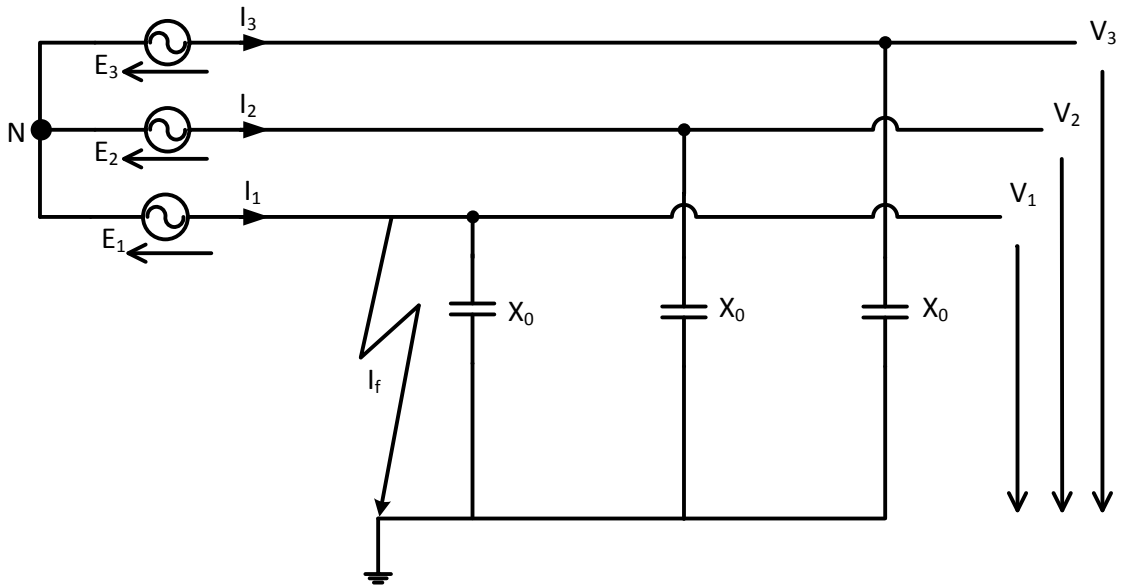


Figure 2.9: Equivalent circuit for an isolated earthed system

### 2.2.2 Solidly Neutral Earthed System

The most common earthing method that is used in industrial/commercial power systems is the solid earthing method [4] and it is recommended for systems with either a system voltage lower than 600V or higher than 15kV. [2]. Solidly earthed power systems have their neutral connected directly to ground without any intentional impedance, see Figure 2.10.

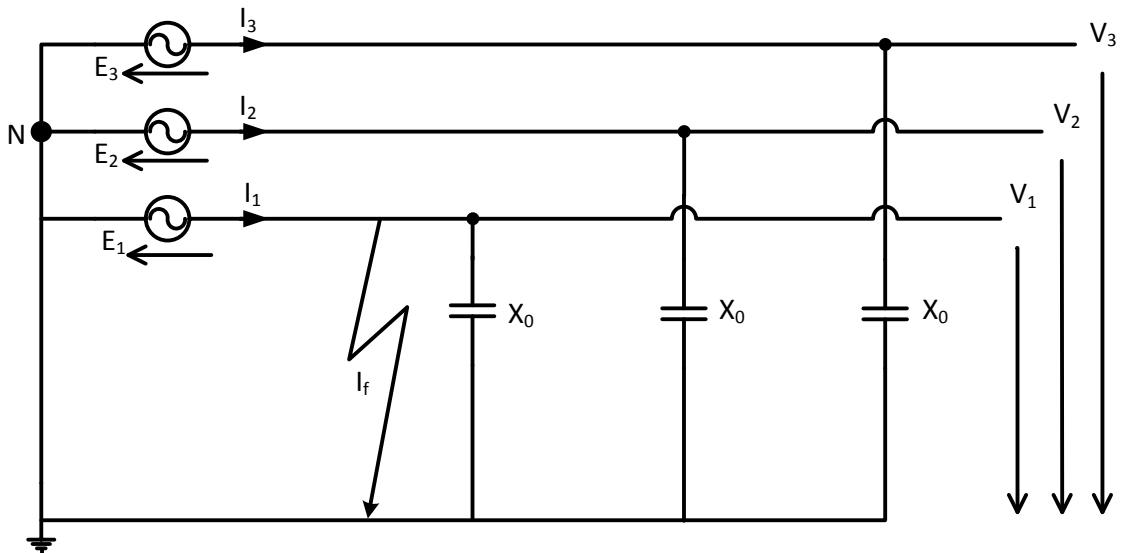


Figure 2.10: Equivalent circuit for solidly earthed system

To take advantage of the benefits of a solidly earthed system, it needs to be determined what degree of earthing is provided in the system. This can be done by comparing the magnitude of the ground-fault current to the three-phase fault current. The earth-fault current needs to be at least 60 % of the three phase-fault current to achieve an effectively earthed system. This can also be expressed in reactance and resistance. To achieve an effectively earthed system, two requirements need to be fulfilled,  $R_0 \leq X_1$  and  $X_0 \leq 3X_1$ , where  $R_0$  and  $X_0$  is the zero-sequence resistance/reactance of the generator or transformer and  $X_1$  is the positive sequence reactance. If the zero-sequence reactance is too great, compared with the positive-sequence reactance, there will be transient overvoltages in the system. If  $R_0$  is too great, the desired suppression of voltage to ground on the unfaulted phases, may be unaccomplished [2].

Normally the zero-sequence impedance of the generators and transformers, which are used in a typical power system, is much lower than the positive-sequence impedance. However, it is for some conditions possible for the zero-sequence impedance to be greater than the positive sequence impedance, e.g. if several transformers/generators (parallel connected) feed the power system [2].

With solidly earthed systems, the coefficient of grounding (COG) is below 80 %, which means that the the system has good control of overvoltages, both transients and temporary overvoltages. The COG is the ratio between line-to-earth voltage and the line voltage [3].

Due to the fact that the impedance to earth of a solidly earthed system is very small, the fault current becomes very high. This is an advantage because it makes it easy to detect it, but also disadvantage because the high current causes high stress on the equipment and it may cause voltage gradient problems [3].

### 2.2.3 Resistance Earthed System

In a resistance earthed system, there is a resistor connected between the transformer's neutral point and ground, see Figure 2.11. A resistance earthed system reduces the ground-fault-current to a manageable level due to the value of the resistor. This result in benefits as preventing damages on equipment in the electrical system, preventing arcing, lower the mechanical stress on the electrical system carrying fault currents, reduced current for expensive equipments and limiting transient overvoltages because of ground faults is limited to 250 % of the normal voltage level. There are two different methods used for resistance earthed system, low-resistance earthed and high-resistance earthed system [2][5].

With a high-resistance earthed system, the earth-fault-current is reduced to less than 10 A. The high resistance-to-earth system should be designed so that the current,  $I_R$  through the resistor is equal to or nearly greater than the total capacitive charging

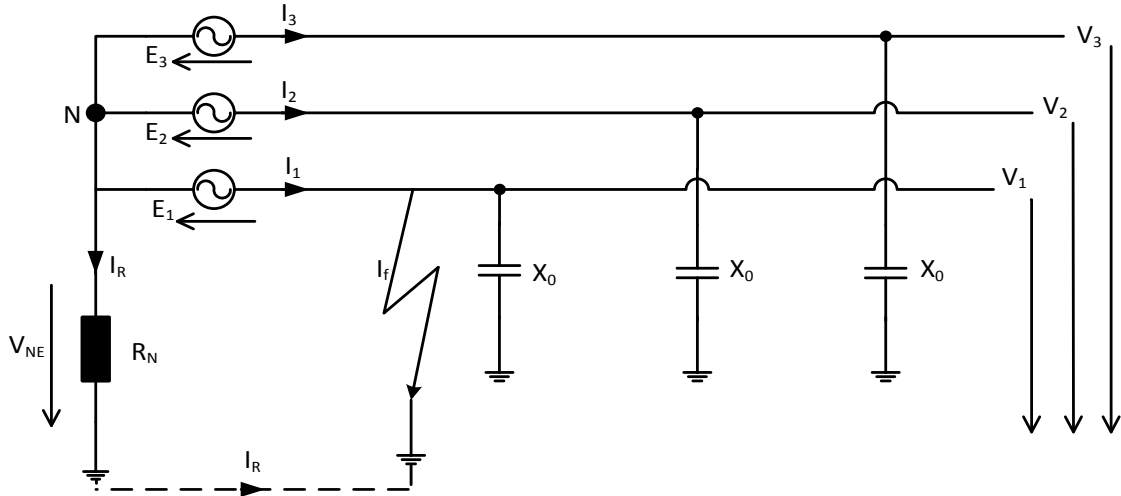


Figure 2.11: Electrical circuit for resistance earthed system

current,  $3I_0$ . The ohmic value of the resistor should be  $R_N \leq X_0/3$ , where  $X_0$  is the capacitive reactance between the phase and ground. Using high-resistance earthing has an advantage of not having to clear the fault directly due to the low fault current. This method is suitable in lower voltage systems but can also be used at some applications for medium voltage system [2][6]. In IEEE Standard 141-1993 it is stated that “*Investigations recommend that high-resistance grounding should be restricted to 5 kV class or lower systems with charging currents of about 5.5 A or less and should not be attempted on 15 kV systems, unless proper grounding relaying is employed*” [5].

Low-resistance earthing is often used in higher voltage systems compared with high-resistance earthing because it is often permitted to handle higher ground-fault-currents, normally in the range 100 – 1000 A. The impact of the charging capacitive current in this configuration can be negligible due to it affects the ground-fault current with a small percentage. Therefore, the ohmic value for the low-resistance to ground can be obtained by  $R_N = V_{NE}/I_f$ , where  $V_{NE}$  is the system line voltage to ground and  $I_f$  is the ground-fault current [2].

Low-resistance earthing has the advantage that permitting high ground-fault currents makes it easy to detect and to activates the protective system, such as overcurrent relays, which trips and disconnect the fault. Additional advantage is that compared with solid earthing it has lower fault current. The transient overvoltages can be more limited for low-resistance earthing than both resonance earthing and isolated earthing [3][7][8].

Disadvantages using low-resistance earthing is that the fault current is relatively high, which can be dangerous for both equipment and persons [3][9].

### 2.2.4 Resonance Earthed System

For electric grids with high voltages or long cable lengths, the capacitive fault currents tends to be larger and is more of concern. By using resonance earthed systems fault currents can be reduced [10]. It is possible to have a resistor in parallel with the reactor to increase the fault detection sensitivity [8].

To limit the reactive part of the line-to-ground fault current, the power system needs to be compensated with inductive reactance. This can be done by connecting a Petersen coil between the transformers' neutral point and earth. Figure 2.12 shows a simplified equivalent circuit, which is often used. Ideal symmetrical three-phase voltage sources are considered and the line resistances and inductances are negligible [11][12].

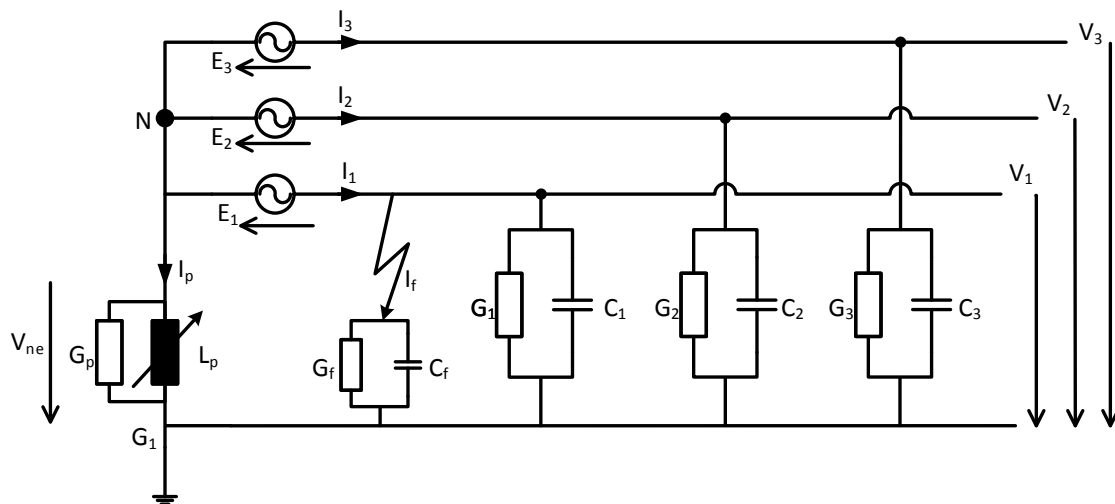


Figure 2.12: Equivalent circuit for resonant earthed system

$E_1, E_2$  and  $E_3$  represents the source voltages,  
 $V_1, V_2$  and  $V_3$  phase voltages,  
 $I_1, I_2$  and  $I_3$  phase currents,  
 $V_{ne}$  neutral-to-earth voltage,  
 $N$  neutral point,  
 $C_1, C_2$  and  $C_3$  line to earth capacitances,  
 $G_1, G_2$  and  $G_3$  line-to-earth conductances,  
 $L_p$  and  $G_p$  inductance and conductance of Petersen coil,  
 $C_f$  and  $G_f$  capacitance and conductance at fault location.

Figure 2.12 can also be represented in a single phase equivalent circuit. For derivation of that circuit, following assumptions needs to be done: 1) Line-to-earth capacitances and conductances are symmetrical, 2) the line-unbalance (capacitive and ohmic) is reduced

to phase 1 [13].

The equivalent circuit in Figure 2.12 gives following equations:

$$0 = I_p + I_1 + I_2 + I_3 \quad (2.59)$$

$$V_{ne}Y_p = I_p \quad (2.60)$$

$$(E_1 + V_{ne})Y_1 = I_1 \quad (2.61)$$

$$(E_2 + V_{ne})Y_2 = I_2 \quad (2.62)$$

$$(E_3 + V_{ne})Y_3 = I_3. \quad (2.63)$$

Now assume that  $C_1 = C_2 = C_3$ ,  $G_1 = G_2 = G_3$ ,  $G_f = \Delta G$  and  $C_f = \Delta C$ , then the following equations are obtained:

$$Y_p = G_p + \frac{1}{j\omega L_p} \quad (2.64)$$

$$Y_1 = (G + \Delta G) + j\omega(C + \Delta C) \quad (2.65)$$

$$Y_2 = Y_3 = G + j\omega G. \quad (2.66)$$

Assuming that the system is a symmetrical three phase system, the voltages can be represented as:

$$E_1 = E_1, E_2 = a^2 E_1 \text{ and } E_3 = a E_1 \quad (2.67)$$

where  $a = e^{-j120^\circ}$ . Then (2.59) can be written as:

$$0 = V_{ne}(Y_p + Y_1 + Y_2 + Y_3) + E_1(Y_1 + a^2 Y_2 + a Y_3) \quad (2.68)$$

or

$$V_{ne} = -\frac{Y_1 + a^2 Y_2 + a Y_3}{Y_p + Y_1 + Y_2 + Y_3} E_1. \quad (2.69)$$

The following equations are obtained from (2.64)-(2.66):

$$Y_1 + a^2 Y_2 + a Y_3 = \Delta G + j\omega \Delta C \quad (2.70)$$

$$Y_p + Y_1 + Y_2 + Y_3 = (3G + \Delta G) + j\omega(3C + \Delta C) \quad (2.71)$$

and by substituting (2.70) and (2.71) into (2.69), results in:

$$V_{ne} = -\frac{Y_U}{Y_u + Y_W + j(B_C - B_L)} E_1 = -\frac{Y_U}{Y_U + Y_0} E_1 \quad (2.72)$$

$$Y_0 = Y_W + j(B_C - B_L) \quad (2.73)$$

where:

$$Y_U = \Delta G + j\omega \Delta C$$

unbalance of the fault location

$$Y_W = 3G + G_p$$

active part of  $Y_0$

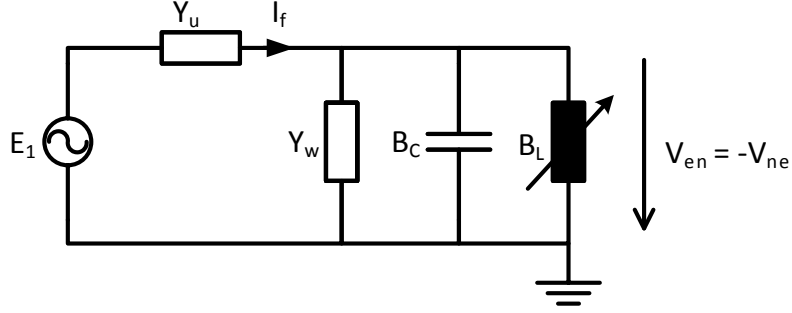


**Figure 2.13:** Single-phase equivalent circuit for resonant earthed system

$$B_C = \omega 3C \quad \text{capacitive part of } Y_0$$

$$B_L = \frac{1}{\omega L_P} \quad \text{inductive part of } Y_0.$$

From (2.72) the single-phase equivalent circuit can be represented, seen in Figure 2.13 [13]

The Petersen coil is adjustable and can be tuned in such way that the inductive current that passes through the coil compensates for the capacitive current in the earth fault. Hence the power system will be set in resonance. Usually the Petersen coil doesn't compensate for the whole fault current due to resistive losses in lines and coil. The current that remains is a residual current, which is very small, and won't be maintained. The fault will extinguish anyway [11].

When the system is in resonance, maximum inductance occurs. This happens when the imaginary part of (2.73) is equal to 0 which results at the resonance frequency:

$$\omega = \sqrt{\frac{1}{3L_P C_e}} \quad (2.74)$$

where  $C_e$  is the line-to-earth capacitance. In practice it is not preferable to obtain perfect resonance to avoid high voltages [14]. Therefore a detuning factor of 8-12 % is used. The detuning factor  $v$  is defined as

$$v = 1 - \frac{1}{3\omega^2 L_P C_e}. \quad (2.75)$$

The system also uses a damping factor defined as

$$\delta_0 = \frac{Y_W}{B_C}. \quad (2.76)$$

The zero sequence component of the impedance of the system is much greater than the positive sequence component, hence the positive component can be neglected. The admittance of the zero sequence component is defined as

$$\underline{Y}_0 = B_C(jv + \delta_0) \quad (2.77)$$

and this result in that the earth-fault current  $I_{Res}$  is obtained as

$$I_{Res} \approx \sqrt{3}U_n B_C(jv + \delta_0). \quad (2.78)$$

where  $U_n = \sqrt{3}E_1$  [13][14].

The Petersen coil can only be adjusted to one single frequency, the nominal frequency. This leads to that the harmonics increases the magnitude of the residual current when fault occurs. The capacitance of the system is constantly changing due to e.g. switching lines, which makes it harder to tune the Petersen coil, hence the Petersen coil needs to be tuned during operation to achieve resonance [12][14].

Advantages by using resonance earthing for power system is first; by reducing the capacitive current, the reactive fault current is reduced and becomes small and second; with a small reactive fault current, arcs cannot maintain themselves and are therefore extinguished [2][15].

The disadvantage with resonance earthing is that normally the Petersen coil is not adjusted for perfect resonance. If there occurs perfect resonance, there will be a high potential between earth and neutral [15]. Another disadvantage is that the transient overvoltages is less limited than the transient overvoltages in low-resistance earthing systems [8].

### 2.2.5 Earthing Transformer

In some power systems, there is no neutral point available but required. Then a zig-zag transformer is used to create an artificial neutral point. The need for this can for example be when an unearthed system needs to be upgraded to high-resistance earthing.

The impedance of the zig-zag transformer itself is low and therefore the fault current will be quite high. Hence the limit of the fault current will be decided by the resistance that is inserted. The resistance can either be inserted between the zig-zig transformer and ground, as seen in Figure 2.14, or inserted directly in the windings [16][17].

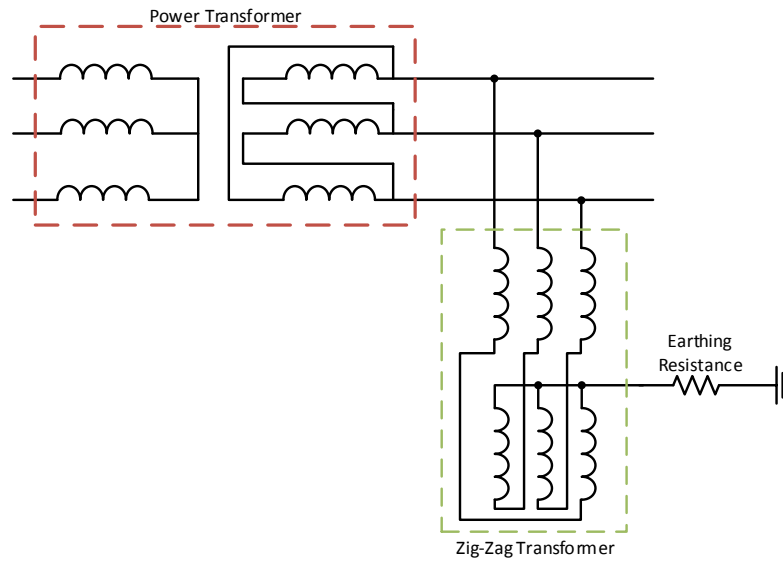


**Figure 2.14:** Equivalent circuit for a Zig-Zag earthing transformer

## 2.3 Earth Electrode

When earthing industrial and commercial power systems, there are a few things that need to be accounted for. A safe and secure solution requires planning e.g. determining the resistance to earth, deciding what kind of construction method should be used and how the earthing electrode should be installed [18].

When determining the earthing resistance of an earth electrode, there are three things that need to be taken into account:

- a) The resistance of the electrode.
- b) The contact resistance between the electrode and the soil.
- c) The resistance of the soil.

The resistance of the soil is seen outwards from the surface of the electrode. Both a) and b) are very small compared with c), hence they can be neglected. The resistance of the soil around the electrode can be seen as the sum of the series resistance of virtual shells of earth. These virtual shells are located outwards from the electrode with decreasing resistance (area of the shells increases), i.e. the shells nearest the rod have the highest resistance. In Figure 2.15 it is visualized how the increase of the resistance decreases further away from the rod [18].

The connection between the system and earth is different for each system which makes this the most important and most difficult thing about the grounding system [18].

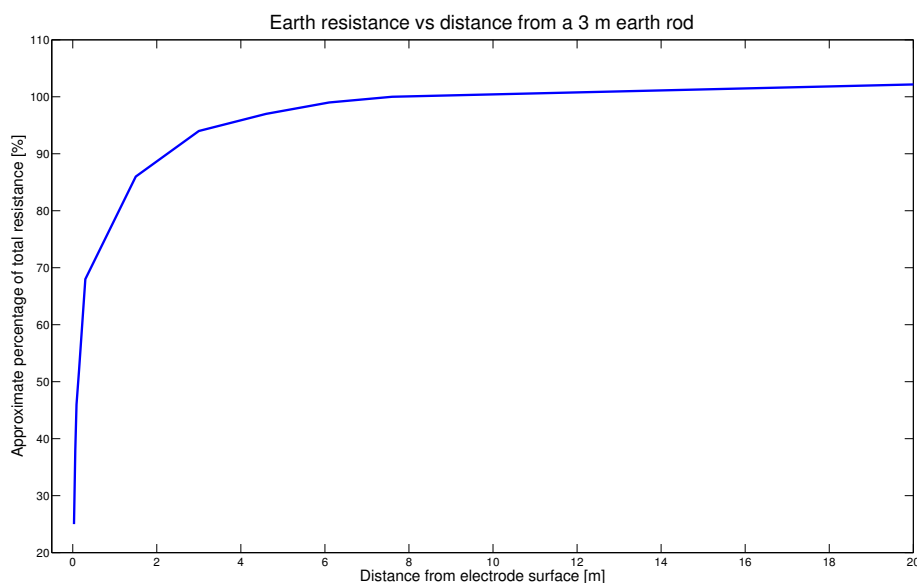


**Figure 2.15:** Earthing resistance from a certain distance from an electrode rod

It is highly recommended to investigate the resistivity of the earth where the connection is made, which can vary depending on depth, temperature and moisture etc. For personnel and equipment safety, the resistance between the connection and earth should be as low as possible. It is recommended to have a resistance between 1-5  $\Omega$  for industrial plant substations and large commercial installations [18].

There are two different methods that are often used to measure the resistivity of the earth. Which method that is best suited depends on the scope of the earthing system and the accuracy. The two different methods are:

a) Low-current method - An extra electrode is buried about 50 m from the earth electrode. Somewhere in the middle between the extra electrode and the earth electrode, a probe is buried. A current is transmitted between the two electrodes and then a voltage is measured between the earth electrode and the probe, thereafter, with Ohm's law, the resistance is calculated. The resistance is then measured both at this point and when the probe is moved in both direction [18].

b) High-current method - When using this method, the extra electrode is placed much further away from the earth electrode than in the low-current method. The electrode is placed about 10 km from the earth electrode. The extra electrode is often another earth electrode which is used in some other substation and the measuring line that is used is often an overhead line that is out of operation. An existing transformer is used as current source, but for better accuracy is preferable to use a separate current source, e.g. a

transportable diesel generator. The measurement is done with a selective voltmeter [18].

Earth electrodes can be e.g. driven electrodes or concrete encased electrodes. Driven electrode is normally a rod driven into the soil. It is usually more effective to use few rods that are buried deep instead of many short rods. For ordinary earth conditions, a rod of 3 m is a minimum standard. Concrete encased electrodes is a semi-conducting medium which has a lower resistivity than average loam soil [18].

## 2.4 Impulse Overvoltage

Impulse voltages frequently cause disturbances in power systems. These kinds of transient overvoltages have peaks much greater than the normal a.c. operating voltage. There are two kinds of transient voltages, lightning overvoltages and switching overvoltages. The shape of a lightning impulse can be seen in Figure 2.16 [19].

Lightning overvoltages are caused by lightning strokes that hit the overhead lines or the busbars of outdoor substations. The amplitude of these voltages are very high, often above 1000 kV or more which injects a high current in to the system. The currents are in the order of 100 kA and sometimes even greater. The traveling wave that occurs by the lightning is very steep and may stress the insulation of the power transformers or other equipment. The front time for the lightning wave,  $T_f$ , is  $1.2 \mu\text{s} \pm 30 \%$  and time to half,  $T_2$ , is  $50 \mu\text{s} \pm 20 \%$ . The lightning impulses are referred as 1.2/50  $\mu\text{s}$  waves. The front time is defined as  $T_2 * 1.67$ . To damp the high voltage transients, power systems

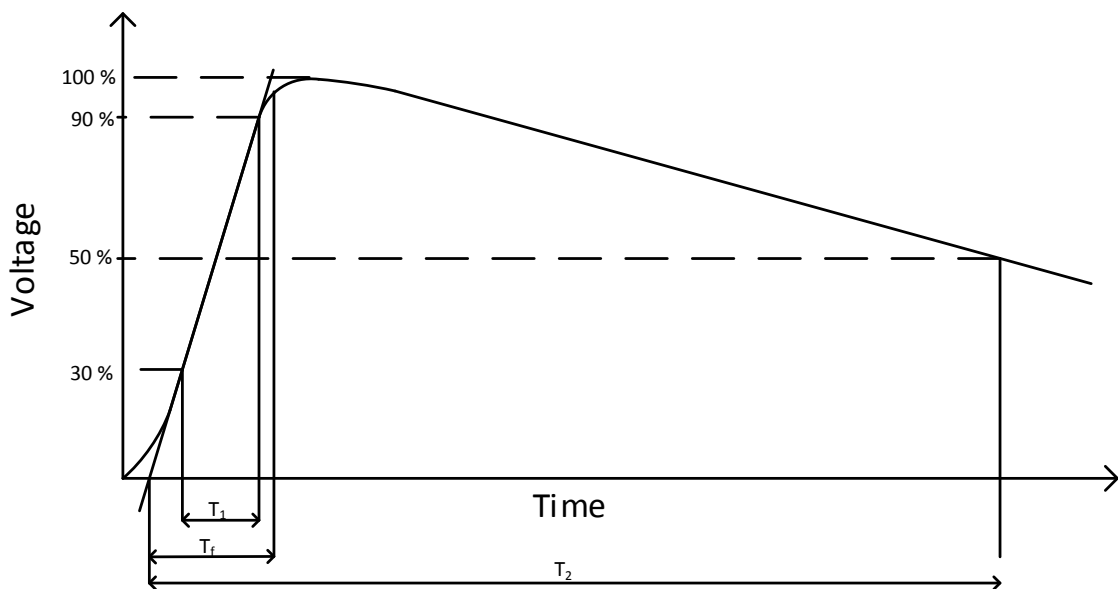
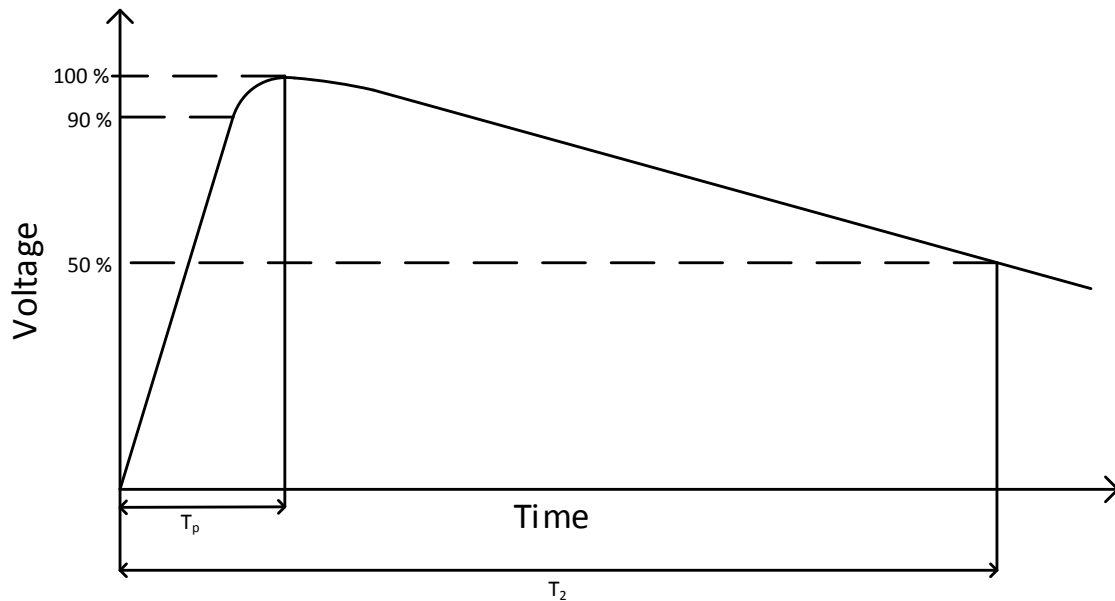


Figure 2.16: General shape of a lightning impulse



**Figure 2.17:** General shape of a switching impulse

are equipped with surge arresters to distort the traveling waves [19]. According to [20], a power system with voltage level of 36 kV should be able to handle a 1.2/50  $\mu$ s impulse with a maximum voltage of 170 kV.

Switching overvoltages has a wave shape as shown in Figure 2.17. These overvoltages doesn't have amplitudes as great as the lightning overvoltages. The switching transients are related to the operating voltage and the shape of the wave is directly influenced by the impedance of the system and the switching conditions. The front of the switching overvoltages are usually flatter than the lightning wave but can still be very dangerous to the insulation of the system, especially in power systems with a rated voltage greater than 245 kV. The time to peak,  $T_p$ , of a standard switching impulse is 250  $\mu$ s  $\pm$  20% and time-to-half,  $T_2$  is normally 2500  $\mu$ s  $\pm$  60% [19].

# 3

## Electrical Regulations and Standards

In Europe, regulations and standards can vary between countries. Many countries are following the standards and regulations published by the European Committee for Electrotechnical Standardization. In Sweden, all design and construction of power installation should comply with regulations and standards that are issued for safe operation and protection of people. In order to achieve a more secure power installation a proper system earthing should be performed according to the regulations and standards published by the Swedish Electrical Authority, Els akerhetsverket and Swedish Electric Standard, Svensk elstandard.

The Swedish Electrical Authority, Els akerhetsverket, has published some regulations regarding electrical safety of power installations for up to 25 kV. Some of these regulations are published in the document ELS AK FS-2008:1, *“Electrical Safety Authority’s regulations and general advice on how electrical installations shall be designed”*, but there are no clear regulations and guidelines how to perform electrical safety for power installations over 25 kV [21].

Swedish Electric standard, Svensk elstandard, has published two documents, *“SS 421 01 01, Power installation exceeding 1 kv a.c.”* and *“SS-EN 50522:2010 Earthing of power installations exceeding 1 kV a.c.”*, both containing import standards regarding system earthing for power installations [22][23].

It is stated in the document ELS AK FS-2008:1 that the protection system for a high-voltage system that is not solidly earthed and containing an overhead line should have high sensitivity to detect earth faults. The protection system should be able to secure faults with a fault resistance up to 5000 ohms. Furthermore, within an electrical installation that exceeds 25 kV and using a common system earthing, the touch voltage should

not exceed 100 V without automatically being disconnected within 2-5 seconds [22].

When system earthing is performed in power installations, such as a wind farm, the requirements from the Swedish Electrical Authority and Swedish Electric Standard should be followed to maintain high electrical safety and safe operation.

# 4

## Mapping of Wind Farms

### 4.1 Survey Methodology

The reason for this survey is to give an insight of what kind of system earthing is used for wind farms around Europe. Companies that operate or own the wind farms were contacted and asked the following questions:

- Which level has the system voltage of the collector grid at the wind farm?
- Which method for system earthing is used in the wind farm?

This information led to an overview of what kind of system earthing methods that are most common. The survey answered the following questions:

- Which is the most common method for system earthing in Europe?
- Which is the most common method for system earthing in Sweden?
- What are the pros and cons regarding the most common method?

How extensive the survey becomes, is directly dependent on how many companies that are willing to participate. To understand the advantages and disadvantages with each method, there was literature studies and simulations in PSCAD for the different methods.

### 4.2 Selection of Wind Farms

The companies that are selected are chosen because of their size in wind energy. The wind farms selected have at least 10 wind turbines and have a collector grid with a voltage level of 36 kV. The wind farms have different geographical locations. Both onshore and offshore wind farms are investigated to see if there are any differences in system earthing.

There are a lot of databases available with information regarding both offshore and onshore wind farms across Europe and also in Sweden. These databases contain information regarding companies owning wind farms, which are appropriate to contact for information regarding system earthing [24][25][26].

From these databases a number of companies, which operate wind farms, in different countries have been contacted. For this study, it is not important which company has what kind of earthing system, but what kind earthing system is used in what country. In Table 4.1 it is presented how many wind farms were contacted for the different countries.

**Table 4.1:** Wind farms in different countries across Europe who have been contacted

| Country        | Wind farms |
|----------------|------------|
| Sweden         | 22         |
| Austria        | 4          |
| Belgium        | 6          |
| Bulgaria       | 1          |
| Croatia        | 1          |
| Cyprus         | 1          |
| Czech Republic | 3          |
| Denmark        | 5          |
| Estonia        | 2          |
| France         | 2          |
| Germany        | 21         |
| Greece         | 2          |
| Italy          | 3          |
| Lithuania      | 1          |
| Netherlands    | 4          |
| Norway         | 4          |
| Poland         | 7          |
| Portugal       | 8          |
| Romania        | 1          |
| Spain          | 15         |
| United Kingdom | 34         |

# 5

## Description of the wind farm

The wind farm that is simulated is based on a small wind farm in Sweden. It consists of two parts, Part A and Part B with four and six wind turbines with a mutual collection grid. The wind farm is connected to a distribution network.

### 5.1 Technical specification

The wind farm has a total capacity of 23 MW. Both parts of the wind farm consist of Enercon E-82 wind turbines, where each turbine has a rated power of 2.3 MW. They have a rotor diameter of 82 meter and have three blades. Each turbine generates an internal voltage of 0.4 kV and are equipped with a turbine transformer rated 33/0.4 kV, Dyn5-coupled, with a rated apparent power of 2500 kVA. The turbines are connected in two radials for each part of the wind farm.

The design voltage of the collector grid is 36 kV and the collector grid from Part A and Part B is connected into a mutual connection point. Thereafter, it is connected to a 77/33 kV-transformer, YNyn0-coupled, located in the substation before reaching the distribution network. The 33 kV-collector grid contains both underground cables with different geometries and transmission lines. An overview can be seen in Figure 5.1.

The length of the inter array underground cables in Part A and Part B can be seen in Table 5.1. Thereafter, there is a distance of 12 kilometers of transmission lines, to the transition point before it in the transition point switches to 7 kilometers of underground cables. The underground cables are then connected to the substation. In Table 5.1 it can be seen what type of cable is used between different locations and the length of the cable.

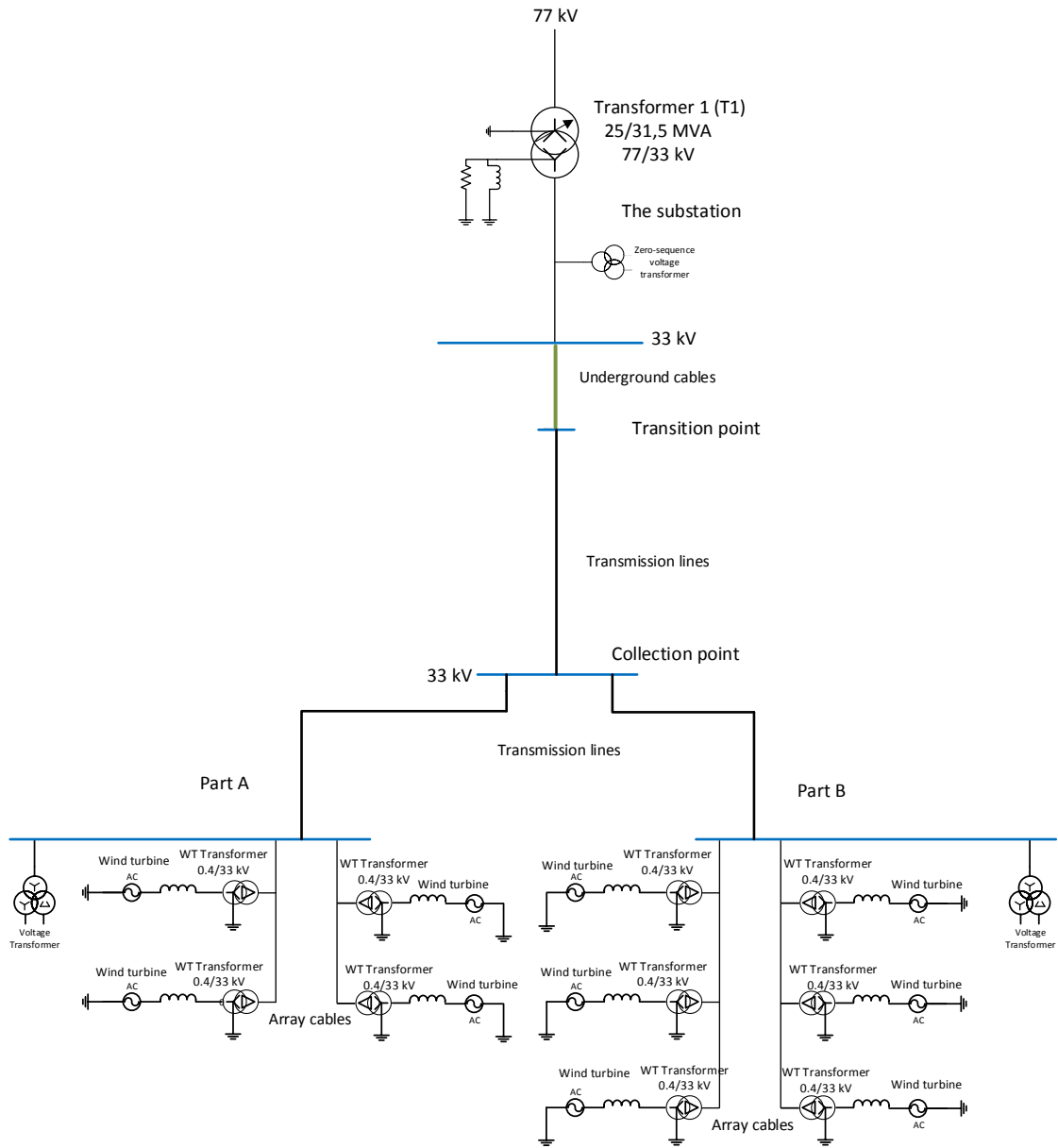


Figure 5.1: Single line diagram of the wind farm

**Table 5.1:** Cable list of the wind farm

| Location                            | Type of cable                          | Cable length [km] |
|-------------------------------------|--|-------------------|
| Substation - Transition point       | AXLJ-TT 36 kV, 3x1x500 mm <sup>2</sup> | 7                 |
| Transition point - Connection point | AL59, 3x1x241 mm <sup>2</sup>          | 9                 |
| Connection point - Part B           | AL59, 3x1x241 mm <sup>2</sup>          | 3                 |
| Connection point - Part A           | AL59, 3x1x241 mm <sup>2</sup>          | 3                 |
| Array cables 1, Part A              | AXLJ-TT 36 kV, 1x3x95 mm <sup>2</sup>  | 1.3               |
| Array cables 1, Part B              | AXLJ-TT 36 kV, 1x3x95 mm <sup>2</sup>  | 2.4               |
| Array cables 2, Part A              | AXLJ-TT 36 kV, 1x3x95 mm <sup>2</sup>  | 1                 |
| Array cables 2, Part B              | AXLJ-TT 36 kV, 1x3x95 mm <sup>2</sup>  | 2.9               |

## 5.2 System earthing of the wind farm

The wind farm consists of two different system earthing methods depending of the voltage level, solidly earthed and resonance earthed system, which can be seen in Figure 5.1.

The 0.4 kV-system is earthed through the 33/0.4 kV-transformers, which is Dyn5-coupled. The transformer coupling indicates that the LV-voltage side are solidly earthed, see Figure 2.10. Although the system is separated for each turbine, they are interconnected through cable screens and earth electrodes at the 0.4 kV-side.

The 33 kV-collector grid of the wind farm is earthed through the LV-side of the 77/33 kV-transformer, YNyn0-coupled, with resonance earthed system consisting of a high-ohmic resistance and a reactor, see Figure 2.12. The high-ohmic resistance is dimensioned to a current of 10 A, which from equation

$$R = \frac{33000}{\sqrt{3} * 10} \approx 1900 \Omega \quad (5.1)$$

results in an ohmic value of 1900  $\Omega$ . The reactor is dimensioned for a current,  $I$ , of 10-100 A. The inductance can be calculated by

$$L = \frac{33000}{\sqrt{3} * I * 2\pi * 50} \quad (5.2)$$

and can be varied between  $L = 0.6065 - 6.065$  H.

The HV-side of the 77/33 kV-transformer is solidly earthed.

## 5.3 Protection of the wind farm

The power system in the wind farm is protected with protection relays, surge arresters and breakers. They should be configured according to Swedish regulations and standards.

The protection system in the substation is measuring the zero sequence voltage with a voltage transformer in between the 77/33 kV-transformer and the 33 kV-busbar, which can be seen in Figure 5.1, to determine if the relays needs to activate and trip the lines.

In accordance with the regulations in chapter 3 the protection equipment should be able to detect a fault current ( $I_f$ ) for a fault impedance of 5000  $\Omega$ , which can be calculated by

$$I_f \approx \frac{33000}{\sqrt{3}(5000 + 1900)} \approx 2.7 \text{ A} \quad (5.3)$$

and result in  $I_f = 2.7$  A.

The surge arrester that are used in the wind farm is MWK27K4. The energy capability is  $5.5 \text{ kJ/kV} \cdot 27 \text{ kV} = 148.5 \text{ kJ}$ , where 27 kV is the operating voltage when the surge arrester starts to conduct.

## 5.4 Earth resistance

The earth resistance in the stations Part A and Part B were measured to  $6.3 \Omega$  and  $22 \Omega$ . Both were measured with the high-current method, which is described in chapter 2.3.

For each wind turbine foundation there is a representative earth resistance. It consists of the resistance of six driven earth rods in the tower that are buried to the ground and connected in an earth ring to a common earth terminal. The earth electrode is buried a short distance from the tower and connected to the earth terminal, see Figure 5.2.

It is stated in the regulations in chapter 3 that for electrical installations with greater voltage than 25 kV, the touch voltage should not exceed 100 V with common system earthing. To achieve this requirement with a fault current of 2.7 A, the earth resistance should not be higher than  $37 \Omega$ , which is calculated by

$$R = \frac{100}{2.7} = 37 \Omega. \quad (5.4)$$

If the earth resistance should exceed  $37 \Omega$  the touch voltage will be higher than 100 V and the electrical installation will not be considered as safe.

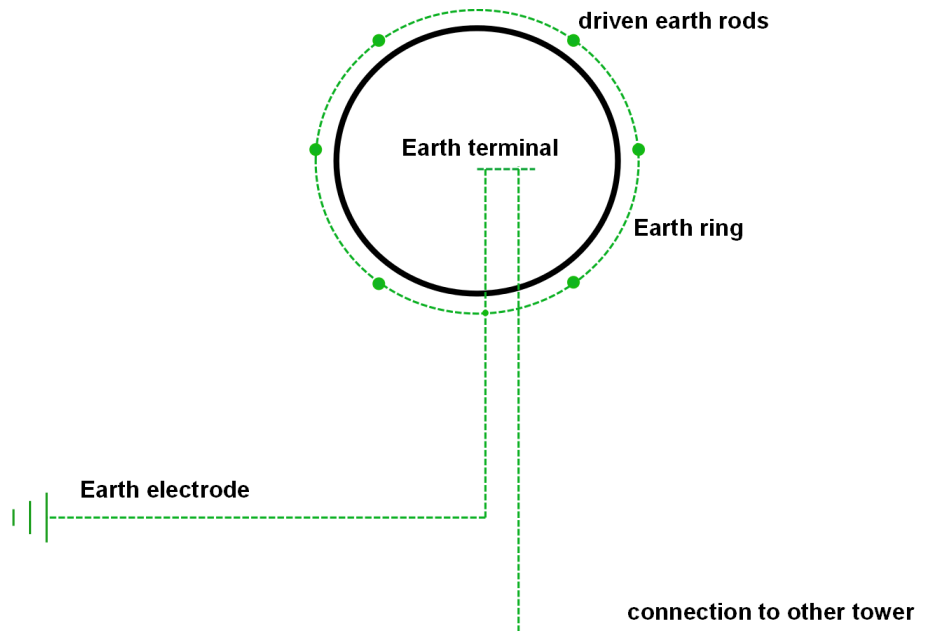


**Figure 5.2:** Earthing of the wind turbine foundation

# 6

## Modeling

### 6.1 Introduction to PSCAD/EMTDC

The simulation program that will be used is PSCAD/EMTDC. PSCAD stands for Power Systems Computer Aided Design and is the graphical user interface, which allows the user to construct schematic circuits, run simulations, and analyze the result. EMTDC stand for Electromagnetic Transients including DC and is an electro-magnetic transient simulation engine. In the following, PSCAD/EMTDC will be referred as PSCAD.

PSCAD includes a lot of different features from simple passive elements, e.g. resistors, inductors and capacitors to more complex models, such as FACTS devices and electric machines [27].

### 6.2 Cables

In PSCAD, cables can be modeled by using the input parameters of their geometry, electrical properties and changing the depth and the horizontal position of the cables in ground. Cables behave different at varying frequencies. Thus, the cables will be modeled as frequency dependent in PSCAD. Two types of coaxial cables can be modeled, one separated coaxial cable model or one model with a collection of coaxial cable within a pipe conductor, which can be used to model three-phases in a coaxial cable, see Figure 6.1. For both types of the cable can the number of conductive, semi-conductive and insulating layers be varied. Each conductive layer is separated with an insulating layer.

The first layer,  $R_0$  is the radius of the conductor. The second layer,  $R_1$  is the thickness of the insulating material. The third layer,  $R_2$  is the radius of the second conductor. The fourth layer,  $R_3$  is the thickness of the second insulating material. The permittivity of the insulating material can be modified to change the behaviour of the cable and is set to 2.3, which is permittivity for PEX cables. Properties and geometric parameters

of the cable can be found in data sheets from manufacturers.

It can be seen in Table 6.1 which settings of the parameters are used for the two different cables for the model in PSCAD.

**Table 6.1:** Settings of the cables in PSCAD

| Parameters for the cable            | radius [mm] | Type       |
|-------------------------------------|-------------|------------|
| <b>AXLJ-TT 18/30(36 kV) 3-phase</b> |             |            |
| $R_0$                               | 5.5         | Conductor  |
| $R_1$                               | 8.3         | Insulation |
| <b>AXLJ-TT 18/30(36 kV)</b>         |             |            |
| $R_0$                               | 12.6        | Conductor  |
| $R_1$                               | 10          | Insulation |
| $R_2$                               | 0.5         | Conductor  |
| $R_3$                               | 3           | Insulation |

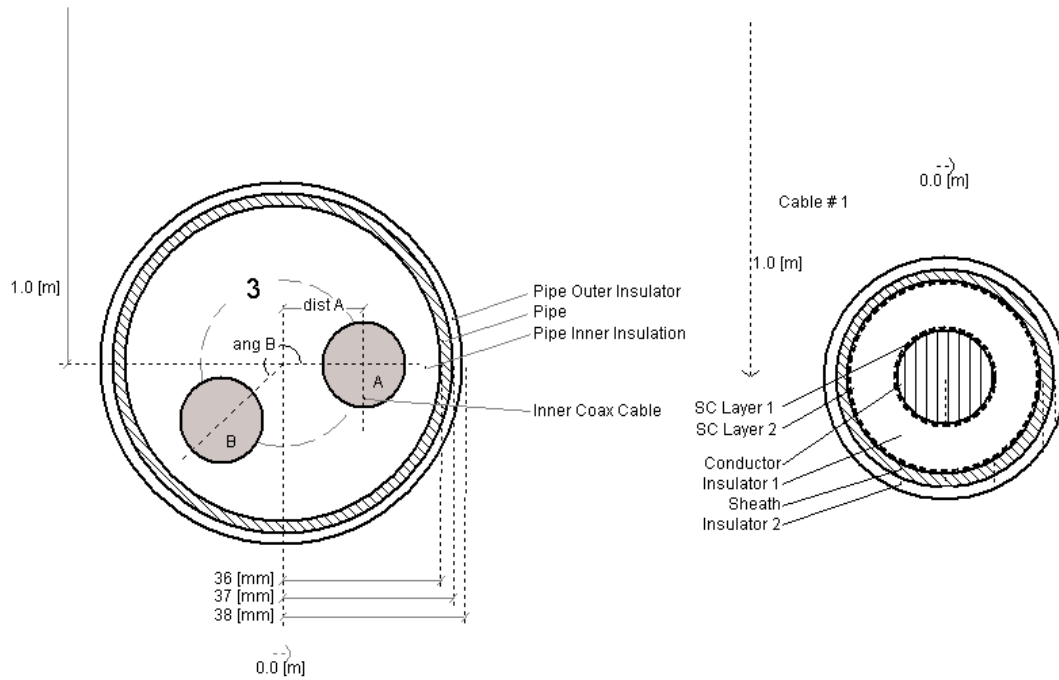


**Figure 6.1:** Example of coaxial cables in PSCAD

### 6.3 Overhead lines

Different pole configurations can be modeled in PSCAD for overhead lines. An overhead line with three conductors with the horizontal spacing between phases,  $d$ , and height above ground,  $h$ , can be seen in Figure 6.2. The behaviour of the overhead line can be modeled by configuring the input parameters,  $h$ ,  $d$ , total number of strands, radius and thickness of the conductors. This to achieve a correct model of the overhead line. It can be seen in Table 6.2 which settings of the parameters are used for modeling in PSCAD.

**Table 6.2:** Settings of the transmission line in PSCAD

| Input parameters for PSCAD        |                 |       |
|-----------------------------------|-----------------|-------|
| Height ( $h$ )                    | [m]             | 12    |
| Distance between phases ( $d$ )   | [m]             | 1.4   |
| Total number of strands           |                 | 19    |
| Total number of outer strands     |                 | 12    |
| Outer radius                      | [mm]            | 10.05 |
| Strand radius                     | [mm]            | 2.01  |
| DC Resistance of entire conductor | [ $\Omega$ /km] | 0.123 |
| Length                            | [km]            | 12    |

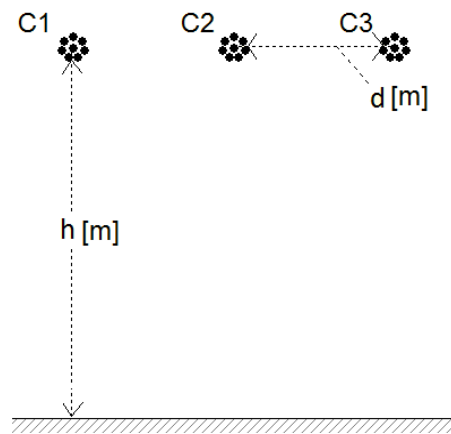


**Figure 6.2:** Overhead line with pole configuration, "Line Constants 3 Conductor Flat Tower" without earth wires in PSCAD.

## 6.4 Wind turbine and transformers

Each wind turbine and the including transformer is modeled as a voltage source with a source inductance connected to a 33/0.4 kV-transformer, see Figure 6.3. The voltage source is modeled as an ideal sinusoidal wave. The value of the inductance is set to  $L = 0.1224$  mH, which represents the inductance for the wind turbine. The value of the inductance for the wind turbine was given for a generator in PSCAD. The LV-side of the transformer is solidly earthed.

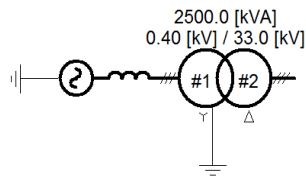


**Figure 6.3:** Model of a voltage source and a 33/0.4 kV-transformer in PSCAD.

## 6.5 77/33 kV-transformer

The 77/33 kV-transformer is modeled as a transformer with stray capacitances, see Figure 6.4. This is due to that the model needs to take into consideration high frequency transients from one side of the transformer to the other, which may occur for switching- or lightning impulses. The values of the stray capacitances,  $C$  can vary between different transformers but following values are used,  $C_{HV} = 3$  nF,  $C_{LV} = 10$  nF, and  $C_{HV-LV} = 10$  nF [28].

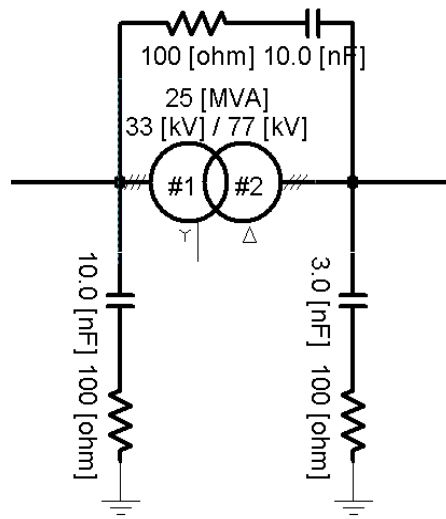


**Figure 6.4:** Model of a 77/33 kV-transformer in PSCAD.

## 6.6 Utility grid

The distribution grid after the 77/33 kV-transformer in the system is modeled as a three-phase voltage source behind an impedance and together representing the utility grid in PSCAD, see Figure 6.5. The grid impedance, also called short-circuit impedance is equal to

$$Z_k = R + jX = 0.68 + j6.78 \Omega. \quad (6.1)$$

The value of the grid impedance was provided from the supervisors of this thesis. The value of the impedance represents the strength of the utility grid. A smaller value of the impedance indicates a stronger grid. Therefore, the grid is weaker if it has a low short-circuit current. The short-circuit current is often used in many cases to describe the strength of the grid. Theoretically, the strongest grid would occur if the short-circuit impedance is equal to zero. Then the short-circuit current would be infinite.



**Figure 6.5:** Utility grid represented by a voltage source and impedance in PSCAD.

### 6.7 Impulse overvoltages

Impulse overvoltages are modeled by a voltage source in series with the phase that is going to be subjected to the voltage pulse. The model in Figure 6.6 was used in order to ensure that the voltage pulse has the right characteristic. This circuit is available in PSCAD but with a current source instead of a voltage source.

$$B = [A]e^{[B]x} = 630e^{-1666666.6t} \tag{6.2}$$

$$F = [A]e^{[B]x} = 630e^{-20000t} \tag{6.3}$$

These equations are used to achieve an amplitude of 630 kV. To achieve an amplitude of 1 MV, 1070 is used instead of 630.

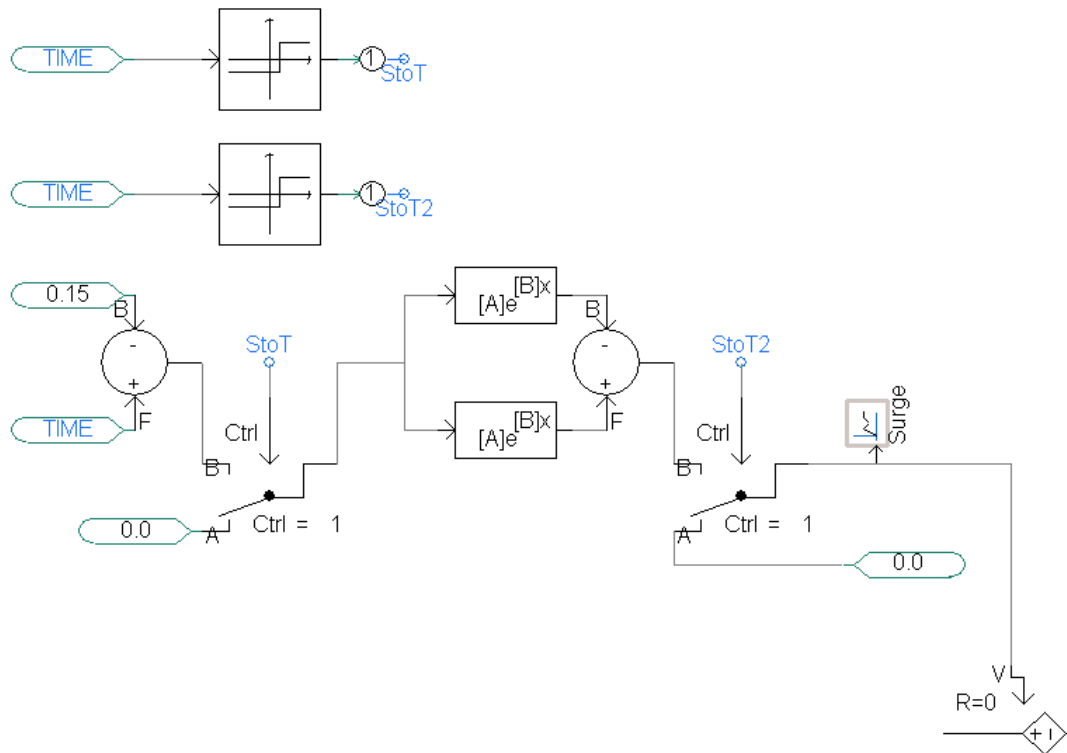


Figure 6.6: Modeling of impulse overvoltage in PSCAD

# 7

## Simulations

The most common methods of system earthing are low-resistance in Europe and resonance earthing in Sweden, see the results in Chapter 8.1. Therefore, these two methods are used for the simulations. The wind farm that the simulations are based on is described in Chapter 5 and the PSCAD-model can be seen in Appendix A.

Low-resistance and resonance system earthing will be used in the simulation to see the behavior of transient overvoltages and fault current for the power system during different type of faults. To simulate and study how different fault scenarios, applied at different locations in the 33 kV-collector grid, would affect the voltage and the system earthing in the power system, certain buses were selected as fault locations. The selected fault locations were the connection point, the transition point and the substation.

Many types of faults can occur in a power system. In this study, line-to-ground faults, line-to-line faults and impulse overvoltages are simulated. A fault impedance of  $1 \Omega$  is used in the simulations for SLG-faults and LLG-faults. For LL-faults a fault impedance of  $0.01 \Omega$  is used. Voltage reduction and transient overvoltages caused by different faults scenarios and the faults impact from the utility grid have been simulated.

Lightning impulses will be simulated to investigate how well surge arresters perform depending on the earth electrode. These simulations will only be performed while using resonance earthing. The lightning impulse occurs at the utility grid, which can be seen in the model in Appendix A, Figure 3.

The fault scenarios that are simulated are

- Single line-to-ground faults (SLG)
- Line-to-line-to-ground faults (LLG)
- Line-to-line faults (LL)

- Impulse overvoltages

The simulations that are performed are presented in both tables and figures for each case. Maximum transient overvoltages, voltage reduction, voltage level for the phases and the fault currents for the power system are presented for each simulation.

In Figure 1-3 in Appendix A, it can be seen where all the measurement points are located in the model during all the simulations. The phases in all the figures in the simulations have different colors, phase  $a$  is equal to blue, phase  $b$  is equal to green and phase  $c$  is equal to red.

## 7.1 Low-resistance earthing

The low-resistance earthing was set to  $20 \Omega$ . This value was used because of some wind farms in the survey indicated that they have low-resistance earthing about  $20 \Omega$ . The result from the simulation due to different applied faults at different locations in the 33 kV-collector grid, can be seen in Table 7.1 and Figure 7.1-7.9. The fault is applied at  $t = 0.15$  s and the duration of the fault is set to  $t = 0.1$  s. The SLG-fault occurs on phase  $b$ , LL-fault and LLG-fault is between phase  $a$  and phase  $c$ .

The maximum fault current has a value of  $|I_f| = 1.27$  kA. This is during a SLG-fault located at the substation, which can be seen in Table 7.1 and Figure 7.1.

The maximum transient overvoltage is during a SLG-fault located at the substation and is equal to  $-60.0$  kV. For LLG-fault and LL-fault the highest transient overvoltages occurs at the substation and is equal to  $-57.2$  kV respectively  $-56.5$  kV, which can be seen in Figure 7.1, Figure 7.4 and Figure 7.7.

SLG-faults causes a voltage rise for the collector grid for phase  $a$  and phase  $c$  on all fault locations, this can be seen in Table 7.1 and Figure 7.1-7.3.

LLG-faults causes a voltage rise on phase  $b$  to a maximum of  $U_b = 39.9$  kV during faults located at the substation, this can be seen in Table 7.1 and Figure 7.4.

LL-faults applied at the substation causes biggest voltage reduction on the utility grid for phase  $a$ ,  $U_a = 9.2$  kV. This can be seen in Table 7.1 and Figure 7.7. The voltage level for the fault phases are reduced during a LL-fault. Furthermore, The fault phases are during this type of fault in phase and at the same voltage level, which can be seen in Figures 7.7-7.9.

The SLG-fault has low impact on the voltage level of the utility grid according to Figure 7.1-7.3. Both LLG-and LL-faults reduces the voltage on phases and causes the utility grid to become unbalanced, this can be seen in Figure 7.4-7.5 and Figure 7.7-7.8. The

**Table 7.1:** The peak value of voltage levels and fault current during faults at different locations with low-resistance earthing.

| Fault            | Fault location   | Fault current [kA] | Voltage level [kV] |            |             |              |
|------------------|------------------|--------------------|--------------------|------------|-------------|--------------|
|                  |                  |                    | Grid               | Substation | 33k Source  | Wind turbine |
| SLG              | Substation       | 1.27               | $U_a=62.6$         | $U_a=46.2$ | $U_a=44.9$  | $U_a=0.31$   |
|                  |                  |                    | $U_b=63.5$         | $U_b=1.27$ | $U_b=1.5$   | $U_b=0.31$   |
|                  |                  |                    | $U_c=61.4$         | $U_c=44.3$ | $U_c=44.6$  | $U_c=0.31$   |
|                  | Transition point | 1.13               | $U_a=62.6$         | $U_a=45.6$ | $U_a=44.7$  | $U_a=0.31$   |
|                  |                  |                    | $U_b=63.1$         | $U_b=5.9$  | $U_b=1.55$  | $U_b=0.31$   |
|                  |                  |                    | $U_c=61.3$         | $U_c=39.6$ | $U_c=43.3$  | $U_c=0.31$   |
| Collection point | 0.94             | $U_a=62.6$         | $U_a=44.7$         | $U_a=44.7$ | $U_a=0.32$  |              |
|                  |                  | $U_b=62.3$         | $U_b=15.7$         | $U_b=0.9$  | $U_b=0.26$  |              |
|                  |                  | $U_c=61.2$         | $U_c=30.15$        | $U_c=36.9$ | $U_c=0.31$  |              |
| LLG              | Substation       | 0.65               | $U_a=34.8$         | $U_a=12.4$ | $U_a=14.0$  | $U_a=0.21$   |
|                  |                  |                    | $U_b=45.2$         | $U_b=39.9$ | $U_b=39.2$  | $U_b=0.35$   |
|                  |                  |                    | $U_c=66.6$         | $U_c=12.9$ | $U_c=12.9$  | $U_c=0.2$    |
|                  | Transition point | 0.6                | $U_a=42.4$         | $U_a=12.6$ | $U_a=10.9$  | $U_a=0.23$   |
|                  |                  |                    | $U_b=54.8$         | $U_b=38.5$ | $U_b=38.9$  | $U_b=0.32$   |
|                  |                  |                    | $U_c=61.1$         | $U_c=16.5$ | $U_c=7.2$   | $U_c=0.11$   |
| Collection point | 0.51             | $U_a=55.9$         | $U_a=16.0$         | $U_a=2.47$ | $U_a=0.25$  |              |
|                  |                  | $U_b=60.4$         | $U_b=36.2$         | $U_b=38.1$ | $U_b=0.29$  |              |
|                  |                  | $U_c=61.2$         | $U_c=25.3$         | $U_c=2.56$ | $U_c=0.035$ |              |
| LL               | Substation       | 0                  | $U_a=9.2$          | $U_a=13.3$ | $U_a=11.6$  | $U_a=0.26$   |
|                  |                  |                    | $U_b=54.6$         | $U_b=26.7$ | $U_b=26.0$  | $U_b=0.28$   |
|                  |                  |                    | $U_c=54.0$         | $U_c=13.5$ | $U_c=14.4$  | $U_c=0.02$   |
|                  | Transition point | 0                  | $U_a=38.2$         | $U_a=18.0$ | $U_a=12.0$  | $U_a=0.26$   |
|                  |                  |                    | $U_b=57.1$         | $U_b=26.7$ | $U_b=25.9$  | $U_b=0.28$   |
|                  |                  |                    | $U_c=57.8$         | $U_c=18.9$ | $U_c=14.0$  | $U_c=0.02$   |
| Collection point | 0                | $U_a=52.7$         | $U_a=22.8$         | $U_a=12.9$ | $U_a=0.27$  |              |
|                  |                  | $U_b=59.8$         | $U_b=26.8$         | $U_b=25.9$ | $U_b=0.27$  |              |
|                  |                  | $U_c=60.8$         | $U_c=23.6$         | $U_c=13.1$ | $U_c=0$     |              |

smallest impact on the utility grid is during faults applied at collection point, which can be seen in Figure 7.6 and Figure 7.9.

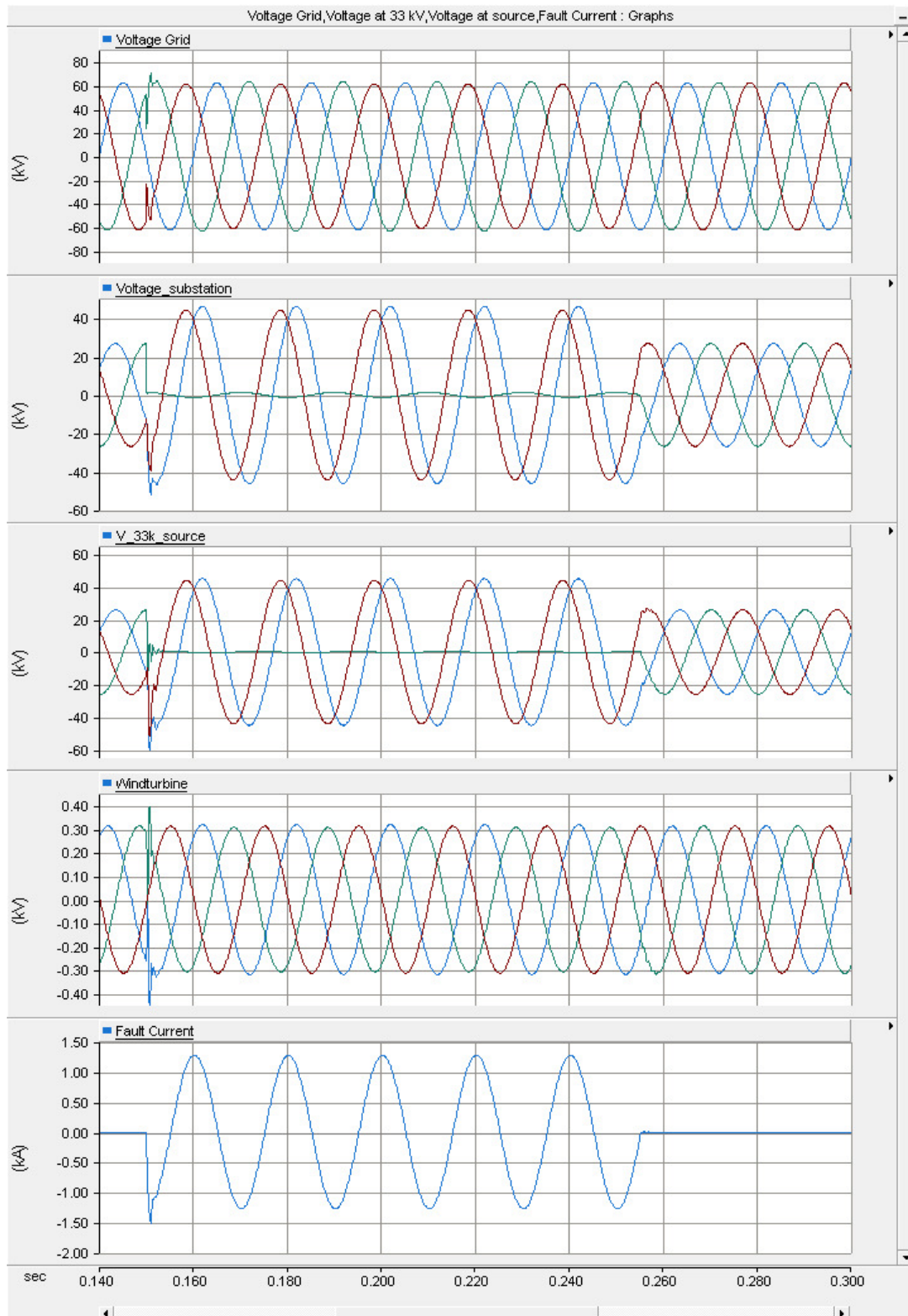


**Figure 7.1:** Voltages and fault current during an SLG-fault that occurs at the substation for low-resistance earthing.

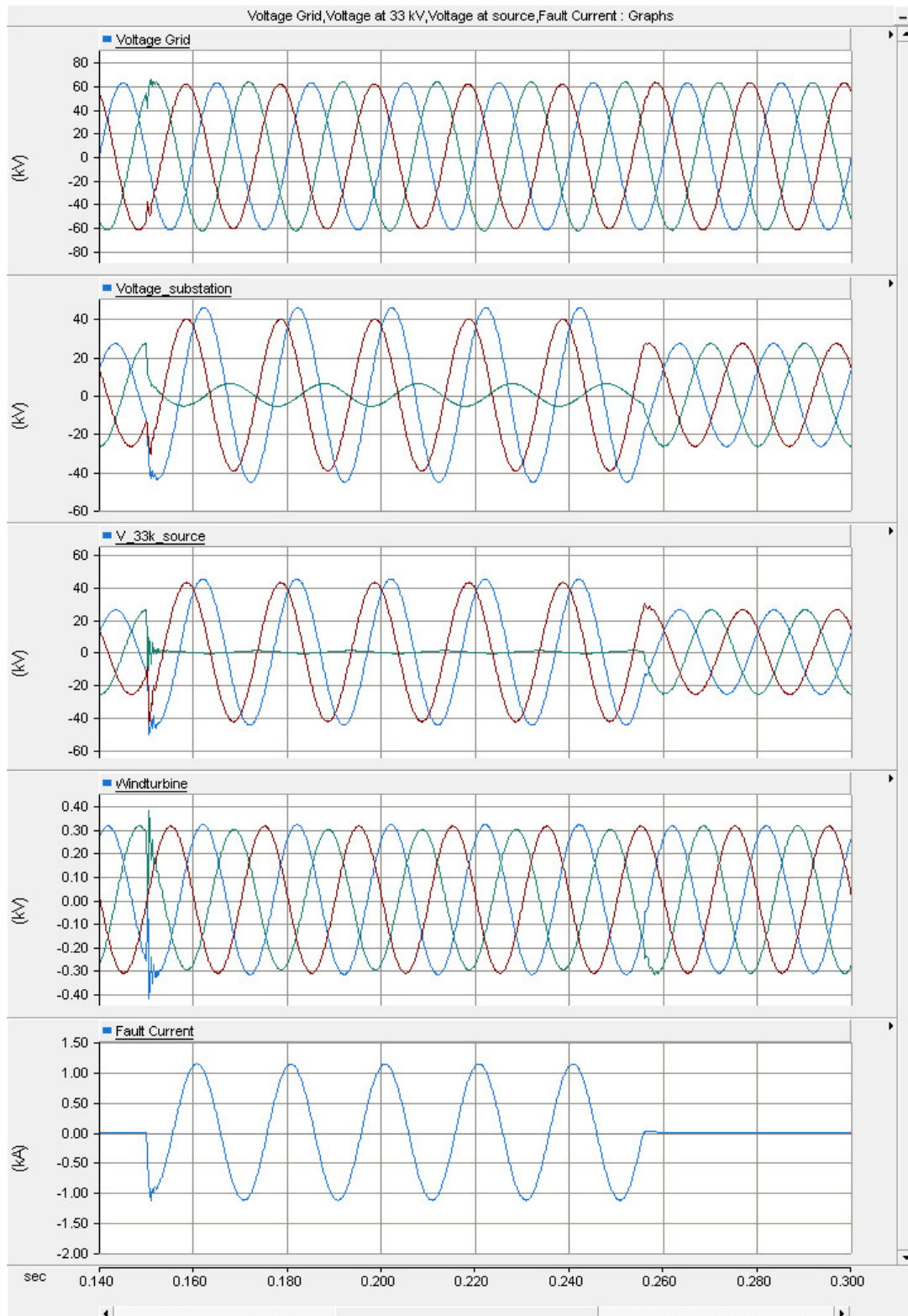


**Figure 7.2:** Voltages and fault current during an SLG-fault that occurs at the transition point for low-resistance earthing.

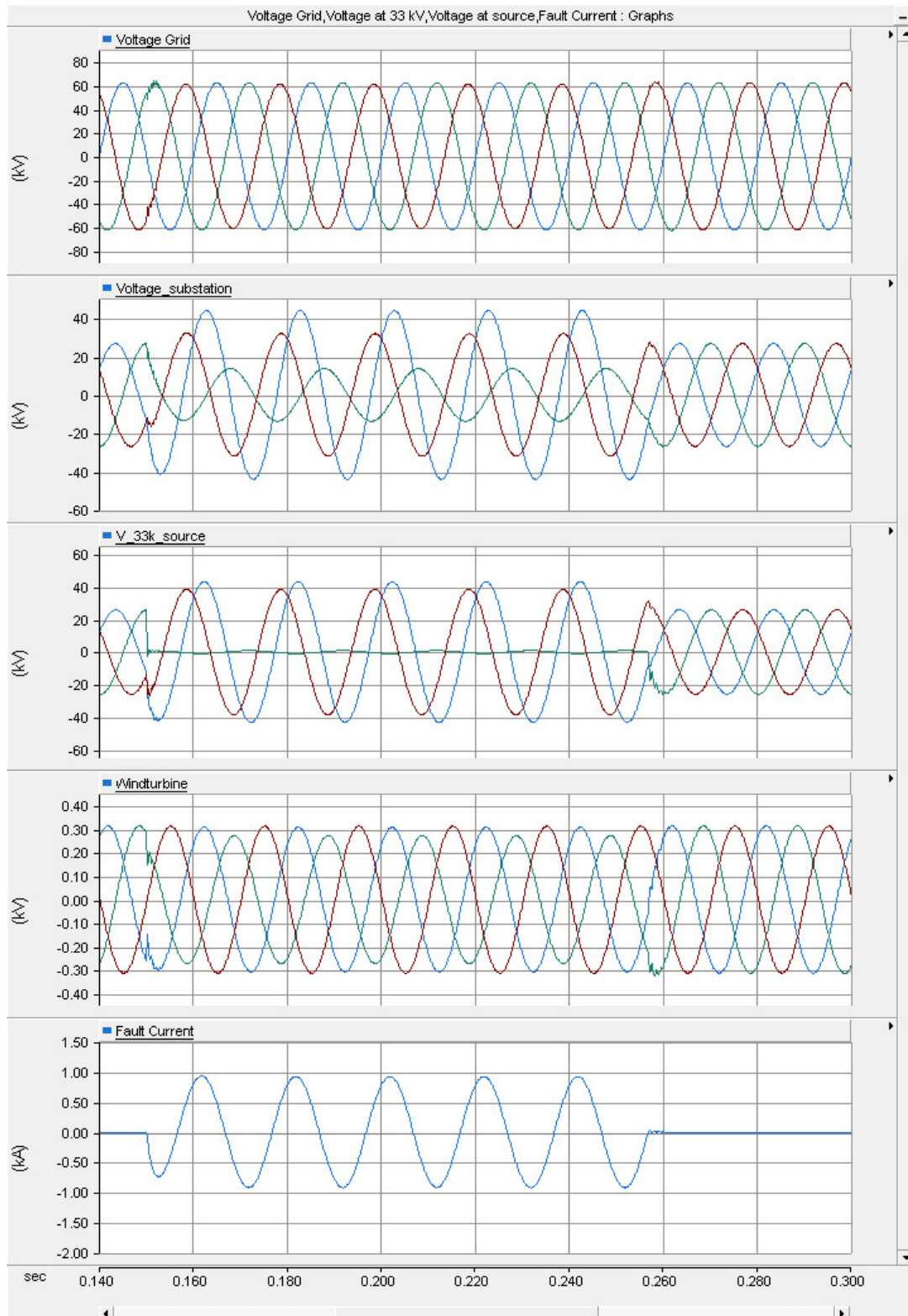


**Figure 7.3:** Voltages and fault current during an SLG-fault that occurs at the collection point for low-resistance earthing.

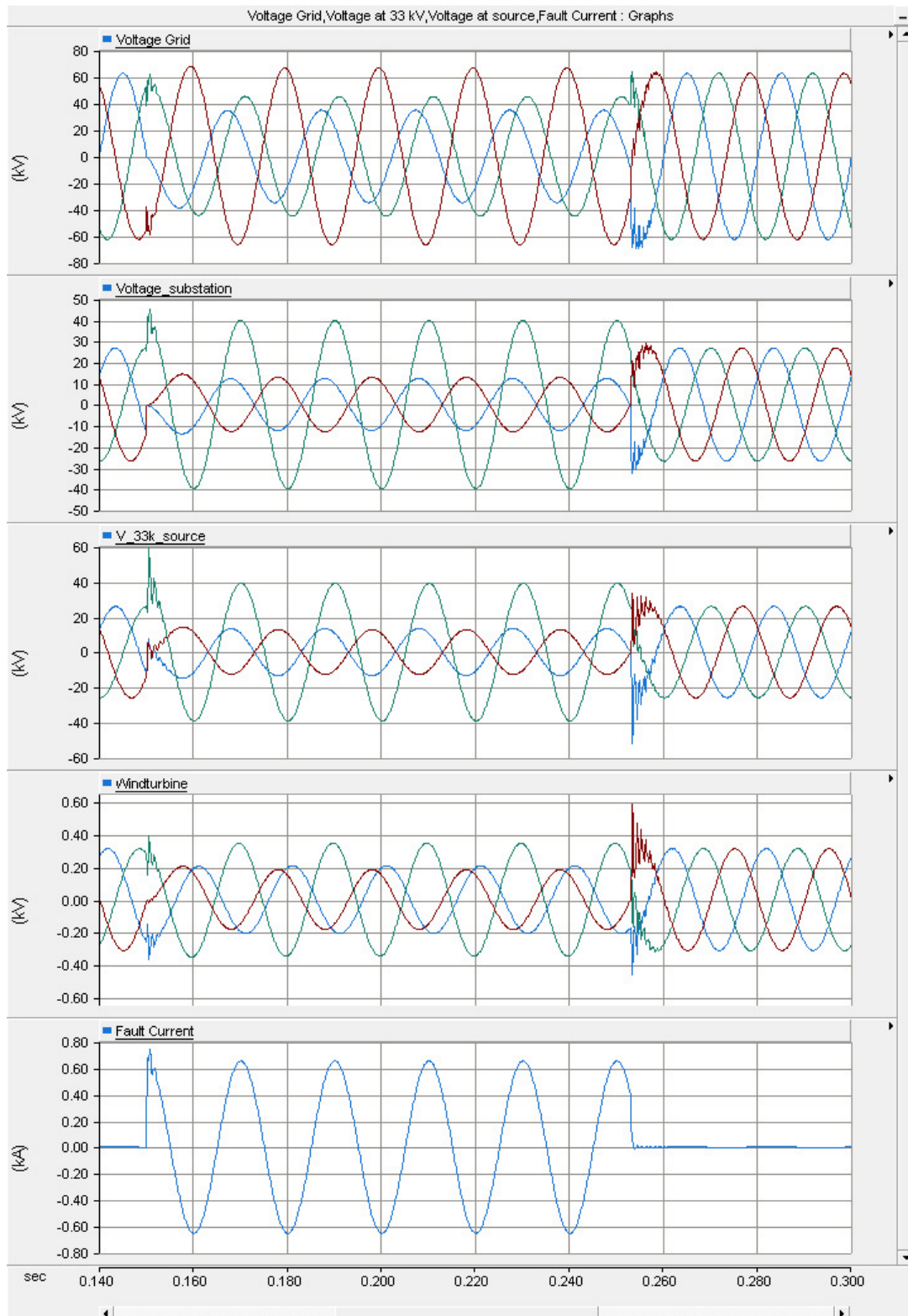


**Figure 7.4:** Voltages and fault current during an LLG-fault that occurs at the substation for low-resistance earthing.

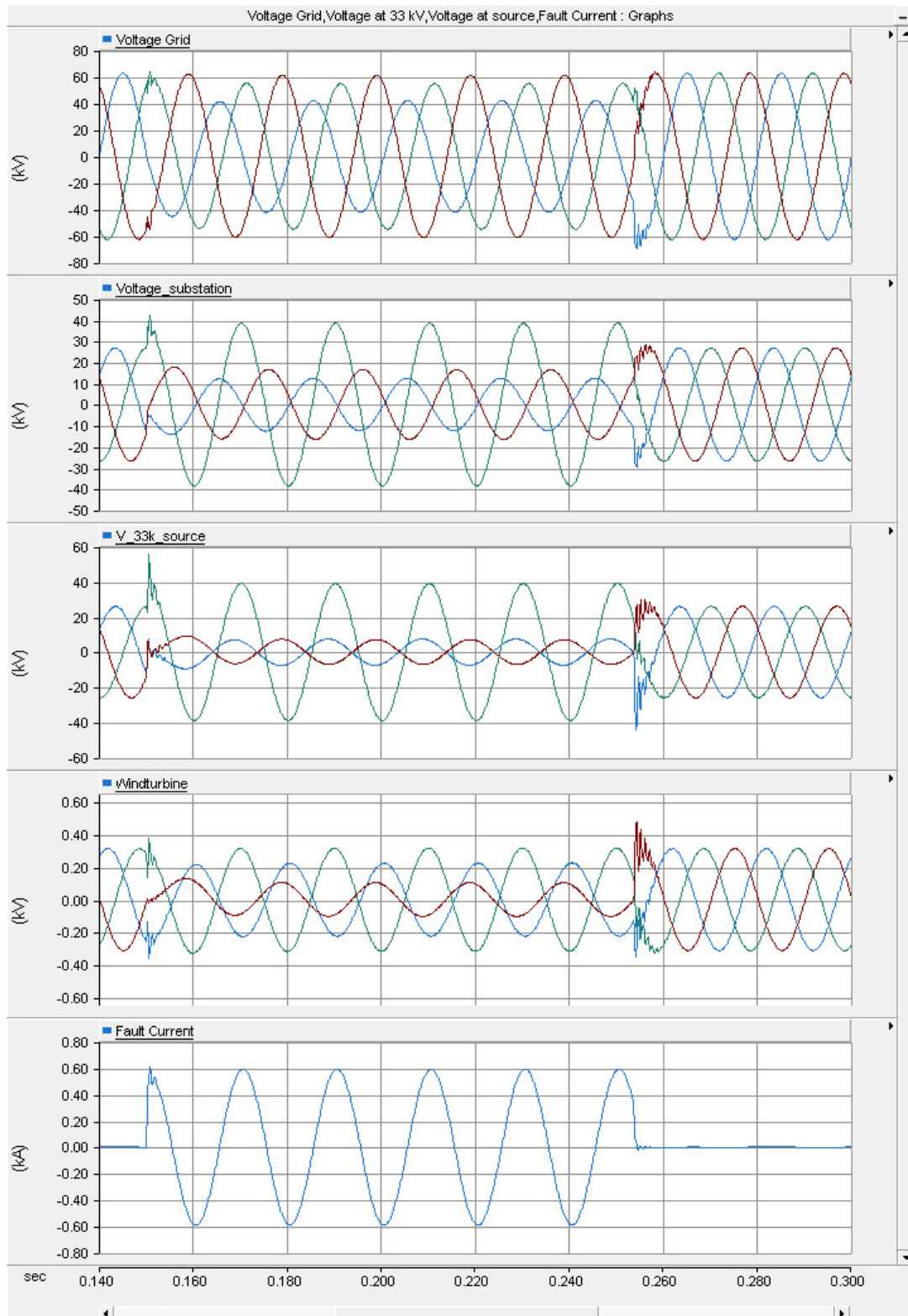


**Figure 7.5:** Voltages and fault current during an LLG-fault that occurs at the transition point for low-resistance earthing.

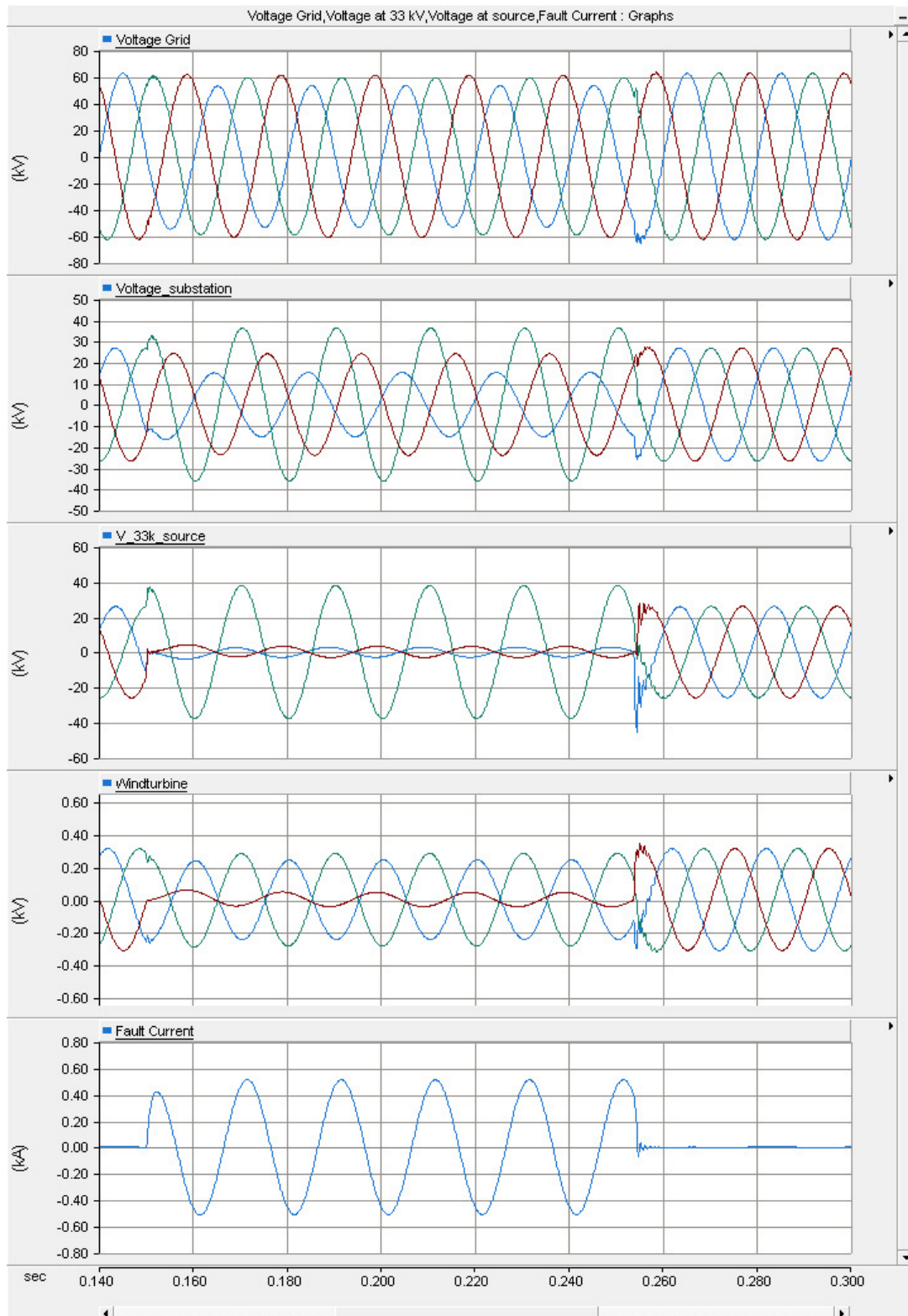


Figure 7.6: Voltages and fault current during an LLG-fault that occurs at the collection point for low-resistance earthing.

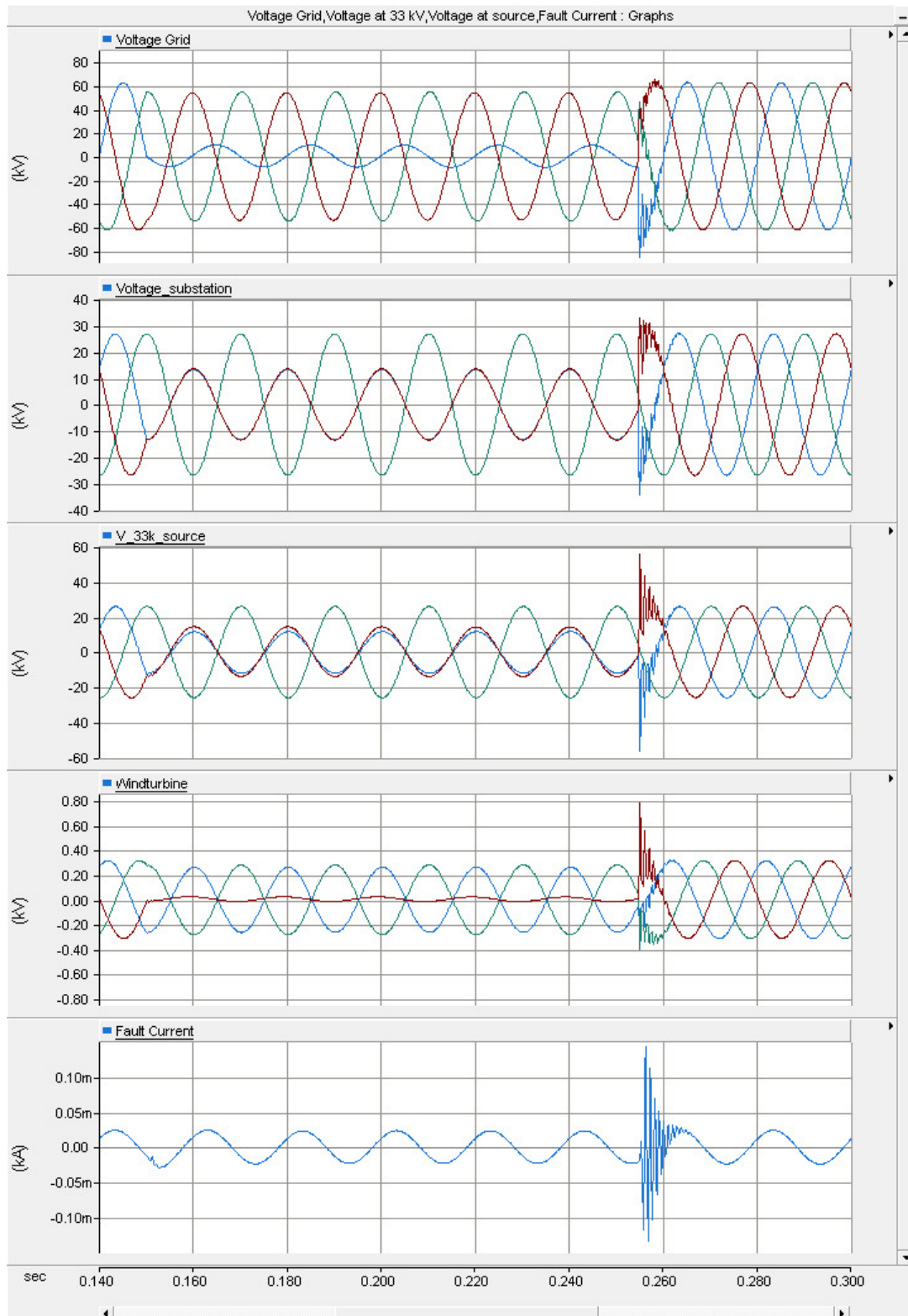


Figure 7.7: Voltages and fault current during an LL-fault that occurs at the substation for low-resistance earthing.

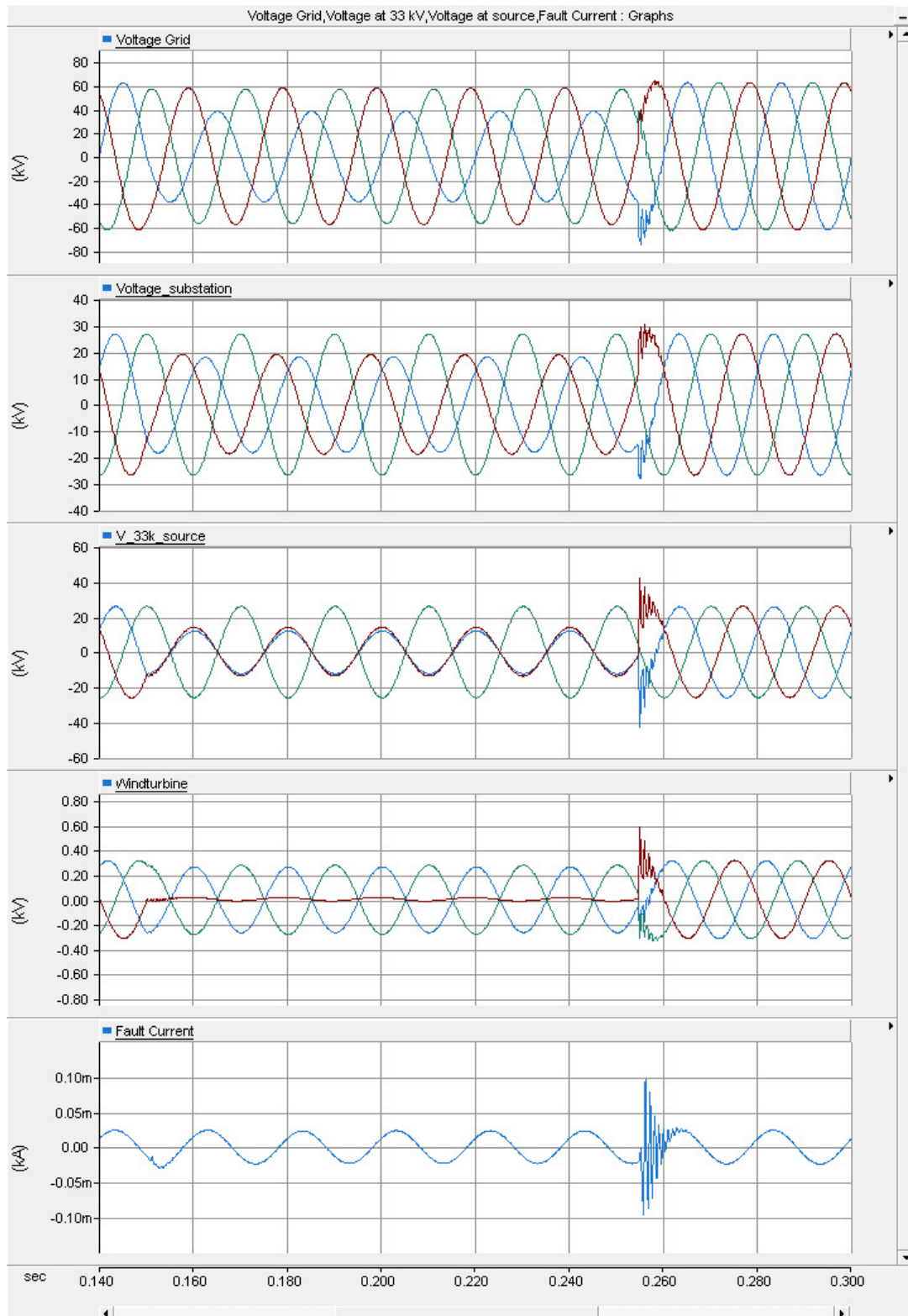
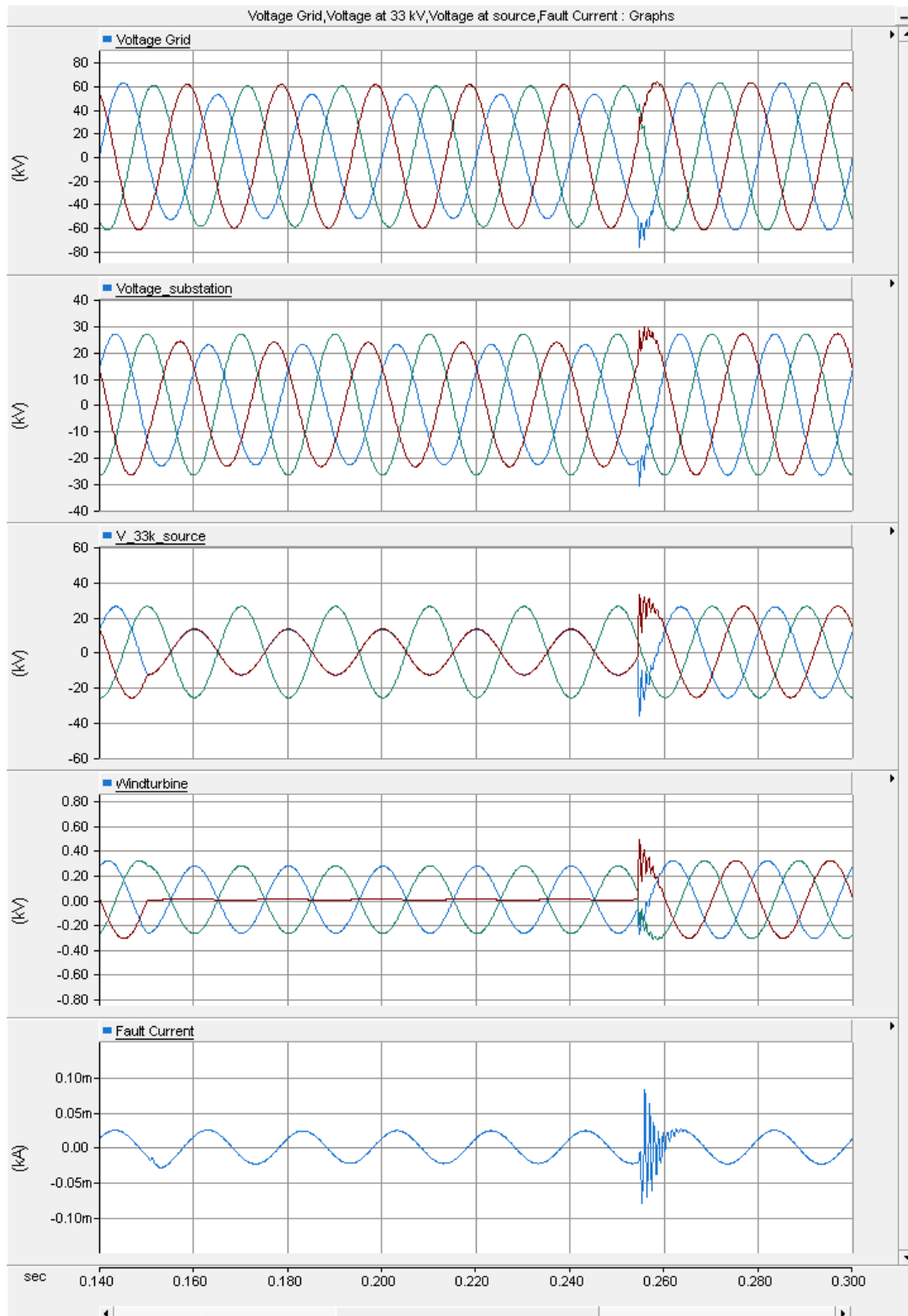


Figure 7.8: Voltages and fault current during an LL-fault that occurs at the transition point for low-resistance earthing.



**Figure 7.9:** Voltages and fault current during an LL-fault that occurs at the collection point for low-resistance earthing.

## 7.2 Resonance earthing

The parameters for resonance earthing were set to,  $L = 0.605$  H and  $R = 1900$   $\Omega$ . This is based on the wind farm that is described in Chapter 5.2. The fault is applied at  $t = 0.15$  s and the duration of the fault is set to  $t = 0.1$  s. The SLG-fault occurs on phase  $b$ , LL-fault and LLG-fault is between phase  $a$  and phase  $c$ .

The results from the simulation due to different applied faults at different locations in the 33 kV-collector grid, can be seen in Table 7.2 and Figure 7.10-7.18.

For resonance earthing, it can be seen from Figure 7.10-7.18 that the fault current is highest for SLG fault,  $|I_{f\_res}| = 0.014$  kA and  $|I_{f\_ind}| = 0.14$  kA. The chosen reactor is dimensioned for a 100 A rms current and the resistor for a 10 A rms current and this is also what is obtained. The values for the current and voltages in Table 7.2 is peak values.

When a SLG-fault is applied at phase  $b$ , it can be seen in Figure 7.10-7.12 that it doesn't matter where in the system the fault occurs, the system will behave almost the same.

For a LLG-fault, seen in Figure 7.13-7.15 the common thread is that the voltage at phase  $a$  and  $c$ , where the fault occurs, decreases and the voltage at phase  $b$  increases.

LL-fault between phase  $a$  and  $c$  can be studied in Figure 7.16-7.18. From the figures, it can be seen that when the fault occurs, the voltage at phase  $a$  and  $c$  decreases to the same level inside the 33 kV-system and phase  $b$  remain almost constant. When the fault occurs at the substation, phase  $a$  and  $c$  are in phase inside the 33 kV-system, but when the fault occurs at the transition point and the collection point, phase  $a$  and  $c$  are only in phase when measuring at the V\_33k\_source.

The highest transient overvoltage occurs during SLG-fault at the substation when measuring at the V\_33k\_source. The transient is -82.4 kV, see Figure 7.10. The highest transient overvoltages during LLG-fault and LL-fault is -62.1 kV and -56.5 kV, see Figure 7.14 and Figure 7.16.

**Table 7.2:** The peak value of voltage levels and fault currents during faults at different locations with resonance earthing.

| Fault | Fault location   | Fault current [kA]                      | Voltage level [kV]                     |  |   |  |
|-------|------------------|---|--|--|---|--|
|       |                  |   | Grid                                   | Substation                             | 33k Source                              | Wind turbine                           |
| SLG   | Substation       | $I_{res} = 0.014$<br>$I_{ind} = 0.14$   | $U_a=62.4$<br>$U_b=62.4$<br>$U_c=62.4$ | $U_a=45.2$<br>$U_b=0$<br>$U_c=45.2$    | $U_a=46.6$<br>$U_b=1.9$<br>$U_c=44.9$   | $U_a=0.31$<br>$U_b=0.31$<br>$U_c=0.31$ |
|       | Transition point | $I_{res} = 0.014$<br>$I_{ind} = 0.14$   | $U_a=62.4$<br>$U_b=62.4$<br>$U_c=62.4$ | $U_a=45.6$<br>$U_b=0$<br>$U_c=45.5$    | $U_a=44.7$<br>$U_b=1.6$<br>$U_c=46.2$   | $U_a=0.31$<br>$U_b=0.31$<br>$U_c=0.31$ |
|       | Collection point | $I_{res} = 0.014$<br>$I_{ind} = 0.14$   | $U_a=62.7$<br>$U_b=62.7$<br>$U_c=62.4$ | $U_a=47.3$<br>$U_b=2$<br>$U_c=45.1$    | $U_a=45.4$<br>$U_b=0$<br>$U_c=45.4$     | $U_a=0.31$<br>$U_b=0.31$<br>$U_c=0.31$ |
| LLG   | Substation       | $I_{res} = 0.007$<br>$I_{ind} = 0.07$   | $U_a=34.6$<br>$U_b=44.8$<br>$U_c=66.2$ | $U_a=12.6$<br>$U_b=40.2$<br>$U_c=12.6$ | $U_a=14.25$<br>$U_b=39.3$<br>$U_c=12.5$ | $U_a=0.21$<br>$U_b=0.35$<br>$U_c=0.19$ |
|       | Transition point | $I_{res} = 0.007$<br>$I_{ind} = 0.07$   | $U_a=41.7$<br>$U_b=54.7$<br>$U_c=61.3$ | $U_a=14.5$<br>$U_b=39.9$<br>$U_c=14.5$ | $U_a=8.86$<br>$U_b=39.4$<br>$U_c=6.9$   | $U_a=0.23$<br>$U_b=0.32$<br>$U_c=0.11$ |
|       | Collection point | $I_{res} = 0.0066$<br>$I_{ind} = 0.064$ | $U_a=55.6$<br>$U_b=60.4$<br>$U_c=60.9$ | $U_a=18.6$<br>$U_b=39.0$<br>$U_c=20.6$ | $U_a=2.7$<br>$U_b=38.2$<br>$U_c=2.1$    | $U_a=0.25$<br>$U_b=0.28$<br>$U_c=0.35$ |
| LL    | Substation       | 0<br>0                                  | $U_a=9.4$<br>$U_b=54.6$<br>$U_c=53.8$  | $U_a=13.3$<br>$U_b=26.8$<br>$U_c=13.5$ | $U_a=11.6$<br>$U_b=25.9$<br>$U_c=14.4$  | $U_a=0.26$<br>$U_b=0.28$<br>$U_c=0.02$ |
|       | Transition point | 0<br>0                                  | $U_a=38.2$<br>$U_b=57.2$<br>$U_c=57.8$ | $U_a=18.0$<br>$U_b=26.7$<br>$U_c=18.9$ | $U_a=12.0$<br>$U_b=26.0$<br>$U_c=14.0$  | $U_a=0.26$<br>$U_b=0.28$<br>$U_c=0.02$ |
|       | Collection point | 0<br>0                                  | $U_a=52.7$<br>$U_b=59.8$<br>$U_c=60.9$ | $U_a=22.8$<br>$U_b=26.8$<br>$U_c=23.6$ | $U_a=12.9$<br>$U_b=25.8$<br>$U_c=13.1$  | $U_a=0.27$<br>$U_b=0.27$<br>$U_c=0$    |

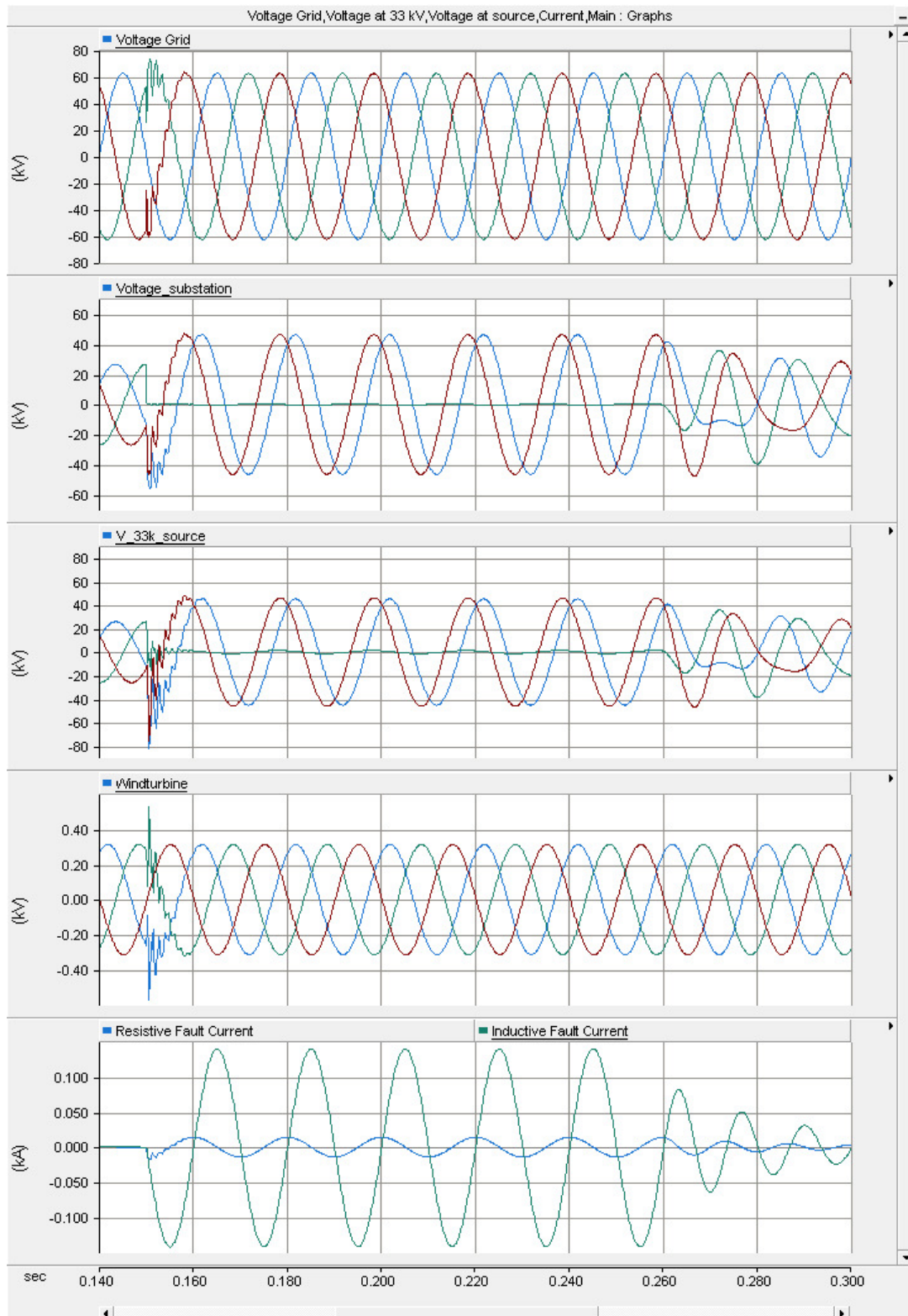


**Figure 7.10:** Voltages and fault currents during an SLG-fault that occurs at the substation for resonance earthing.

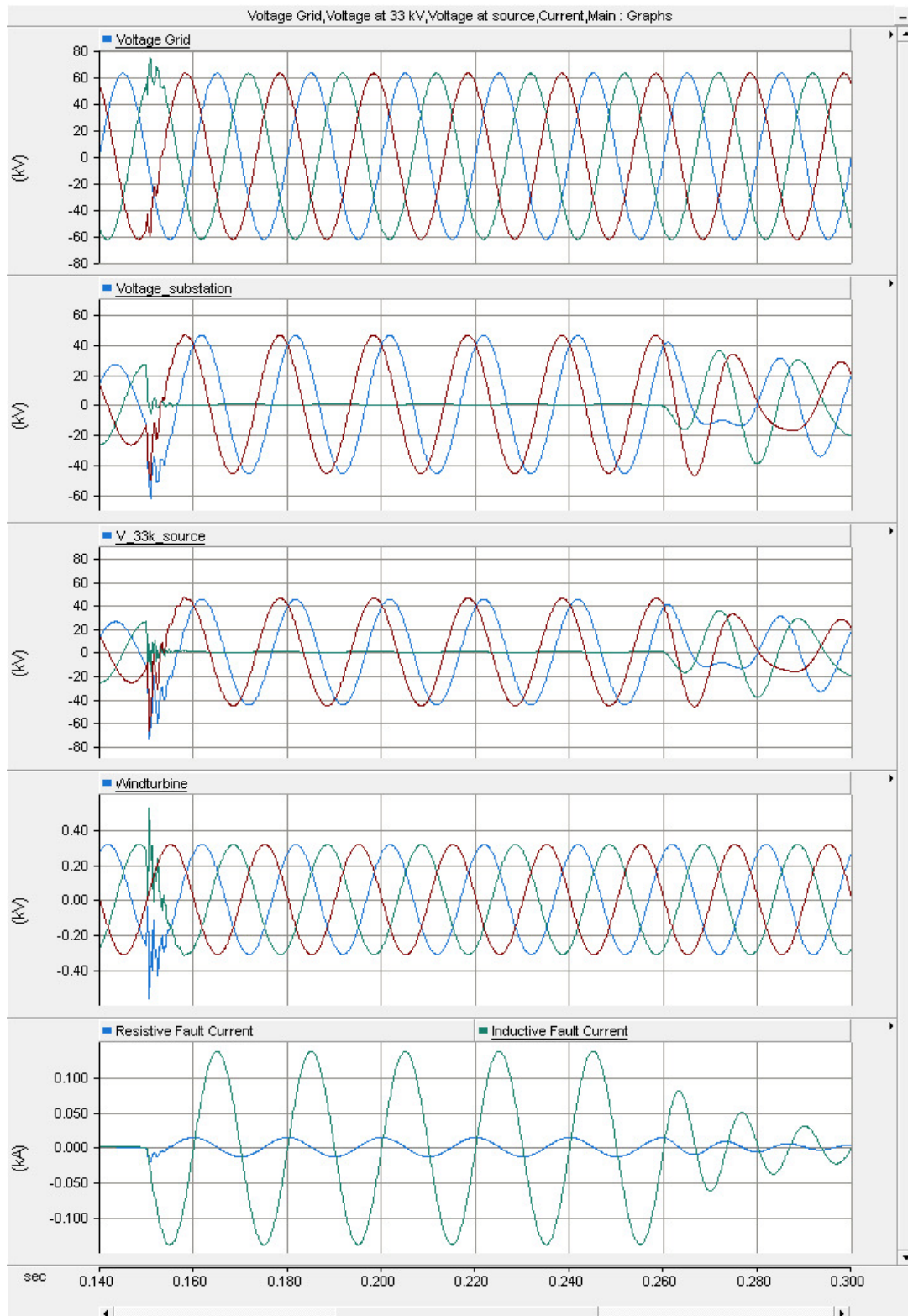


**Figure 7.11:** Voltages and fault currents during an SLG-fault that occurs at the transition point for resonance earthing.

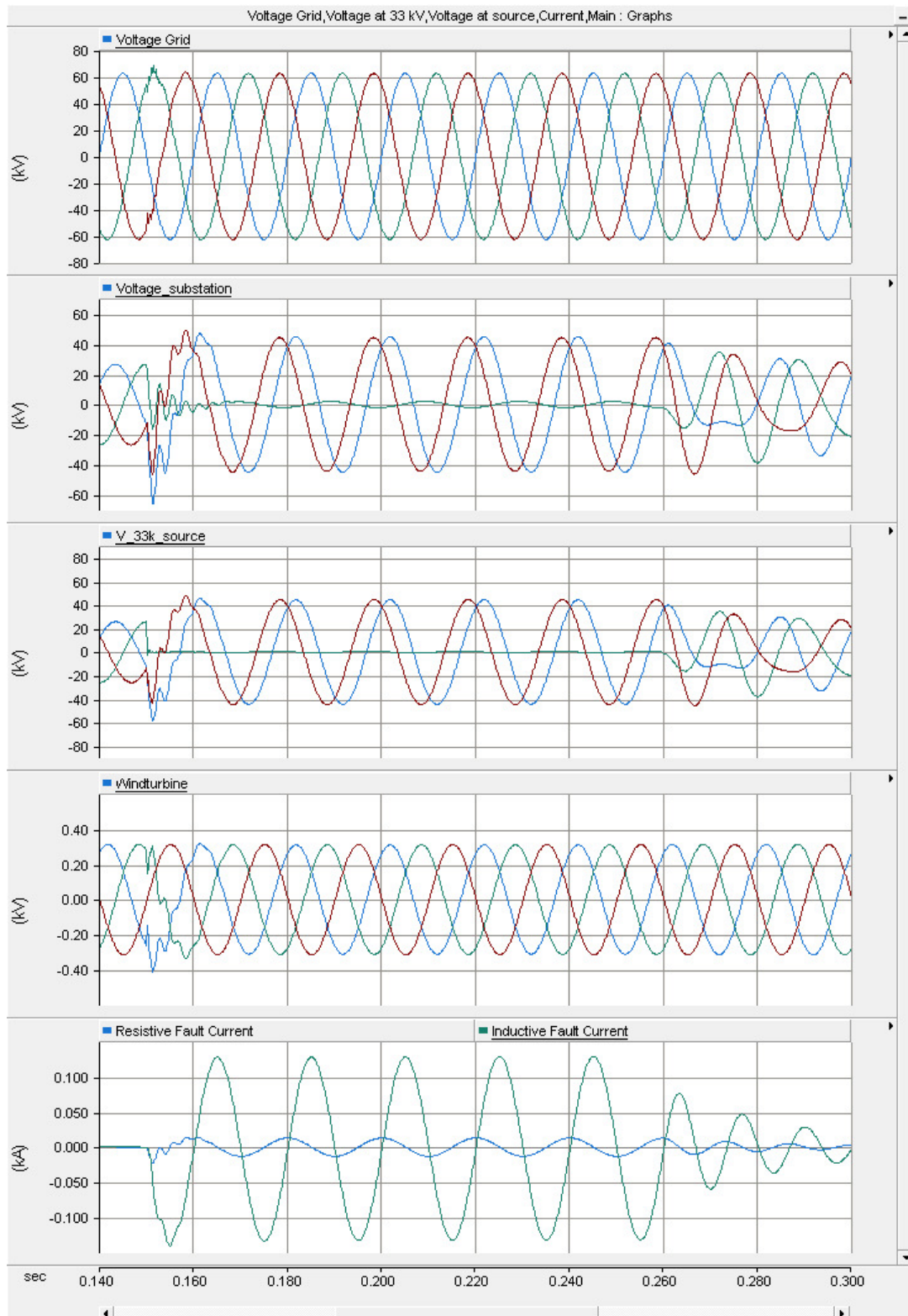


**Figure 7.12:** Voltages and fault currents during an SLG-fault that occurs at the collection point for resonance earthing.

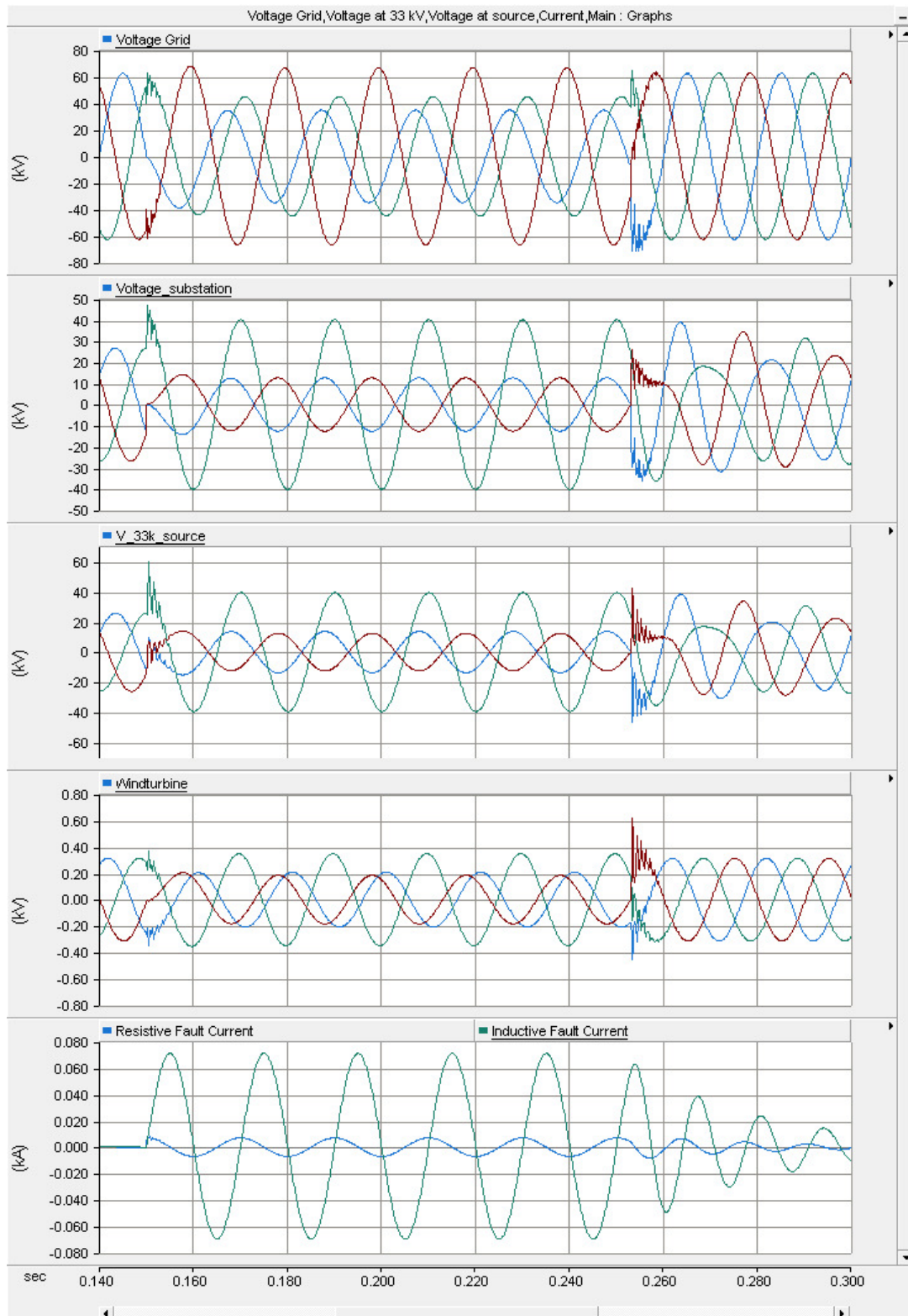


**Figure 7.13:** Voltages and fault currents during an LLG-fault that occurs at the substation for resonance earthing.

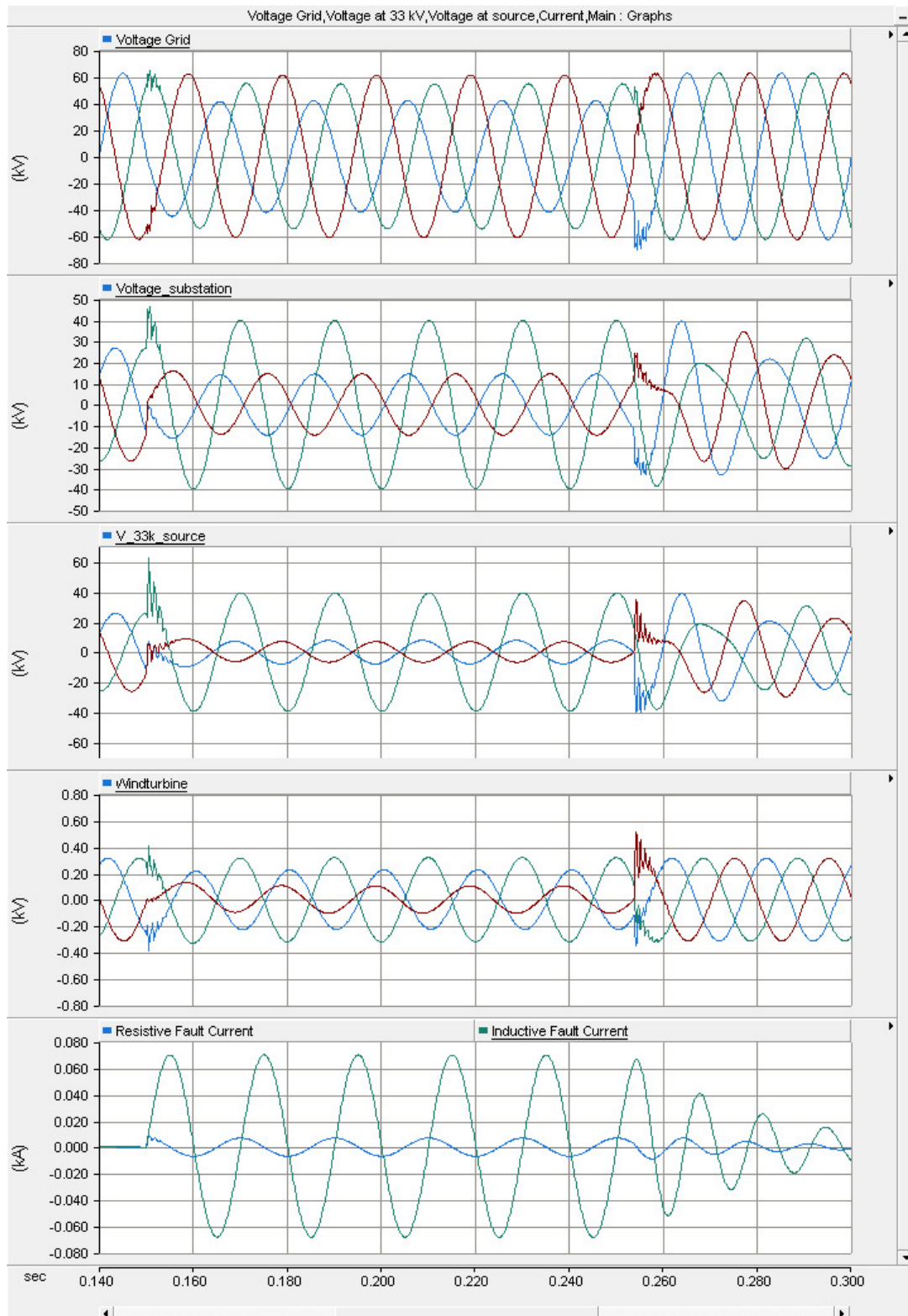


**Figure 7.14:** Voltages and fault currents during an LLG-fault that occurs at the transition point for resonance earthing.

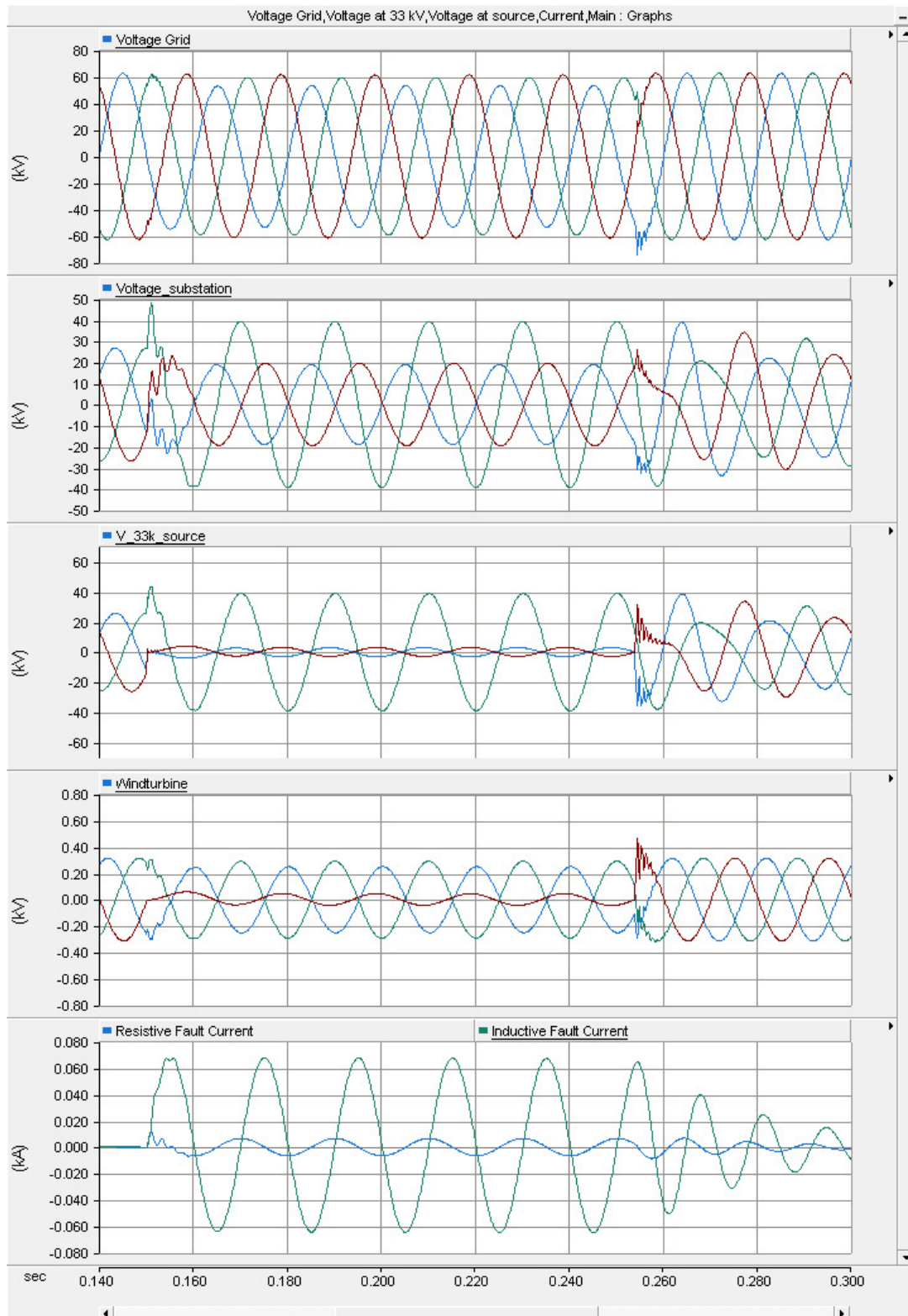


**Figure 7.15:** Voltages and fault currents during an LLG-fault that occurs at the collection point for resonance earthing.

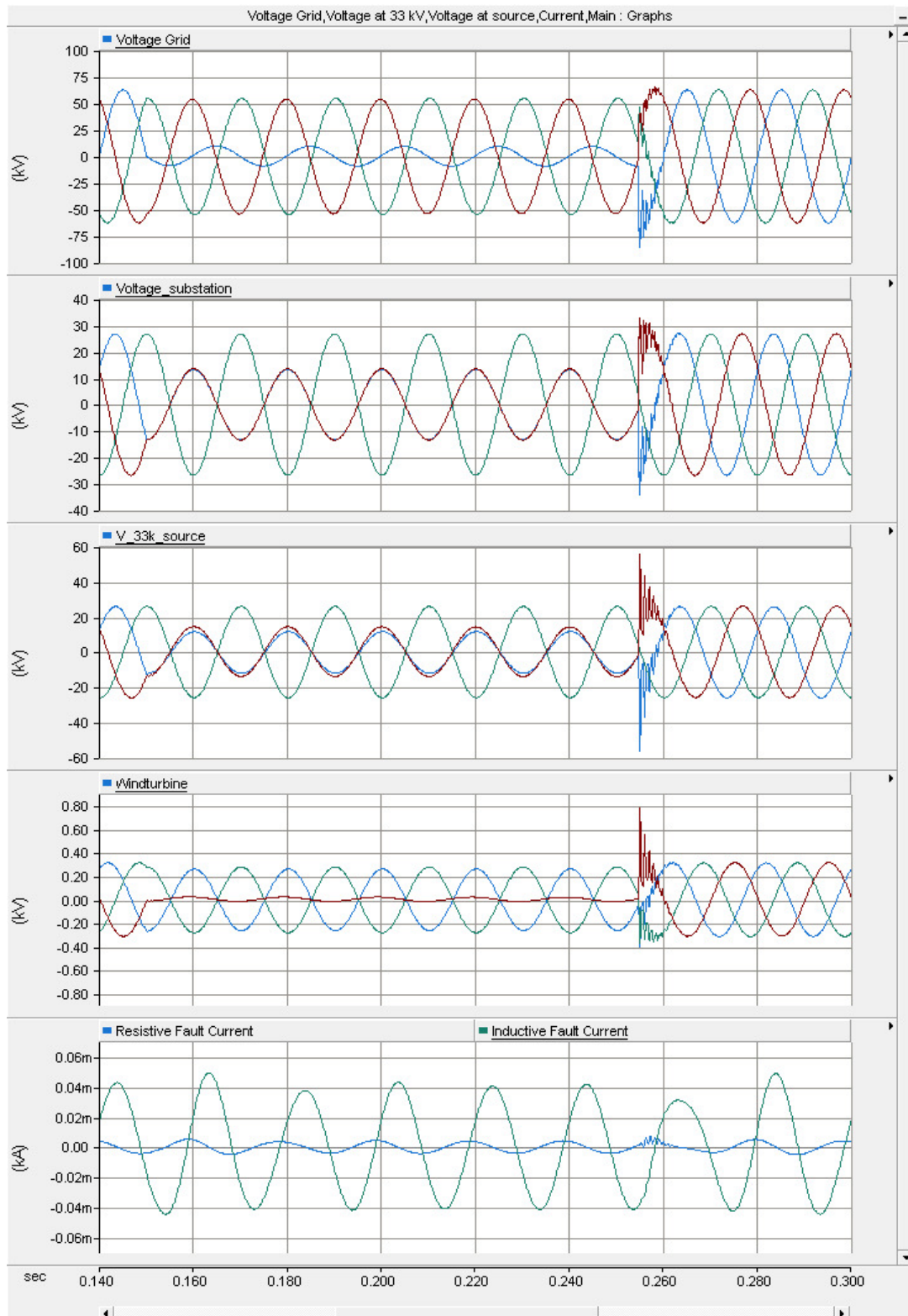


**Figure 7.16:** Voltages and fault currents during an LL-fault that occurs at the substation for resonance earthing.

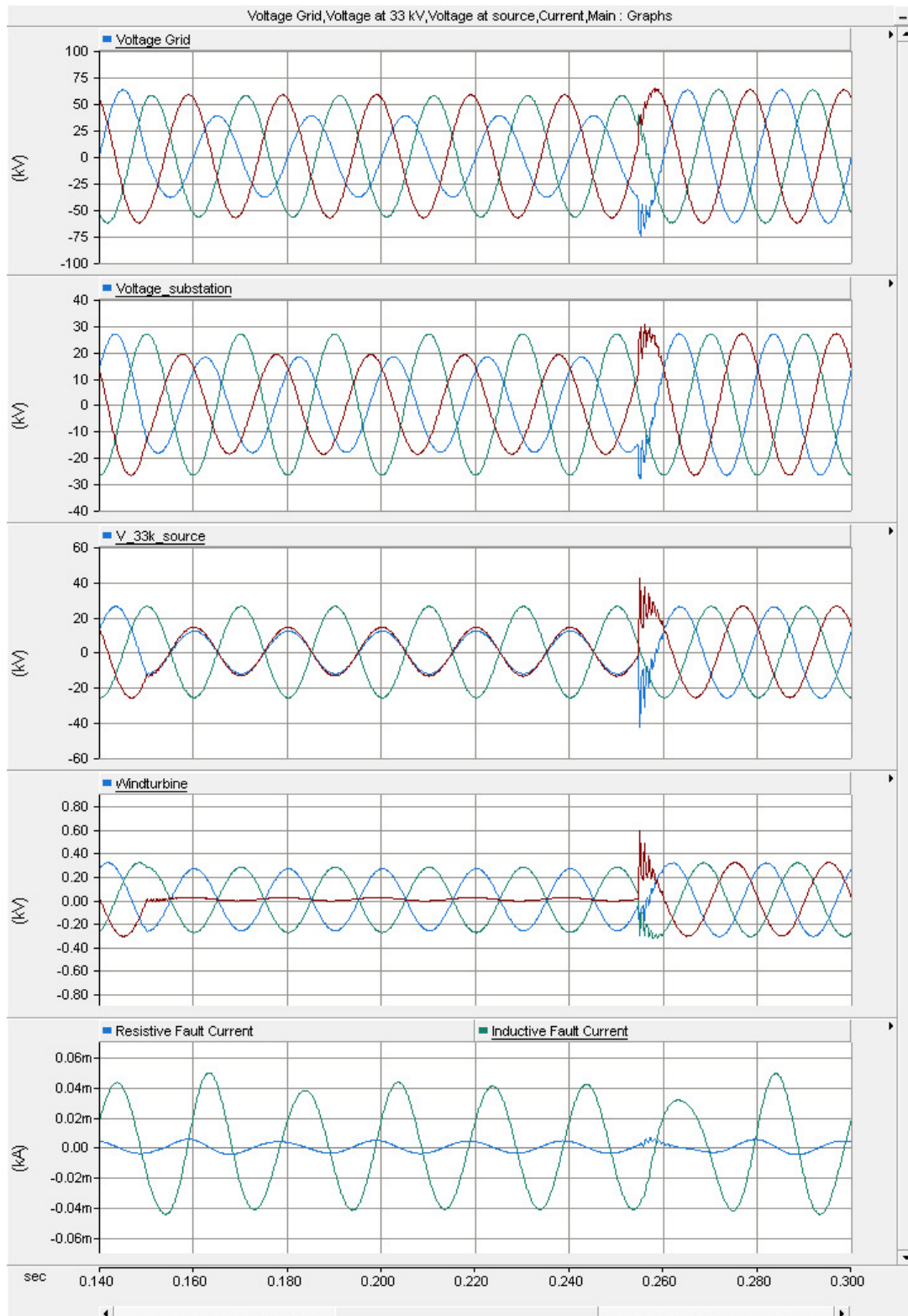


**Figure 7.17:** Voltages and fault currents during an LL-fault that occurs at the transition point for resonance earthing.

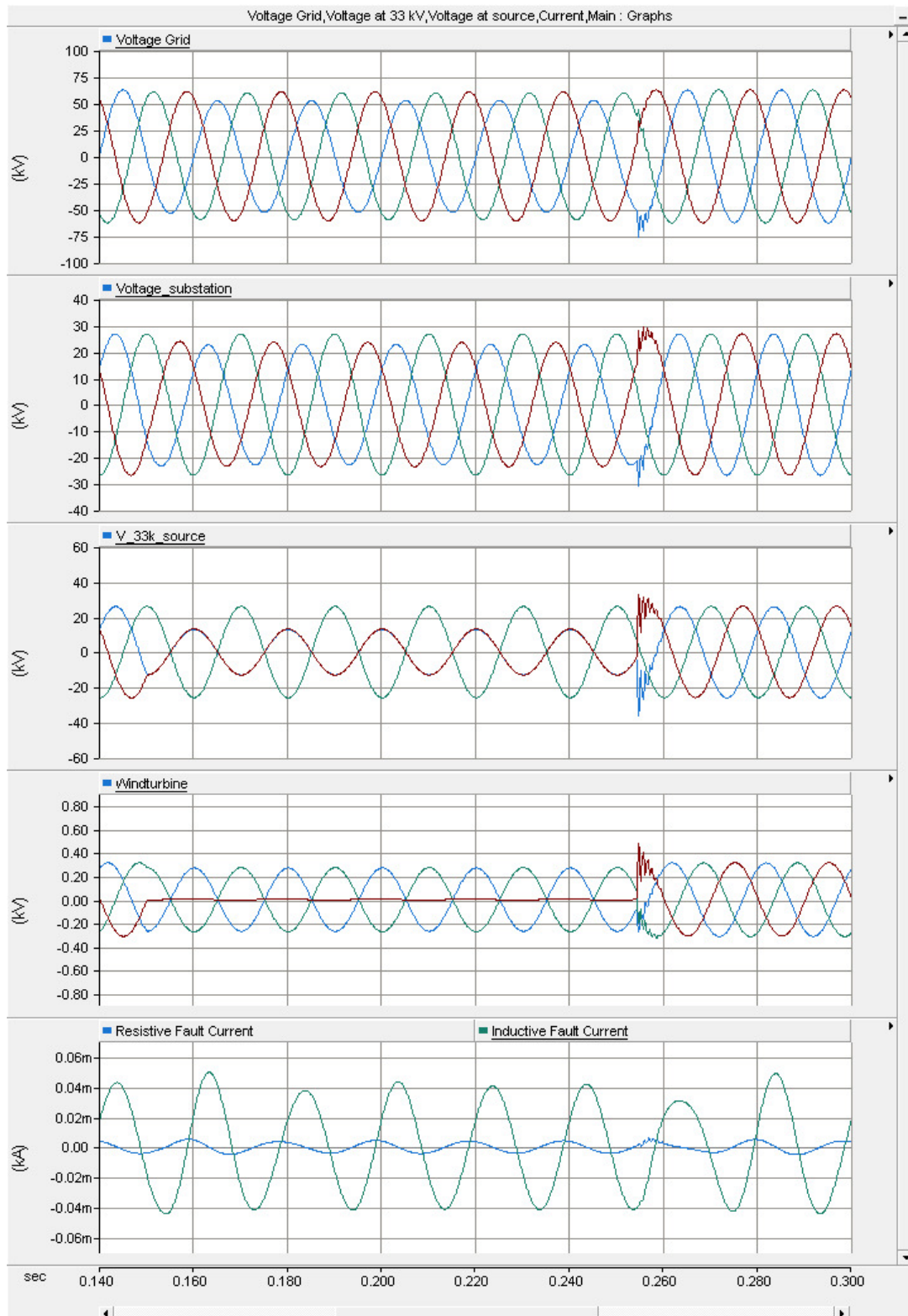


**Figure 7.18:** Voltages and fault currents during an LL-fault that occurs at the collection point for resonance earthing.

### 7.3 Lightning impulse for resonance earthing

Impulse overvoltage simulations were done for two different amplitudes, 600 kV and 1 MV, which represents two different lightning impulses. The lightning impulses occur at the utility grid, which is at the 77 kV side of the 77/33 kV transformer. A 77 kV system is designed, according to [29], to be able to withstand a lightning impulse of 605 kV. Hence the chosen value of 600 kV. The amplitude of 1 MV is chosen to see what is happening to the system when the lightning impulse is slightly higher.

The voltage rating of the surge arrester was set to 27 kV. During the simulations, the resistance representing the earth electrode was set to two different ohmic values,  $R = 1 \Omega$  and  $R = 40 \Omega$ . In Chapter 2.3 it is stated that the resistance of the earth electrode should be in the range of 1-5  $\Omega$ . Therefore, the resistance of the earth electrode was set to 1  $\Omega$ . Furthermore,  $R = 37 \Omega$  were calculated in Chapter 5.4. In order to have a margin for the simulations, the earth electrode were set to  $R = 40 \Omega$  for the high-resistance earth electrode.

The result from the simulations can be seen in Figure 7.20-7.23 and in Figure 7.25-7.28.

#### 7.3.1 Lightning impulse of 600 kV

A lightning impulse with an amplitude of 600 kV, see Figure 7.19, occurs at the collector grid. The result in Figure 7.20 and Figure 7.22 shows that the voltage at the 77 kV side of the 77/33 kV transformer increases to about 320 kV. There is no surge arrester on this side of the transformer, which is why the voltage increases to the same level regardless the value of the earth electrode. Surge arresters are, on the other hand, installed at the 33 kV side of both the 77/33 kV and the 33/0.4 kV transformer. In Figure 7.20 the earth electrode is set to 1  $\Omega$ . With this earth electrode the voltage increases to a maximum of 49.5 kV at the 77/33 kV transformer and a maximum of 47.1 kV at the 33/0.4 kV transformer. When the impedance of the earth electrode was increased to 40  $\Omega$ , see Figure 7.22, the voltage next to the surge arresters increases to a maximum of 58.9 kV and 53.4 kV.

From Figure 7.21 and Figure 7.23 it can be seen that the surge arresters are operating and the current is higher when using a lower resistance for the earth electrode. The figures also shows that the energy stored by the surge arrester is higher for the 1  $\Omega$  earth electrode configuration.

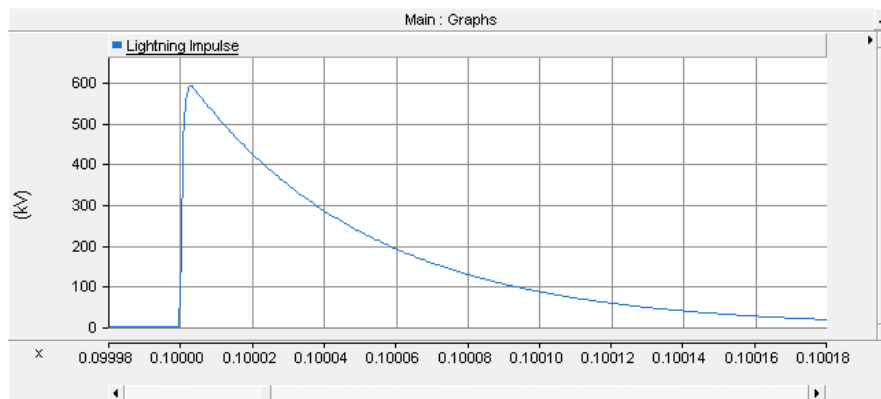


**Figure 7.19:** Simulated lightning impulse with an amplitude of 600 kV.

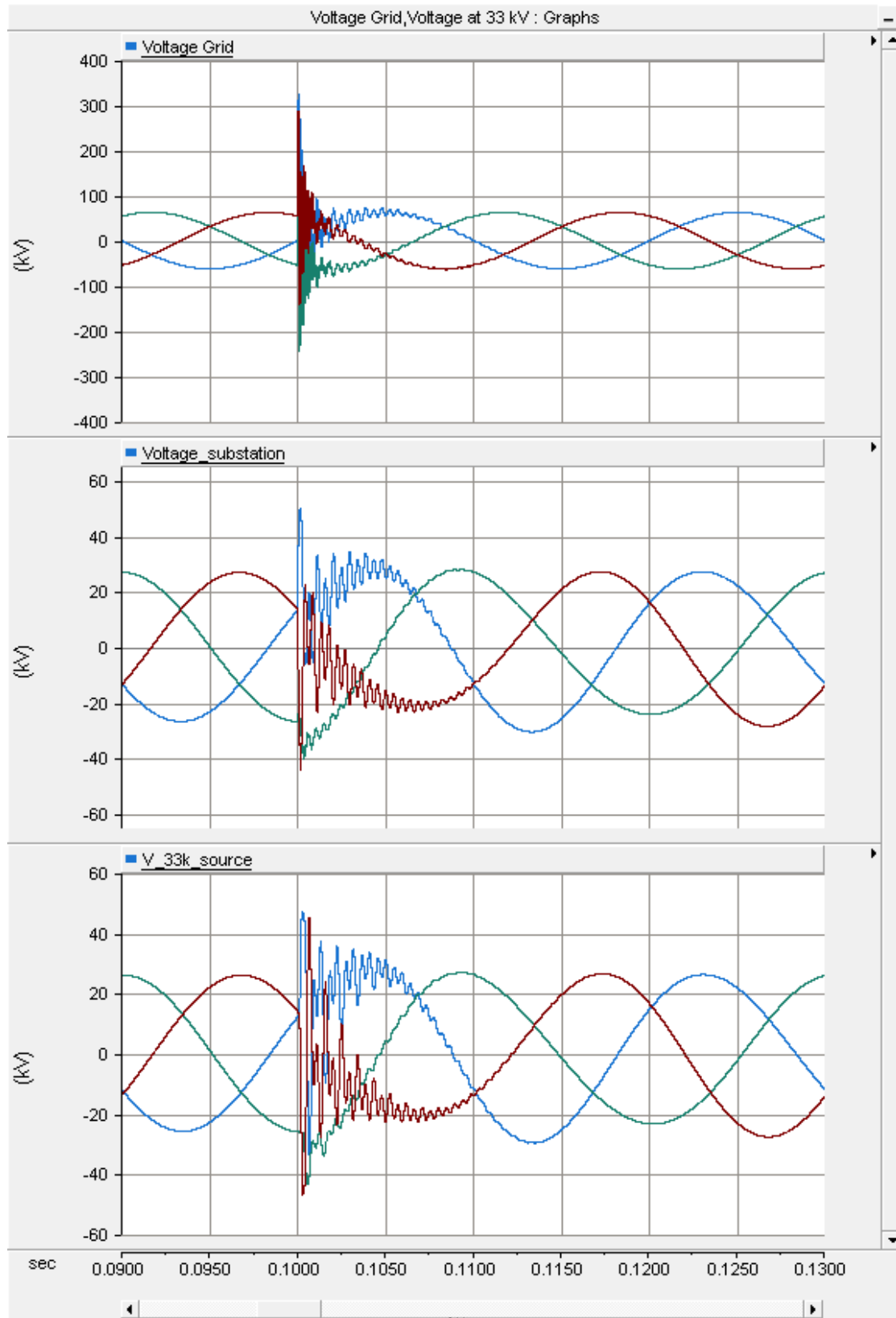


**Figure 7.20:** 600 kV lightning impulse at the utility grid with a surge arrester with an earth electrode of 1 Ω.

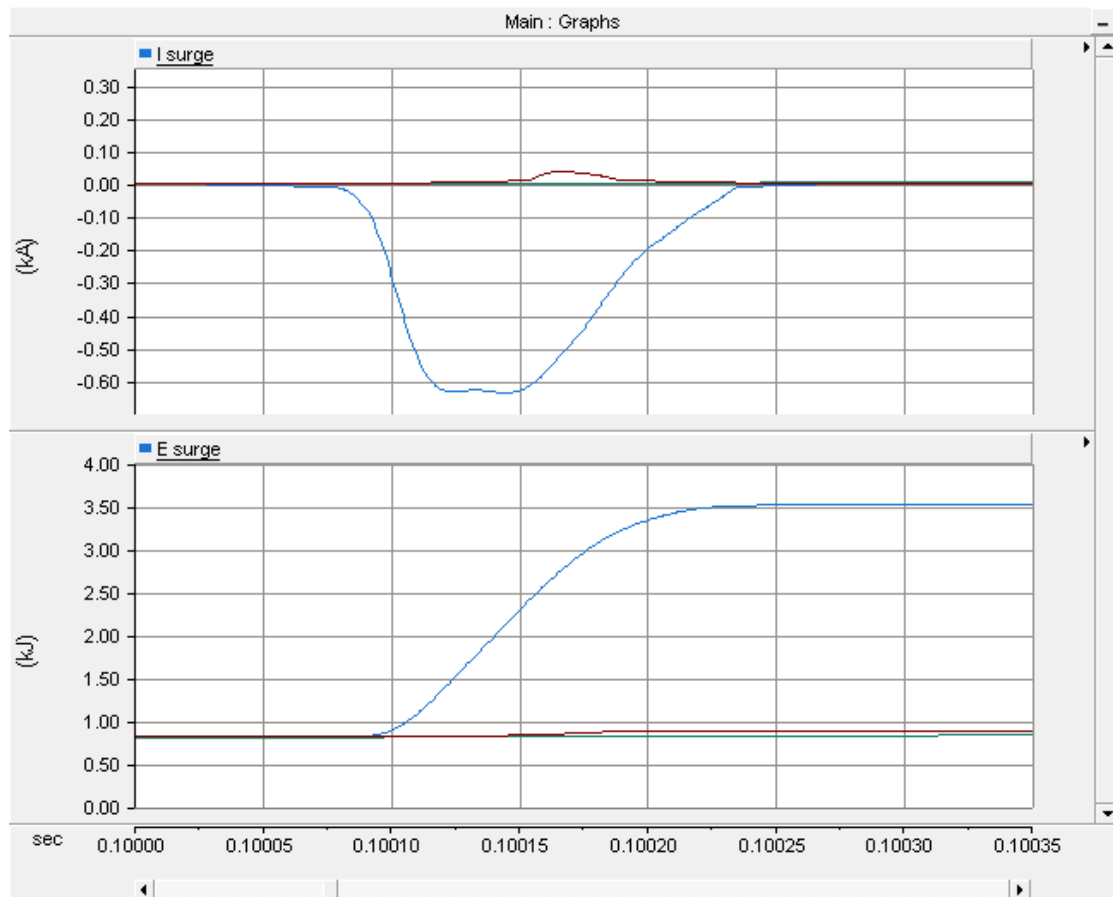


**Figure 7.21:** Current and Energy for a surge arrester with an earth electrode of  $1 \Omega$  and an amplitude of 600 kV.

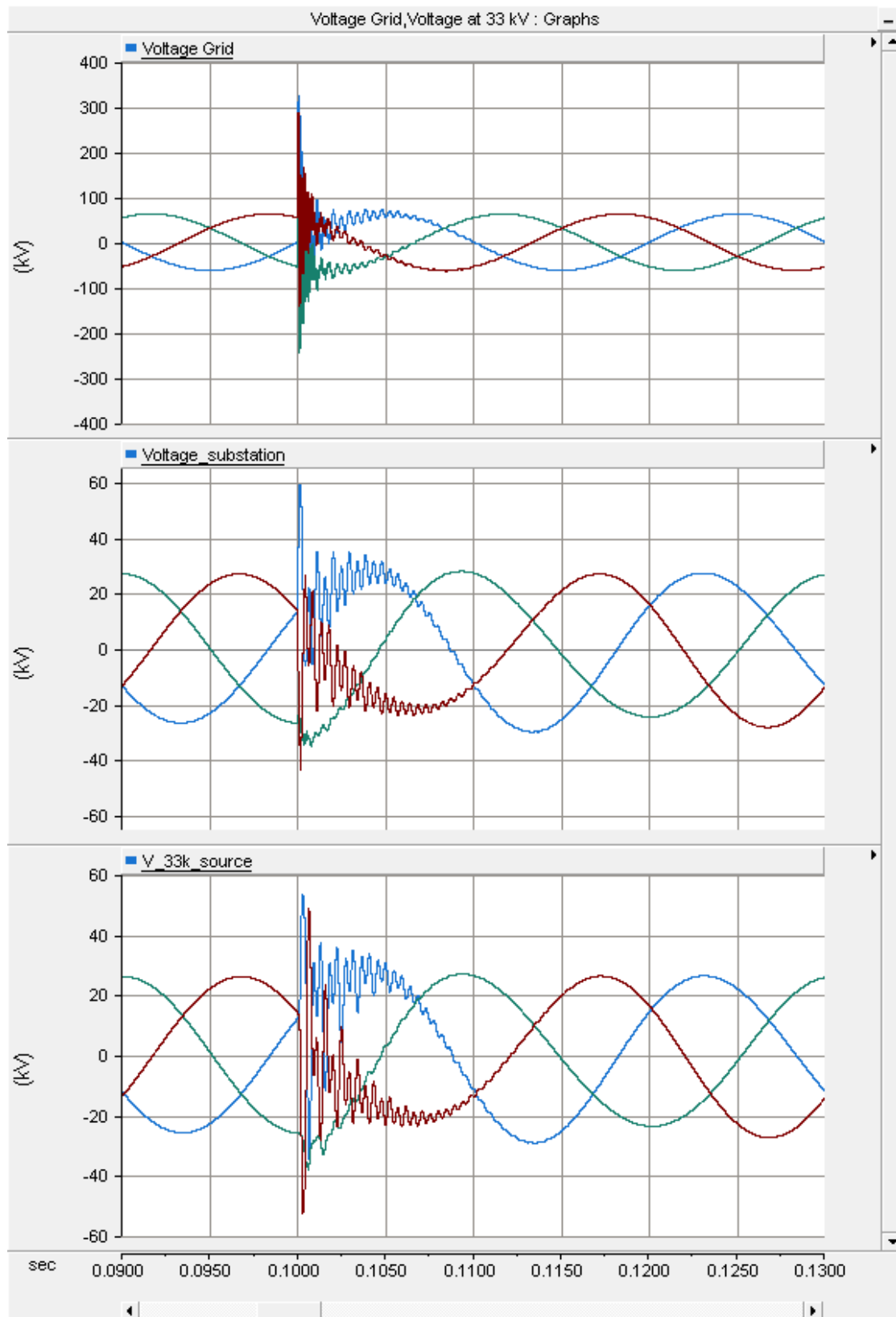
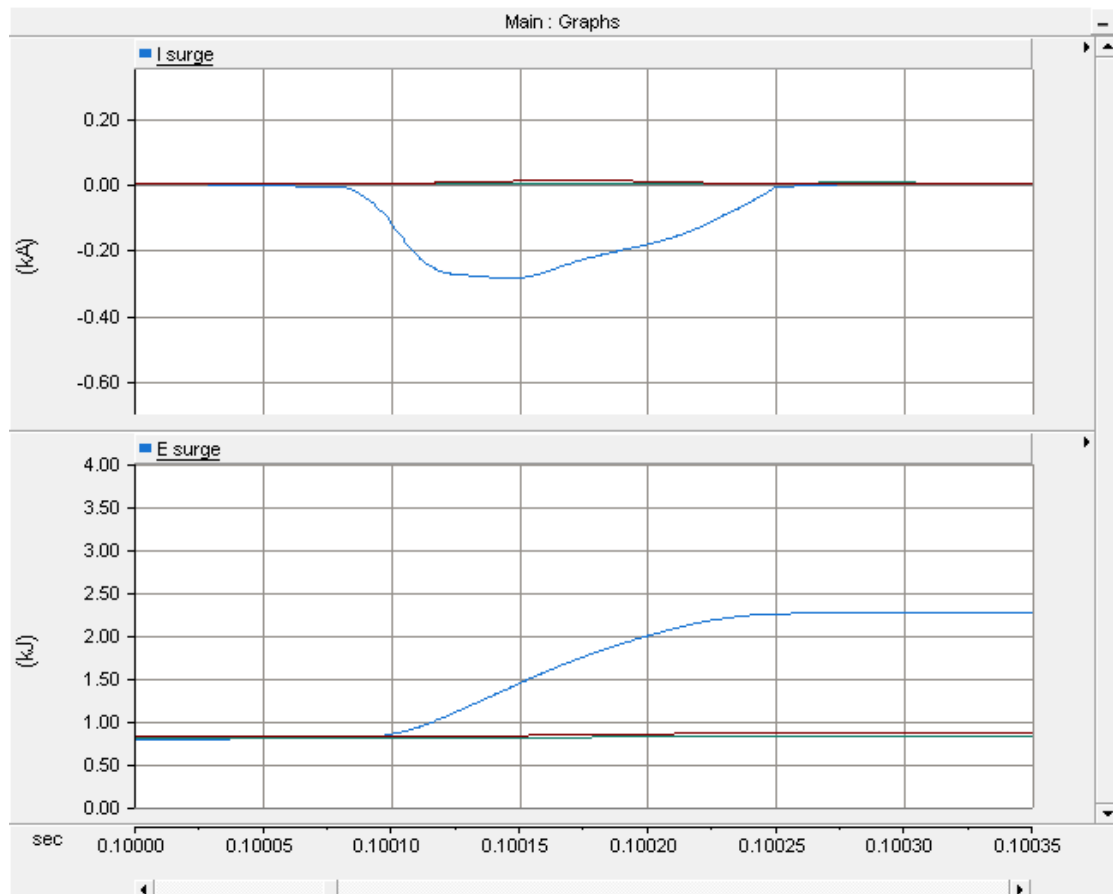


Figure 7.22: 600 kV lightning impulse at the utility grid with a surge arrester with an earth electrode of 40 Ω.



**Figure 7.23:** Current and Energy for a surge arrester with an earth electrode of  $40 \Omega$  and an amplitude of 600 kV.

### 7.3.2 Lightning impulse of 1 MV

When increasing the amplitude of the lightning impulse to 1 MV, see Figure 7.24, it can be seen from Figure 7.25 and Figure 7.27 that the value of the resistance of the earth electrode has an even greater impact compared with the 600 kV lightning impulse. When using  $40\ \Omega$ , the impulse increases the voltage inside the power system to 80.6 kV respectively 58.5 kV, but for  $1\ \Omega$ , the voltage only increases to 53 kV and 47.4 kV.

In order to prevent the voltage from increasing as much as for  $40\ \Omega$ , the surge arrester absorbs a higher amount of energy. For the  $1\ \Omega$  case, see Figure 7.26, the surge arrester absorbs 11.2 kJ. For the  $40\ \Omega$  case, see Figure 7.28, the surge arrester only absorbs 6.1 kJ.

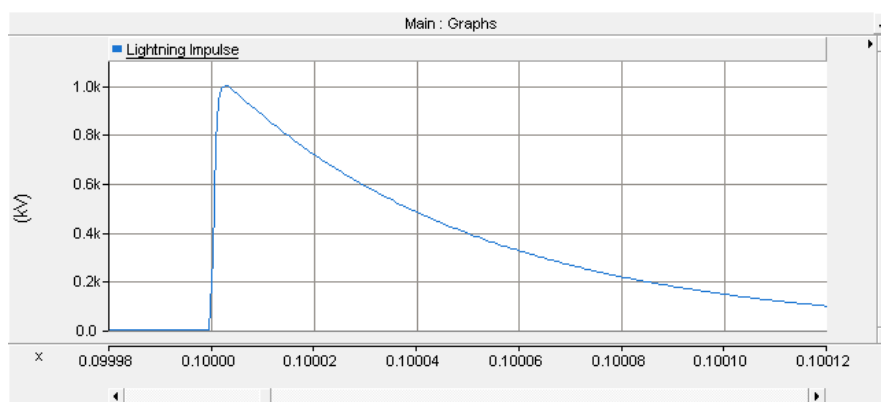


**Figure 7.24:** Simulated lightning impulse with an amplitude of 1 MV.

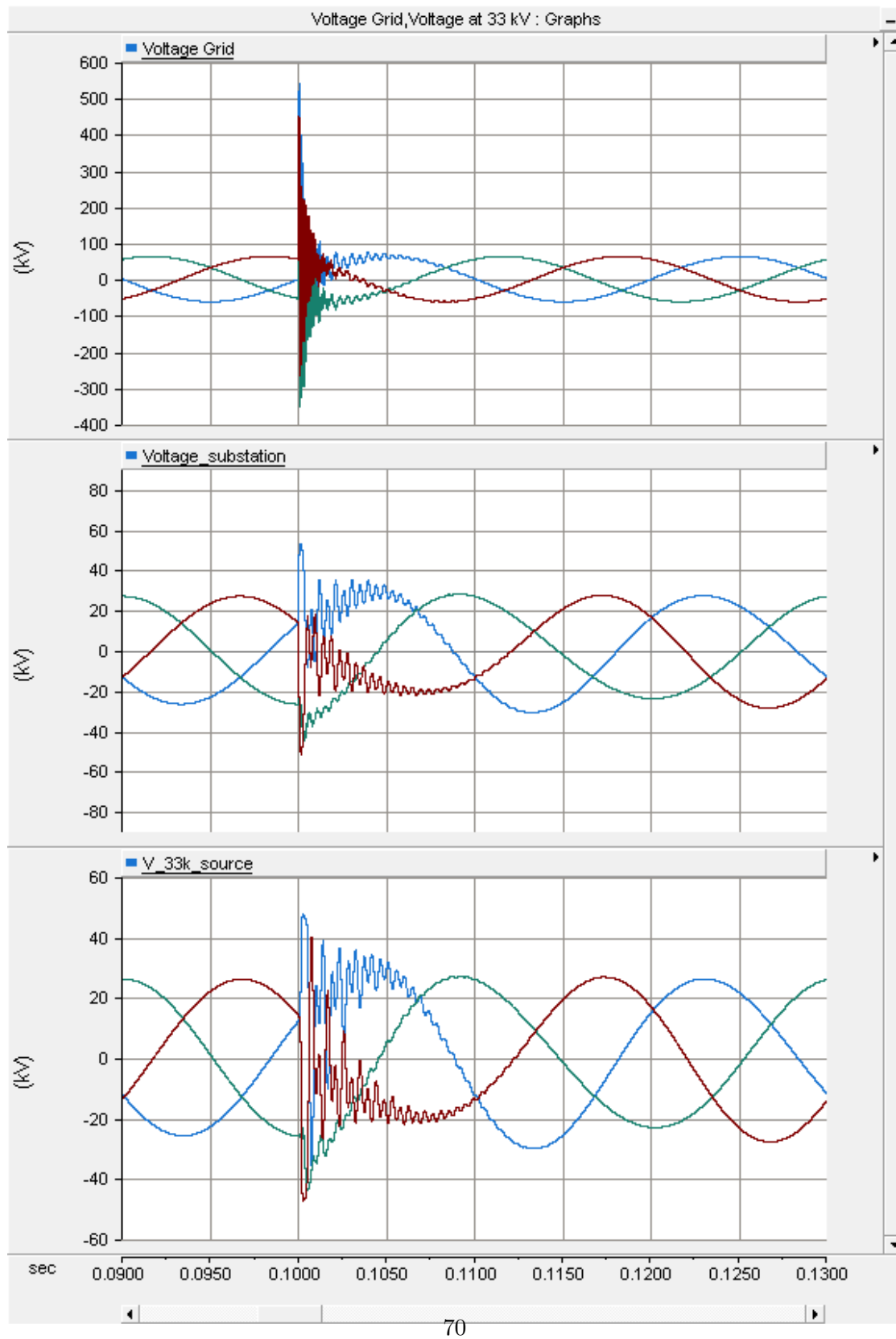


**Figure 7.25:** 1 MV lightning impulse at the utility grid with a surge arrester installed at the substation with an earth electrode of  $1 \Omega$ .

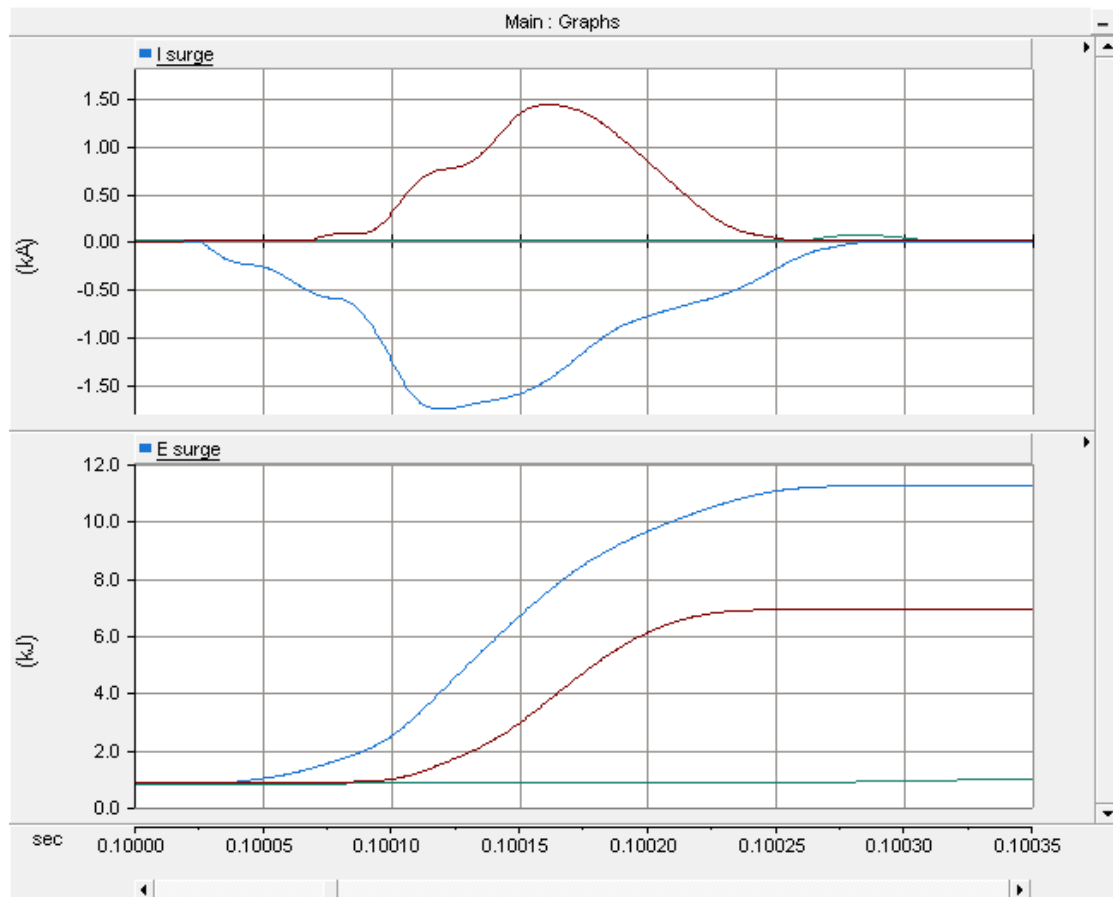


**Figure 7.26:** Current and Energy for a surge arrester, installed at the substation, with an earth electrode of  $1 \Omega$  and an amplitude of 1 MV.

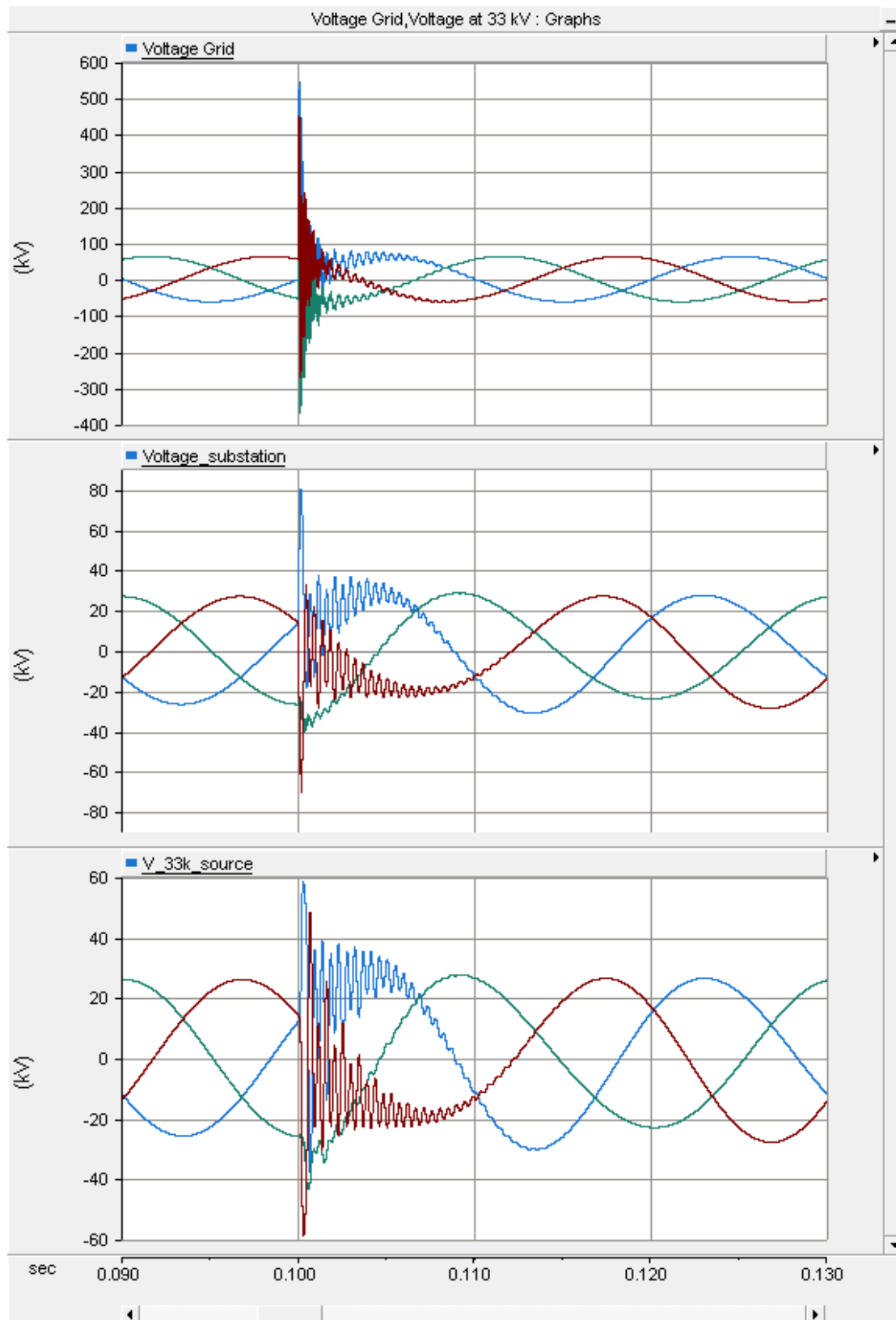
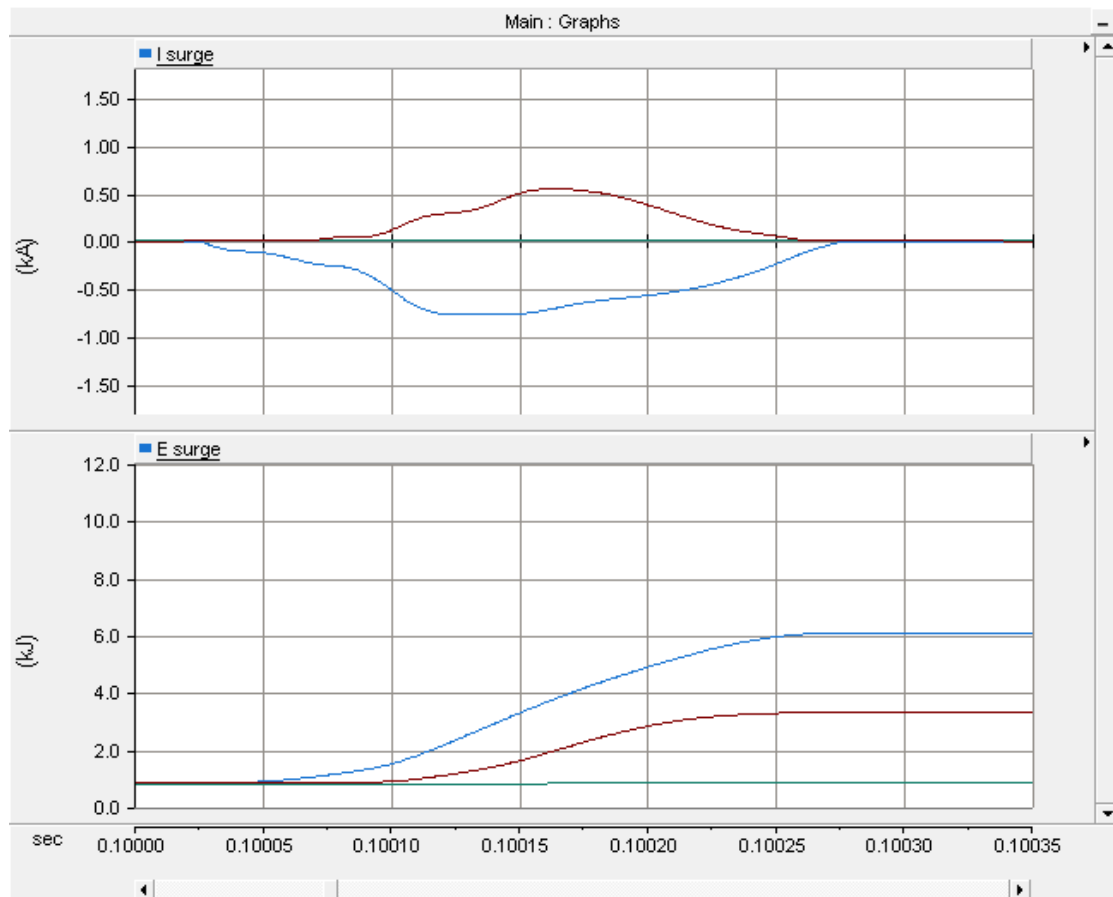


Figure 7.27: 1 MV lightning impulse at the utility grid with a surge arrester installed at the substation with an earth electrode of  $40 \Omega$ .



**Figure 7.28:** Current and Energy for a surge arrester, installed at the substation, with an earth electrode of  $40 \Omega$  and an amplitude of 1 MV.

# 8

## Result

### 8.1 Survey

A lot of companies were contacted but only a handful of them responded. Some companies in certain countries were more helpful than others, e.g. companies in Sweden and United Kingdom. In these countries most of the wind farm companies responded, but there was no response from companies in certain countries, e.g. Spain and France.

A table of how many wind farms in Sweden that participated in the survey is presented in Table 8.1. Table 8.1 also includes what kind of system earthing the wind farms are using.

**Table 8.1:** Type of earthing methods that is used for different wind farms across Sweden

| Country | Type of earthing system             | Number of wind farms |
|---------|-------------------------------------|----------------------|
| Sweden  | Resonance                           | 20                   |
|         | Earthing transformer/Resonance      | 1                    |
|         | Low resistance                      | 2                    |
|         | Earthing transformer/Low-resistance | 1                    |
|         | Isolated                            | 1                    |

How many wind farms that participated in Europe and what kind of system earthing the wind farms are using is presented in Table 8.2.

**Table 8.2:** Type of earthing methods that is used for different wind farms across Europe

| Country      | Type of earthing system              | Number of wind farms |
|--------------|--------------------------------------|----------------------|
| Austria      | Low-resistance                       | 3                    |
| Belgium      | Solid                                | 2                    |
| Denmark      | Solid                                | 1                    |
|              | Low resistance                       | 1                    |
|              | Earthing transformer/Low resistance  | 1                    |
|              | Isolated                             | 1                    |
| England      | Low-resistance                       | 8                    |
| Germany      | Low-resistance                       | 3                    |
| Ireland      | Low-resistance                       | 2                    |
| Italy        | Isolated                             | 1                    |
| Netherlands  | Earthing transformer/Solidly earthed | 1                    |
| Norway       | Low-resistance                       | 1                    |
| Portugal     | Low-resistance                       | 1                    |
| Scotland     | Low-resistance                       | 3                    |
|              | Earthing transformer                 | 1                    |
| Wales        | Low-resistance                       | 1                    |
| <b>Total</b> | Low-resistance                       | 24                   |
|              | solid                                | 3                    |
|              | Isolated                             | 2                    |
|              | Earthing transformer                 | 2                    |

## 8.2 Simulation

A comparison between the different fault scenario simulations with low-resistance earthing and resonance earthing is presented in Table 8.3. From the simulation it can be seen that the voltage levels of all phases are almost the same, despite different system earthing method. It can also be seen that the voltage behaves the same for the both methods when the fault is moved.

The fault current, unlike the voltage, differs a lot for the different earthing methods. As expected, the low-resistance method provides a system with a much higher fault current than the resonance earthing method. When using resonance earthing, the fault current seems to be the same at the different locations for the same type of faults. For

the low-resistance method on the other hand, the fault current reduces further away from the substation. For both resonance and low-resistance earthing, the highest fault current occurs for SLG-faults.

**Table 8.3:** The peak value of voltage levels and fault current in comparison of low-resistance-and resonance earthing during SLG-, LLG-and LL-faults. Measured at Substation

| Fault      |                    | Low-resistance | Resonance                         |
|------------|--------------------|----------------|-----------------------------------|
| Substation |                    |                |                                   |
| SLG        | Fault Current [kA] | 1.27           | $I_{res} = 0.014, I_{ind} = 0.14$ |
|            | $U_a$              | 46.2           | 45.2                              |
|            | $U_b$ [kV]         | 1.27           | 0                                 |
|            | $U_c$              | 44.3           | 45.2                              |
| LLG        | Fault Current [kA] | 0.65           | $I_{res} = 0.007, I_{ind} = 0.07$ |
|            | $U_a$              | 12.4           | 12.6                              |
|            | $U_b$ [kV]         | 39.9           | 40.2                              |
|            | $U_c$              | 12.9           | 12.6                              |
| LL         | $U_a$              | 13.3           | 13.3                              |
|            | $U_b$ [kV]         | 26.7           | 26.8                              |
|            | $U_c$              | 13.5           | 13.5                              |
| Transition |                    |                |                                   |
| SLG        | Fault Current [kA] | 1.13           | $I_{res} = 0.014, I_{ind} = 0.14$ |
|            | $U_a$              | 45.6           | 45.6                              |
|            | $U_b$ [kV]         | 5.9            | 0                                 |
|            | $U_c$              | 39.6           | 45.5                              |
| LLG        | Fault Current [kA] | 0.6            | $I_{res} = 0.007, I_{ind} = 0.07$ |
|            | $U_a$              | 12.4           | 14.5                              |
|            | $U_b$ [kV]         | 38.5           | 39.9                              |
|            | $U_c$              | 16.5           | 14.5                              |
| LL         | $U_a$              | 18.0           | 18.0                              |
|            | $U_b$ [kV]         | 26.7           | 26.7                              |
|            | $U_c$              | 18.9           | 18.9                              |
| Collection |                    |                |                                   |
|            | Fault Current [kA] | 0.94           | $I_{res} = 0.014, I_{ind} = 0.14$ |

SLG

|     |                    |       |                                     |
|-----|--------------------|-------|-------------------------------------|
|     | $U_a$              | 44.7  | 47.3                                |
|     | $U_b$ [kV]         | 15.7  | 2.0                                 |
|     | $U_c$              | 30.15 | 45.1                                |
| LLG | Fault Current [kA] | 0.51  | $I_{res} = 0.0066, I_{ind} = 0.064$ |
|     | $U_a$              | 16.0  | 18.6                                |
|     | $U_b$ [kV]         | 36.2  | 39.0                                |
|     | $U_c$              | 25.3  | 20.6                                |
| LL  | $U_a$              | 22.8  | 22.8                                |
|     | $U_b$ [kV]         | 26.8  | 26.8                                |
|     | $U_c$              | 23.6  | 23.6                                |

The maximum transient overvoltages during the faults are shown in Table 8.4. From the table it is seen that the amplitude of the transient overvoltages is greater when using resonance earthing. The largest transient overvoltage is 82.4 kV and occurs during a SLG-fault. For LL fault, the transient overvoltages are the same amplitude for both the earthing methods. For both low-resistance and resonance earthing, the transient overvoltages are greater for SLG-fault than for the other faults. It can be noticed that during LL fault, the transient overvoltages behave the same as when using low-resistance earthing.

The result from the impulse simulation with different ohmic value of the earth electrode can be seen in Table 8.5. The results indicate that if a lightning impulse of 600 kV occurs on the utility grid, a higher value of earth electrode for the surge arrester will expose the collector grid for a greater voltage. The current through the surge arrester decreases if there is a higher value for the earth electrode.

If the lightning impulse instead have an amplitude of 1 MV, it is even clearer that the surge arrester is dependent on the resistance of the earth electrode. For the worst case, where the voltage level differs the most is when measuring at substation. The voltage increases during a 1 MV lightning impulse with 52 % compared with 19 %, which is during a 600 kV lightning impulse.

**Table 8.4:** Transient overvoltage comparison between low-resistance earthing and resonance earthing

| Fault | Location   | Max. Transient Voltage [kV] |           |              |           |
|-------|------------|-----------------------------|-----------|--------------|-----------|
|       |            | Voltage_substation          |           | V_33k_source |           |
|       |            | Low-res.                    | Resonance | Low-res.     | Resonance |
| SLG   | Substation | -51.9                       | -56.7     | -60.0        | -82.4     |
|       | Transition | -42.6                       | -62.5     | -50.7        | -73.9     |
|       | Collection | -                           | -65.6     | -            | -58.8     |
| LLG   | Substation | 45.2                        | 47.5      | 57.2         | 60.3      |
|       | Transition | 42.1                        | 46.6      | 57.9         | 62.1      |
|       | Collection | -                           | 48.5      | -42.7        | 43.5      |
| LL    | Substation | -34.0                       | -34.1     | -56.5        | -56.5     |
|       | Transition | 30.2                        | 30.2      | -42.8        | -42.9     |
|       | Collection | -30.7                       | -30.8     | -36.2        | -36.2     |

**Table 8.5:** The peak value of voltage levels of 33 kV-collector grid, current through the surge arrester and energy during a lightning impulse of 600 kV and 1 MV.

| Earth electrode    |            | 600 kV impulse |             | 1 MV impulse |             |
|--------------------|------------|----------------|-------------|--------------|-------------|
|                    |            | 1 $\Omega$     | 40 $\Omega$ | 1 $\Omega$   | 40 $\Omega$ |
| Lsurge             | $I_a$      | -0.64          | -0.29       | -1.75        | -0.77       |
|                    | $I_b$ [kA] | 0              | 0           | 0            | 0           |
|                    | $I_c$      | 0.036          | 0           | 1.42         | 0.55        |
| E_surge            | $E_a$      | 3.5            | 2.25        | 11.2         | 6.1         |
|                    | $E_b$ [kJ] | 0.82           | 0.82        | 0.9          | 0.92        |
|                    | $E_c$      | 0.89           | 0.85        | 6.9          | 3.3         |
| Voltage_substation | $U_a$      | 49.5           | 58.9        | 53           | 80.6        |
|                    | $U_b$ [kV] | -40.2          | -35.3       | -45          | -40.75      |
|                    | $U_c$      | -44.0          | -43.4       | -52          | -70.80      |
| Voltage_33k_source | $U_a$      | 47.0           | 53.4        | 47.4         | 58.5        |
|                    | $U_b$ [kV] | -43.3          | -38.3       | -44.5        | -43.2       |
|                    | $U_c$      | -47.1          | -52.6       | -47.3        | -59.4       |

# 9

## Discussion

It can be difficult to get in touch with small wind farm owners and operators in certain countries. Because of this, larger companies were more involved in the survey. Furthermore, for some countries only one company responded. This can result in misleading information regarding system earthing method used in some countries. The survey can provide insight into which method is commonly used for wind farms greater than 10 turbines with a voltage level of 36 kV.

It can be seen in Chapter 8, Table 8.2 that some wind farm owners or operators only answered that they are using earthing transformer as earthing method, as described in Chapter 2.2.5. However, this is not a clear answer because it may for example be solidly earthed or resistance earthed after the earthing transformer. Most often earthing transformer is used when earthing needs to occur at a point where a neutral point is missing, e.g. at a delta side of a transformer.

Some companies did respond for the survey but the voltage level for the collector grids was too low. E.g. some wind farms that were contacted in Norway had a 20 kV collector grid and a wind farm in Cyprus had a 12 kV collector grid. Therefore, they were not included in the survey.

It has not been investigated in the survey if there is any correlation between system earthing and if the wind farm is located onshore or offshore. It can be more common to use a particular type of system earthing at for example offshore wind farms.

A few companies wanted to be anonymous in the survey. Therefore, it was determined that no company would be presented in the survey, but only which country the wind farms are located in.

The lengths of the two radial cables were combined for both parts of the wind farm

for the PSCAD-model, see Appendix A. In addition, the length of the overhead lines between the connection point and part A and part B were combined together with the length between the connection point and the transition point for the PSCAD-model.

In the simulation there was no fault scenario on the radial cables for the wind farm, but only after the collection point on the collector grid. Therefore, all wind turbines could be represented by a voltage source for both parts of the wind farm, see Appendix A.

The value of the inductance for the wind turbine was given from the embedded generator in PSCAD. This value was used for the model because Enercon could not provide with the value of the wind turbine E82.

The value of the fault impedance for the simulations was varied between  $1 \Omega$  for SLG-and LLG-fault and  $0.01 \Omega$  for LL-fault. A high ohmic value for the fault impedance would affect and reduce the transient overvoltages and the voltage increase for the phases for these simulated type of faults.

Impulse overvoltages were simulated only for resonance earthing because that was the earthing system used in the specific wind farm described in Chapter 5. It was investigated how this wind farm using resonance earthing works with surge arresters with low-and high-resistance earth electrodes.

From the simulations with surge arresters it could be noticed that the surge arrester could withstand both 600 kV and 1 MV lightning impulses. However, a 77 kV system would probably not be able to handle a lightning impulse of 1 MV, which is mentioned in Section 7.3.

During some simulations with  $40 \Omega$  earth electrode and with a impulse of 3 MW, the voltage increases higher than 170 kV, which means that the system will not withstand a lightning impulse of 3 MV, when having a high value of the resistance of the earth electrode. This can lead to severe consequences for the power system. It is important to ensure that a power installation has a low resistance of the earth electrode, from Chapter 2.3 it is recommended to have a resistance less than  $5 \Omega$ .

For the simulations of impulse overvoltages, the voltage amplitude is determined instead of the amplitude of the current. A lightning strike contains a very large current, which has not been considered when the voltage amplitude is instead determined. The voltage amplitude was chosen to be controlled and determined because there was a certain voltage level that should be simulated. It may have been more accurate to simulate a transmission lines or underground cables before 77 kV-transformer at the utility grid where the lightning strike occurs.

# 10

## Conclusions

From the results of the survey in Section 8.1 and Table 8.2, it can be seen that low-resistance earthing is the most common method for system earthing for wind farms with a collector grid at 36 kV in Europe. Using low-ohmic resistance will usually result in high fault current in a range of 100-1000 A, as mentioned in Subsection 2.2.3. A great advantage is that the high fault current is easy for the protection system to detect and to disconnect the fault line. Additional advantage with low resistance earthing is that compared with solid earthing, it has lower fault current. The transient overvoltages can be more limited for low-resistance earthing than both resonance earthing and isolated earthing. A disadvantage for this method is that the relatively high fault current can be dangerous for persons and equipment in the electrical power system.

In Sweden, it is instead more common to use resonance earthing for wind farms with a collection grid at 36 kV, which can be seen in Table 8.1. By varying the value of the Petersen coil, it is possible to neutralize the capacitive current between the conductors and earth, which is described in more detail in Subsection 2.2.4. The advantage with resonance earthing is that when phase-to-earth fault occurs, the capacitive current is reduced by the inductive current from the coil. With a small fault current, the arcs cannot maintain themselves and therefore extinguish. The disadvantage with resonance earthing can be that if perfect resonance occurs, there will be a high voltage potential difference between earth and the neutral point.

This survey indicates that even though the collector grid is at 36 kV, wind farms in Sweden are frequently using resonance earthing and in Europe it is more common with low-resistance earthing.

By comparing low-resistance earthing and resonance earthing in Table 8.3, it can be concluded that the fault current is much greater for low-resistance compared with resonance earthing, which is also mentioned in Subsection 2.2.3 and Subsection 2.2.4. Furthermore,

it can be seen that both low-resistance and resonance earthing are nearly at the same voltage level during these simulated type of faults.

From the results, it can be seen in Table 8.4 that the collector grid is exposed to higher transient overvoltages during SLG-faults and LLG-faults for resonance earthing compared with low-resistance earthing. These transient overvoltages can cause damage and degradation on the equipment. The greatest impact of transient overvoltages occurs for SLG-faults. It can be concluded that low-resistance earthing is limiting the transient overvoltages for these simulated types of faults.

The simulations of a lightning impulse led to the result in Table 8.5. According to the table, it can be seen that the amplitude of the impulse inside the collector grid is highly dependent of the earth electrode resistance. It can also be seen that it is more important for higher lightning impulses to have an earth electrode with a low resistance. The voltage difference between 600 kV and 1 MV impulse when using 1  $\Omega$  resistance is very small compared with the 40  $\Omega$  resistance. For 1  $\Omega$  it differs, when measuring at the substation, 3.5 kV and for the 40  $\Omega$  case, it differs 21.7 kV.

As mentioned in Section 2.4, a power system with voltage level of 36 kV should be able to handle a 1,2/50  $\mu$ s impulse with a resulting maximum voltage of 170 kV. For both 600 kV and 1 MV lightning impulses, the voltage inside the system is lower than 170 kV which means that, looking at the 36 kV system, it should be able to handle the impulses using both 1  $\Omega$  and 40  $\Omega$  earth electrode. However, as mentioned in Section 7.3, the 77 kV system is designed to handle a 605 kV lightning impulse, which means that it probably won't be able to withstand a 1 MV lightning impulse.

The high amplitude of the impulse inside the system is not the only thing that needs to be accounted for when designing a power system. When the surge arrester keeps the voltage at a safe level during lightning impulses, a high amount of energy is absorbed by the surge arrester. According to the data sheet, the surge arrester has an energy capability of 148.5 kJ. For the two impulses simulated in Section 7.3, the energy absorbed by the surge arrester is much less than this. Hence the surge arrester should be able to handle the lightning impulses with that amplitude, even with a high resistance earth electrode.

# References

- [1] H. Saadat, *Power system analysis*. PSA Publishing, 2010.
- [2] Donald W. Zipse and Gene Strycula, “142-2007 - IEEE Recommended Practice for Grounding of Industrial and Commercial Power Systems,” *Institute of Electrical and Electronics Engineerings, Inc*, 2007.
- [3] Mats Östman, “The pros and cons of alternative grounding systems,” *Wärtsilä Technical Journal*, 2009.
- [4] D. Shipp and F. Angelini, “Characteristics of Different Power Systems Neutral Grounding Techniques: Facts & Fiction,” *IEEE 1988 Industry Applications Society Technical Conference*, 1988.
- [5] Donald W. Zipse, Robert Beaker, Kenneth Nicholson, Jerry Brown, Daleep Mohla, Charles Dennis, Milton Robinson, S. I. Venugopalan, “141-1993 - IEEE Recommended Practice for Electric Power Distribution for Industrial Plants,” *Institute of Electrical and Electronics Engineerings, Inc*, 1993.
- [6] Joseph Sottile, Thomas Novak and Anup Tripathi, “Best Practices for Implementing High-Resistance Grounding in Mine Power Systems,” *Industry Applications Conference, 2007. 42nd IAS Annual Meeting. Conference Record of the 2007 IEEE*, 2007.
- [7] Paul, D. and Venugopalan, S.I., “Low-resistance grounding method for medium voltage power systems,” *Industry Applications Society Annual Meeting, 1991., Conference Record of the 1991 IEEE*, 1991.
- [8] Jeff Roberts, Dr. Hector J. Altuve, and Dr. Daqing Hou, “Review Of Ground Fault Protection Methods For Grounded, Ungrounded, And Compensated Distribution Systems,” tech. rep., Schweitzer Engineering Laboratories, Inc., 2001.
- [9] Lei Li, Lixiao Duan, Jingshu Zhou, Jian Zhang, Wenzhong Zhou, and Bo Li, “Analysis and Comparison of Resonance Grounding with Low Resistance Grounding,” *Critical Infrastructure (CRIS), 2010 5th International Conference*.

- [10] L. Winell, *Elkraftsystem 2*. Liber AB, 2003.
- [11] J. Parmar, “Types of neutral earthing in power distribution (part 2),” 2012.
- [12] B. Dolník and J. Kurimský, “Contribution to earth fault current compensation in middle voltage distribution networks,” *PRZEGLĄD ELEKTROTECHNICZNY*, no. 2, pp. 220–224, 2011.
- [13] G. Druml, A. Kugi, and B. Parr, “Control of Petersen Coil,” *International Symposium on Theoretical Electrical Engineering*, 2001.
- [14] K.-H. Rofaklski and J. Schlabbach, *Power System Engineering - Planning, Design, and Operation of Power Systems and Equipment*. Wiley-VCH, 2008.
- [15] R. N. Conwell and R. D. Evans, “The Petersen Earth Coil,” *American Institute of Electrical Engineers, Journal of the (Volume:41 , Issue: 2 )*.
- [16] S. Jadhavar, “Grounding transformer.” <http://electriciantheory.blogspot.se/2013/04/grounding-transformer.html>. Accessed: 2014-03-21.
- [17] B. Brown, “Section 6: System grounding.” [http://static.schneider-electric.us/assets/consultingengineer/appguidedocs/section6\\_0307.pdf](http://static.schneider-electric.us/assets/consultingengineer/appguidedocs/section6_0307.pdf). Accessed: 2014-03-21.
- [18] H. Lindmark, *Eldistributionsanläggningar, Kompendieblad i avsnittet Elkraftteknisk Mätteknik*. Högskolan i Trollhättan/Uddelvall, Institutionen för Teknik, 1999.
- [19] E. Kuffel, W. S. Zaengl, J. Kuffel, *High Voltage Engineering: Fundamentals*. Butterworth-Heinemann, 2000.
- [20] Svenska Elektriska Kommissionen, SEK, *Högspänningshandboken*. Svenska Elektriska Kommissionen, SEK, 2005.
- [21] Carina Larsson, “Elsäkerhetsverkets föreskrifter och allmänna råd om hur elektriska starkströmsanläggningar ska vara utförda; ELSÄK-FS 2008:1 ,” tech. rep., Elsäkerhetsverket, 2008.
- [22] Svenska Elektriska Kommissionen, SEK, “Starkströmsanläggningar med nominell spänning överstigande 1 kV AC; SS 421 01 01,” tech. rep., Svenska Elektriska Kommissionen, SEK, 2004.
- [23] European standard, “Earthing of power installations exceeding 1 kV a.c.; SS-EN 50522,” tech. rep., CENELEC, 2010.
- [24] M. PIERROT, “The wind power database.” [http://www.thewindpower.net/country\\_europe\\_en.php](http://www.thewindpower.net/country_europe_en.php). Accessed: 2014-02-14.
- [25] Energimyndigheten, “Vindbrukskollen.” <http://www.vindlov.se/sv/>. Accessed: 2014-02-07.

- 
- [26] 4C Offshore, “4c offshore.” <http://www.4c offshore.com/windfarms/>. Accessed: 2014-02-14.
- [27] Manitoba HVDC Research Centre a division of Hydro International Ltd., *PSCAD - Power Systems Computer Aided Design*.
- [28] T. Abdulahovic, “Analysis of High-Frequency Electrical Transients in Offshore Wind Parks,” tech. rep., Chalmers University of Technology, Department of Energy and Environment, Division of Electric Power Engineering, 2011.
- [29] IEEE Power & Energy Society, “IEEE Standard for General Requirements - C57.12.00,” tech. rep., 2010.



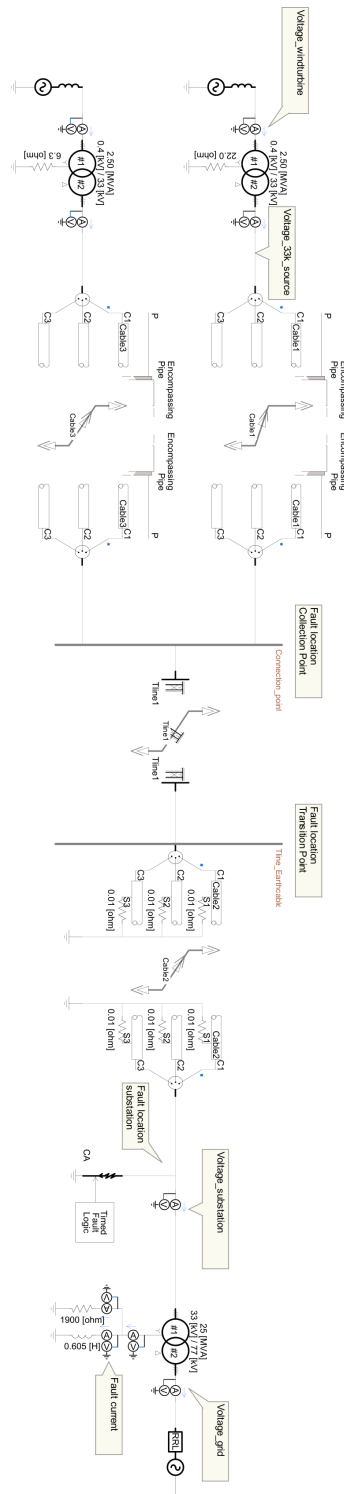


Figure 2: PSCAD-model for resonance earthing simulations.

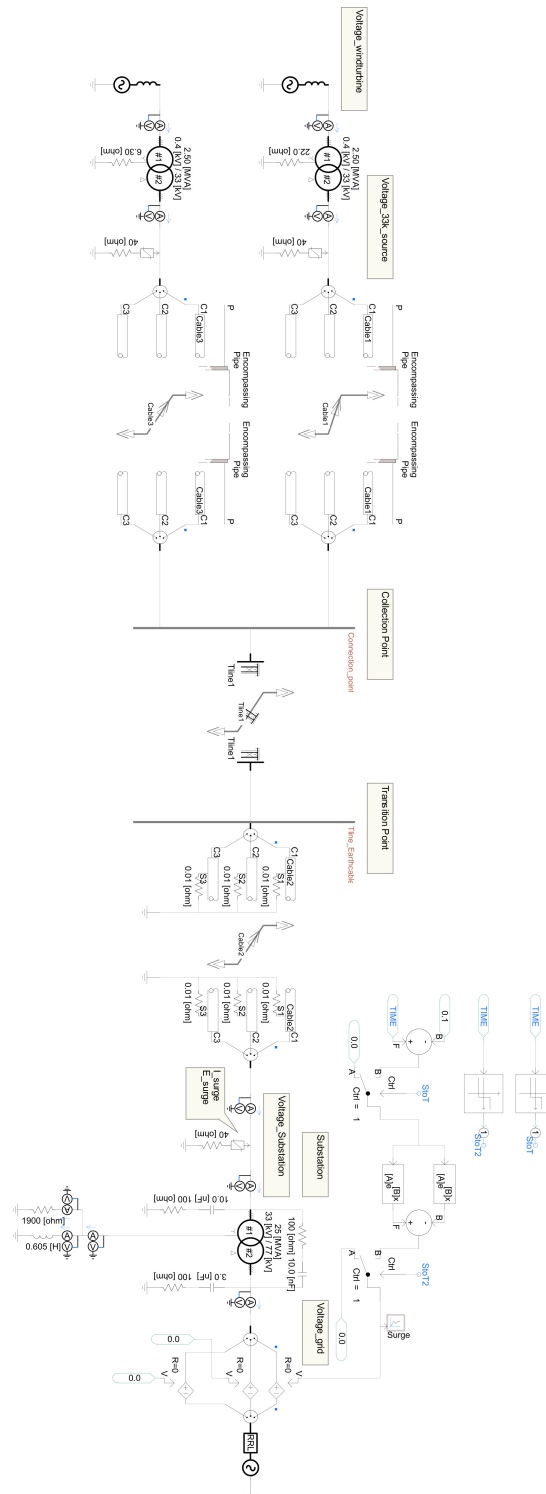


Figure 3: PSCAD-model for lightning simulations.